PG&E Supplemental Response to NRC Additional Slope Stability Questions For Diablo Canyon Independent Spent Fuel Storage Installation (ISFSI) License Application

NRC Request No. 1:

Provide a revised estimate of the rock-mass strength considering the effects of rock-mass weakening owing to stress relief from previous excavations for borrow material and expected future excavation for ISFSI construction.

PG&E Response:

The NRC identified four concerns in the rock-mass strength characterization area and concluded that PG&E should provide a revised estimate of rock-mass strength characterization based on Hoek (2003). PG&E re-evaluated the rock mass strength characterization using Hoek (2003). In addition, PG&E requested Dr. Hoek to perform an independent review of its original characterization of the rock mass strength. Based on PG&E's re-evaluation and Dr. Hoek's independent review, PG&E concluded that the original characterization of the rock mass at the ISFSI site was appropriate and no revision is necessary. The bases of PG&E's conclusion are presented below. Dr. Hoek's written review comments are included in Attachment 1-1. RocLab printouts are included in Attachment 1-2.

Value of mi For Dolomite

The values of mi for dolomite rock at the ISFSI were assigned by comparing the mineralogical and sedimentological characteristics of the exposed rock in exploratory trenches against the estimated values of mi presented by Hoek (2000) for similar rock types. No laboratory triaxial tests were performed on hard dolomite, and therefore laboratory-derived mi values were not determined. Dr. E. Hoek stated in his review:

> *"The selection of the Hoek-Brown mi values given in your notes appears to be very reasonable. For relatively simple rock masses such as dolomites and sandstones, the values of mi tend not to vary a great deal from those quoted in the various Hoek-Brown papers. Consequently, it is unusual to check these values by means of laboratory tests. In any case, mi is the least important parameter in the determination of rock mass properties and even large variations in its value do not normally have a significant impact on the derived strength properties."*

The sensitivity evaluation of mi performed in Calculation GEO.DCPP.01.19, Revision 1, submitted in PG&E Letter DIL-02-005, dated May 16, 2002, substantiates that mi has the least impact of the three input variables (Uc, GSI, mi) used in the Hoek-Brown analyses for the ISFSI. Based on this substantiation and Dr. Hoek's independent review, PG&E concludes that the mi values presented in GEO.DCPP.01.19, Revision 1,

and used for the ISFSI rock mass strength analysis, are valid and do not require modification.

Disturbance factor "D"

The newest update to the Hoek-Brown equations presented in the Rocscience RocLab program (RocLab version 1.006; Rocscience, February 7, 2003) includes a disturbance factor "D" to account for rock mass stress relief dilation and blast damage. The D value is intended to factor future dilation and blast disturbance of the rock mass during excavation (if blasting is proposed to be used) for data that is collected from a previously-excavated, undisturbed rock mass. It should be noted that blasting will not be used for excavation of the ISFSI.

All measured parameters that feed into the Hoek Brown analysis already factor the stress-relief effects from the 1971 excavation, which was achieved by ripping without blasting. Trenches and borehole imaging showed that rock mass dilation from the 1971 excavation extends about 3 to 4 ft below the surface, and discontinuities are in tight contact below this depth. The measured values represent the zone that has experienced stress-relief from the 1971 excavation for 30 plus years. Using these parameters collected from the surface outcrops and shallow trenches for zones that would experience a much smaller scale of stress relief from excavation, such as the proposed cut for the ISFSI pads, would thus be conservative.

The proposed excavation for the new ISFSI pad/cut will be accomplished using large earth-moving equipment. Blasting will not be used for excavation of the ISFSI. Rock mass disturbance should only extend several to several tens of meters horizontally behind the excavated face. Therefore, the localized ISFSI cutslope horizontal stress relaxation will not affect the rock mass strength in the deep rock zones below the cutslope, and in the hillside above the immediate area of the cutslope excavation (more than several tens of meters uphill from the cutslope face). The Hoek-Brown shear strength envelopes with the Disturbance Factor set at zero are appropriate for stability analyses of deep seated stability of rock masses above clay beds. The stability analyses performed for shallow rock failures in the cutslope face, and used for design of the cutslope rock anchor design, were based on discontinuity-specific strengths (Barton-Choubey method) that are lower than the Hoek-Brown shear strength envelopes and that fully-account for any horizontal stress relief dilation of the rock mass in, and immediately behind, the cutslope face. PG&E believes that the Barton-Choubey strength values appropriately model the strength conditions in the post-excavation cutslope rock mass. The Barton-Choubey strengths, representing the strength along rock discontinuities, are much less than the Hoek strength that represents the strength for the fractured rock mass.

Based on Dr. Hoek's evaluation the of borrow slope history and planned ISFSI excavation, he concluded the following.

> *"In terms of the blast damage factor and related stress relief, I fully agree that this will only penetrate for a relatively small distance in your slopes, which have been created by means of relatively gentle civil engineering blasting. Even if this blasting is badly done it does not come close to large open pit blasting where it is not uncommon to blast a million tons in one blast sequence and where the blast damage can extend 100 m or more behind the slope crest. Hence, for your problem, I consider that it is entirely appropriate to set D=0 for deep-seated failures."*

Based on PG&E's review and Dr. Hoek's independent review, PG&E concludes that the disturbance factor, D, should be set at zero for the stability analysis of the deep seated rock mass at the ISFSI, and also for derivation of shear strength envelopes for the confined dolomite and sandstone behind and below the localized cutslope zone of horizontal stress relief dilation (extending several meters to several tens of meters behind the cutslope face).

Revised estimate of rock mass strength

The NRC recommended that the rock mass strength used for the ISFSI deep slope stability analysis be revised using the new RocLab program and D factor (RocLab, version; Rocscience, 2003). PG&E reprocessed its data using the new RocLab program (Attachment 1-2). For the reanalysis, all input parameters were the same as used in Calculation GEO.DCPP.01.19, Revision 1. As discussed previously, no changes are needed for the three input variables: mi, Uc, or GSI. Additionally, the D factor was set at zero for all re-analysis runs.

The output shear strength envelopes from the new RocLab program are the same as the original shear strength envelopes presented in Calculation GEO.DCPP.01.19, Revision 1, and the envelope curves lie on top of each other when the output curves are plotted to the same scale.

Dr. Hoek reviewed Calculation GEO.DCPP.01.19, Revision 1 spreadsheets and curves, and stated the following:

> *"The calculation of the Hoek-Brown parameters has not changed for a long time and there is no difference between the spreadsheets that you have used and the latest RocLab program. What is different is the determination of equivalent Mohr-Coulomb parameters and the introduction of the blast damage factor D."*

PG&E's reanalysis and Dr. Hoek's review shows that the shear strength envelopes presented for the in-situ rock mass ISFSI dolomite and sandstone do not need to be revised.

Rock Mass Friction Angle of 50 Degrees

The lower-bound Mohr-Coulomb rock mass strength values of ϕ = 50 degrees, cohesion = 0 remain valid and below the Hoek-Brown shear strength envelope values (which have not changed in the re-analysis) for the stress range applicable for the stability evaluation of deep-seated sliding in the hill slope above the ISFSI.
Dr. Hoek stated the following based on his review:

> *"The estimate of ϕ = 50 degrees provided by Skip Hendron can be approximated by putting in a slope height of about 60 m for the RockLab analysis of dolomite. This may be a reasonable slope height for your problem but you will note that you also have a cohesion of 0.6 Mpa. Hence Hendron's estimate is good, in terms of slope, but very conservative in terms of cohesion."*

Based on PG&E's and Dr. Hoek's review, PG&E concluded that no changes are required in the rock mass shear strength envelopes or assumed low-bound friction angle of 50 degrees.

Conclusion

The mi values used in the original ISFSI Hoek-Brown analyses are appropriate. As discussed, the disturbance factor, D, should be set at zero for evaluation of the rock mass at the ISFSI, and the shear strength envelopes resulting from the original Calculation GEO.DCPP.01.19, Revision 1 spreadsheets and new RocLab program with D=0 are the same. The low-bound Mohr-Coulomb rock mass strength values of ϕ = 50 degrees, cohesion = 0 remain valid and below the Hoek-Brown shear strength envelope values (which have not changed on re-analysis) for the stress range applicable for the stability evaluation of deep-seated sliding in the hill slope above the ISFSI.

Based on the results of PG&E's review, re-analyses using the RocLab program (Attachment 1-2), and independent review by Dr. Hoek, the input parameters and calculated rock mass shear strength envelopes presented in Calculation GEO.DCPP.01.19, Revision 1, remain valid.

NRC Request No. 2:

Provide an assessment of the seismic stability of the cask-storage pad considering the effects of earthquake loading (inertial loading from the structures superimposed on the loading associated with the free-field ground motion), the occurrence of clay beds underneath the storage pad site, and the failure modes illustrated in Figure 2-1.

PG&E Response:

The NRC's request identified the following concerns:

(1) Only the free-field ground motion was considered in PG&E's analysis. The inertial forces from the storage pads and any pre-existing constructed structures were not included. The induced horizontal shear stress in the subsurface material owing to the inertial forces from the pads is expected to be significant.

(2) There are two potential failure modes that need to be considered in an assessment of the subsurface materials under the storage pad, but only one of the modes was considered by PG&E.

(3) PG&E did not provide documentation of the analysis for the single failure mode that was performed.

To address all three NRC concerns, PG&E has provided documentation for the analyses of the two NRC postulated failure modes in Calculation GEO.DCPP.03.01, Revision 0 (Attachment 2-1) and in a PG&E evaluation of potential failure of the foundation beneath the ISFSI pads (Attachment 2-2). In the two attachments, the inertial loads from the pad and the casks are included and thus induced shear stress on the clay beds is considered. Both analyses showed that even with conservative assumptions of the clay bed being continuous from the pad location to the canyon wall for the horizontal bedding surface failure mode case, or that the clay beds are oriented in a way to facilitate rotational type bearing failure for the second failure mode case, the foundation materials have adequate margin of safety to resist shear failure on the clay beds induced by the inertial loading during the design basis earthquake. The analysis results summarized below are presented separately for the two potential failure modes and detailed analysis results can be found in the attachments.

Potential Failure Dominated By Movement On A Horizontal Bedding Surface

In PG&E's evaluation, the failure model consisted of a slide mass extending from the cut slope to the canyon wall for a distance of about 510 ft, with a width of 490 ft (corresponds to 7 pads), and a depth to the shallowest clay bed of 50 ft. The weight of this rock mass is about 1,749,300 kips. Also included in the model is the 7 fully loaded pads weighing a total of 108,500 kips. The pads and the rock mass are assumed to attach rigidly so that the inertial force from the combined mass is fully exerted on the underlying clay layer during the design basis earthquake.

The pseudo-static analysis performed for this failure mode analysis uses a seismic coefficient of 0.5 times the design peak ground acceleration of 0.83 g (Kramer, 1988, Page 436). The resistance forces come from the shear resistance from the clay bed below, the rock mass strength, which the sliding mass has to detach from in the back, and the two lateral boundaries, which were assumed to have the strength of faults. The results show that the factor of safety is 1.02 and the estimated displacement of this combined mass is about 2.5 inches.

The safety factor is considered acceptable because of the following conservative assumptions: (1) the clay bed for the zone of 490 ft by 510 ft is continuous, (2) the clay beds offset by the surficial faults have no interlocking effects, (3) there is no interlocking of rock asperities in this large area, and (4) the ISFSI pads are fully coupled to the underlying rock foundation and thus the horizontal inertial force imposed by the pads fully contributes to the sliding potential of the underlying rock mass. There is no geologic evidence that: (1) the clay bed zone is continuous to the canyon wall face, (2) there is no interlocking potential between surficial faults, and (3) there is no interlocking potential of rock asperities in this large area. Also, the assumption that the pads are fully coupled to the rock is conservative because the ISFSI pad sliding dynamic analysis, described in SAR Section 8.2.1.2.3.2, states there is 0.41 to 1.21 inches of pad-to-foundation decoupling potential due to one or more of the ground motions analyzed. When the slippage occurs at the contact interface, the inertial loads from the loaded pads cannot be fully exerted to the foundation rock. The amount of inertial load that can be transferred to the foundation is limited to frictional resistance at the contact interface.

The existing raw water ponds between the ISFSI pads and the canyon wall were formed by excavation into the rock foundation. Because the mass of water is only about half of that of the rock mass, it is concluded that the raw water ponds do not adversely impact the sliding analysis and the analysis was conservatively performed assuming the raw water ponds were not present. It should be noted that the raw water ponds are lined to preclude loss of water and any seepage into the foundation.

The proposed CTF structure will be excavated into the foundation rock. With the unit weight of the reinforced concrete of 145 pcf, similar to the unit weight of the in-situ rock of 140 pcf used in the analysis, and by neglecting the approximately 14-ft circular hole in the middle of the CTF structure, the current analysis would have conservatively overestimated the inertial force from the CTF structure.

The water treatment facility, tanks, and buildings shown in SAR Figure 2.1-2 have limited concrete structure above ground and their masses are not significant when compared to the ISFSI pad with casks. The conservatism built into the raw water ponds and the CTF excavations would be more than adequate to cover the limited above ground mass associated with the water treatment facility, tanks, and buildings.
On the above basis, PG&E concluded that horizontal bedding failure mode has adequate safety margin. Detailed documentation of this calculation is provided in Attachment 2-1 to this response.

<u>Potential Rotational Failure Along a Combined Surface Consisting of Inclined Joints and Horizontal Bedding</u>

PG&E evaluated an alternate failure model postulated by the NRC. This slide mass, with fully loaded ISFSI pads, is assumed to rotate on a combination of inclined joints

and horizontal bedding surfaces caused by the inertial force induced rocking of the cask and pads.

The mass of the fully-loaded ISFSI pads are accounted for by the seismically-induced stress distribution determined in Calculation PGE-009-CALC-003, submitted by PG&E Letter DIL-01-004, dated December 21, 2001. In this calculation, a number of combinations of vertical and horizontal seismic coefficients were used to perform a series of pseudo-static analyses. The worse case, in terms of generating the highest bearing stress on the ground, was 6.95 kips on the edge of a 68-ft-wide pad. Under this load combination, about 26 ft of the pad on the opposite side tends to lift off the foundation. As such the load distribution was assumed to vary linearly from 0 to 6.95 kips on the remaining portion on the pad that is still in contact with the foundation. This triangular unbalanced distribution of the pad loads on a portion of the foundation could cause the development of a rotational type of failure if the geometry of the underlying inclined joints and clay beds permits.

The geometry features for each of the pads were developed to identify the most susceptible pad to a rotational type failure. The development and documentation of the pad and foundation cross sections is included in Attachment 2-2.

A slope stability program was used to search the most critical failure surface based on the worst case combination of inclined joints and clay beds under the pad, and the triangular distribution of the surface loads induced by the inertial force from the pad and casks. Under these conditions, the most critical factor of safety is 3.34, demonstrating such mode of failure is not credible.

Alternatively, a bearing capacity approach was used by assuming the foundation is composed of a homogeneous material with the property of clay beds, or the bearing capacity failure geometry is entirely developed along bowl-shaped clay bed segments. This is an extremely conservative approach as clay beds have been demonstrated to be sub-horizontal and any joints that comprise part of the failure surface would have strengths higher than the clay beds. Even under these extremely conservative assumptions, the foundation material has shown to have an adequate factor of safety. Detailed documentation on the two analyses performed for the rotation type failure mode is included in Attachment 2-2.

Conclusions

Based on PG&E's analysis and documentation attached to this request, it is concluded that the foundation material underneath the pad has adequate safety margins for the two failure models, horizontal bedding and rotational.

NRC Request No. 3:

Provide an assessment of effect of the proposed ISFSI excavation on the long-term static stability of the hill slope above the ISFSI considering both clay-bed controlled failure modes and generalized slip circle type failure modes.

PG&E Response

PG&E has performed additional evaluations to address NRC concerns for: (1) the potential for a generalized slip-circle type failure of the cutslopes and hill slope above the ISFSI and (2) the effect of the cutslope (i.e., the proposed excavation for construction of the ISFSI) on the stability of the hill slope above the ISFSI. The results of the evaluations found that the clay bed failure of the slopes governed the design and the effect of the cutslope on slope stability was minimal. The evaluations and PG&E responses to other issues raised by the NRC are discussed below.

Generalized Slip Circle Type Failure Model Evaluation

Originally, PG&E did not consider circular type failure models because colluviums and surficial deposits covering the rock slope, for which such type of failure is feasible, were removed during the 1971 excavation. Any potential slope failures of the exposed competent rock that is visible today above the ISFSI pads are usually controlled by structural discontinuities (i.e., joints, bedding planes and clay beds that exist between intact rocks) as stated in SAR Section 2.6.5.1.1. PG&E performed additional analyses to address the above concerns and to verify that the original assumption that the failures along structural discontinuities control. A letter report documenting the analyses, including the input parameters, program used, and analyses results is included as Attachment 3-1.

Using the cut slope and hill slope stability evaluations documented in calculations GEO.DCPP.01.21, Revision 1 and GEO.DCPP.01.24, Revision 1 (submitted in PG&E Letter DIL-01-004, dated December 21, 2001), new analyses were performed to study a rotational (circular) type failure mode of the cut slope and hill slope for Section I-I'. In performing the analyses, an assumption was made that the rock mass behind the hill slope and the cut slope is significantly fractured such that the dimensions of the rock fragments are small compared to the failure geometry. The purpose of this assumption is to allow the modeling of the rock mass as a homogeneous continuum using Hoek strength, or a friction angle ϕ of 50° for the rock mass.

The first analysis performed was for the Section I-I' without the proposed cutslope near the toe. These results were used as the baseline case from which a comparison with the post toe cut stability analysis results can be made to establish the effect of the proposed cut on the overall slope stability.

Several circular slip circles were searched and analyzed ranging from deep circle (Figure 3 in Attachment 2-1) to shallow circle (Figure 2 in Attachment 2-1). The results show that the deeper circle has the higher factor of safety and the factor of safety decreases as the circles become shallower, as would be expected for slopes that are comprised of purely cohesionless material. The limiting failure mode, or the failure mode that has the lowest factor of safety for cohesionless slopes, would correspond to an infinite slope failure, or extremely shallow failure surface that resembles surface raveling. For the slope at Section I-I' of about 20°, the factor of safety for an infinite slope failure can be simplified to tan (50°) / tan (20°) or a factor of safety of about 3.26. Based on the results of this analysis, the following three conclusions were made.

(1) Shallow failures are more likely than deep seated failures for the purely cohesionless slope modeled for Section I-I'

(2) The minimum factor of safety for the hill slope under the condition existing before the toe cut is about 3.26.

(3) The computed factors of safety, using generalized slip circles in the model of the slope as a homogeneous continuum with strength friction angle of 50°, are higher than the factor of safety for the potential masses sliding on clay beds. The computed factors of safety for masses sliding on clay beds range between 1.62 and 2.86 as presented in the SAR Table 2.6-3. As a result, the slide mass models presented in the SAR Section 2.6.5.1.1 form the basis for the mitigation design for rock masses displacements from the cutslope and hill slope above the ISFSI.

The second analysis performed was on a geometry that includes the proposed excavation near the toe and with the 5-ft centered pattern rock anchors modeled as individual anchors on the section. Rock mass behind the rock anchors is modeled as homogeneous continuum with a friction angle of 50°. The analysis performed a search to find the circular failure surface that yields the lowest factor of safety. The resulting critical circle is shown in Figure 4 in Attachment 3-1 and is located immediately behind the rock anchor system. The factor of safety for this critical failure circle is 3.27. Figure 5 is a deep-seated rotational circle and a circle that extends further uphill. Both figures show higher computed factors of safety than the critical slip circle shown in Figure 1 of Attachment 3-1. Based on the results of the second analysis, the following conclusions were made.

(1) The critical failure surface that develops behind the rock anchors is one that immediately skirts the end of the anchor-reinforced zone. The computed factor of safety for this failure surface is 3.27.

(2) Deep-seated rotational failure below the rock reinforcement and failures that propagate further up slope are less likely than failures that develop

immediately behind the reinforced zone as they show higher computed factors of safety.

(3) The computed factors of safety are significantly higher than the 1.5 typically required for static slope stability and it are also higher than the static factors of safety for the various slide masses as presented in SAR Table 2.6-3.

(4) The factor of safety for failure developed behind the reinforcement zone is close to the minimum factor of safety for the existing slope without the toe cut and without the reinforcement. This would imply that, with the planned rock anchors, the proposed excavation near the toe does not adversely impact the hill slope stability.

Clay Bed Strength

The NRC identified a concern that the shear strength of the clay beds, which was used by PG&E, may overestimate the static strength of the clay. The NRC concluded that the safety factors used by PG&E are acceptable despite the NRC concern that PG&E may have overestimated the rock mass strength. Therefore, the NRC concluded that the long-term stability of the hill slope would be adequate for the conditions evaluated by PG&E.

PG&E based its evaluation of the clay bed strength on the design guideline published by the U.S. Government (NAVFAC DM-7, 1986; USBR Design Standards for Embankment Dams, 1987; and U.S. COE Stability of Earth and Rock-fill Dams, 1970). The PG&E basis is provided as follows: Different strength characterizations are used for the fine grained materials (such as the clay beds encountered at ISFSI), for different loading conditions, depending on how the excess pore water pressures generated in the material from external loading are considered and accounted for (USBR, 1987; USCOE, 1970). For long-term static stability loading conditions, excess pore pressure typically has sufficient time to dissipate and does not accumulate. The most reliable test to determine these parameters is from triaxial tests with pore pressure measurements (USBR, 1987). The effective strength Mohr circles can be determined by subtracting the excess pore pressure for the total strength Mohr circles. Consolidated undrained triaxial test results can also be used to derive undrained strengths for soils (Duncan, Wright, and Wong, 1990). Direct shear test apparatus do not allow pore pressure measurements, and thus cannot be used to determine the effective strength parameters for fine-grained soils reliably, unless the strain rates are so small that excess pore pressure generated from loading can fully dissipate and does not accumulate. On the above basis, consolidated undrained (CU) tri-axial test results are used as the prime test to determine the drained and undrained strength for the clay beds. To supplement triaxial test results, some direct shear tests were also performed for selected clay bed samples. The direct shear tests performed are grouped into three categories depending on the loading sequence and the strain rates. Table 3-1 summarizes the direct shear

tests performed for the project as documented in Data Report G (submitted in PG&E Letter DIL-01-005, dated December 21, 2001):

Table 3-1

Summary of Direct Shear Tests

Type of Test	Strain Rate (inch/min)	Purpose of Test	No. of Tests
Drained monotonic	0.002	Drained strength for long term static loads	3
Undrained monotonic	0.02 to 0.025	Undrained strength for short term rapid loads	6
Undrained cyclic	0.2	Undrained strength for short term rapid loads	4

The slower strain rate used in the drained monotonic direct shear tests was selected to allow excess pore pressure to dissipate during the tests such that the test results can be combined with CU tri-axial tests to determine drained strength for long-term static stability assessment. The strain rate was selected based on consolidation stage characteristic of the clay samples when vertical loads were applied to the fully softened samples in the direct shear apparatus. Strain rates 10 to 100 times higher were used to simulate the undrained condition that is typically exhibited during seismic rapid loading.

Accordingly, the static strength for the clay beds was obtained by using consolidated undrained triaxial tests with pore pressure measurements supplemented with drained monotonic loading. Undrained strength was obtained from consolidated undrained triaxial tests, undrained monotonic and cyclic direct shear tests. These interpretations represent the state-of-practice based on the previously cited guidelines, and accepted practice of the profession (Duncan, Wright, and Wong, 1990). The undrained shear strength envelope was reviewed and accepted by PG&E's Seismic Hazards Review Board as documented in the Board's letter to PG&E, dated September 28, 2001 (Attachment 3-2).

Conclusions

PG&E reviewed the basis used by NRC to derive the clay bed strength and concluded that the clay bed strength documented in Calculation GEO.DCPP.01.31, Revision 1, (Attachment 3-3) remains valid. Based on the analysis performed for this request for circular slip failures, PG&E has demonstrated that the proposed excavation near the toe, with the planned rock anchors installed, does not adversely impact the stability of hill slope above the ISFSI pads. Rotational type failure developed immediately behind the reinforced zone has a factor of safety of 3.27. The computed factor of safety is higher than those for the slide mass models and thus does not control the design. The

factors of safety for deep-seated circles and failure surfaces that propagate further up slope have even higher factors of safety and thus are even less credible.

NRC Request No. 4

Provide an appropriate mitigation against the potential instability of the hill slope above the ISFSI during a potential design-basis earthquake. An approximate mitigation may consist of a support system to stabilize the slope, a change in the geometry of the natural slope by selective excavation and filling, a change in the geometry of the proposed cut slope, and engineered rock barrier to protect the ISFSI structures from potentially unstable masses, or any combination of these and other features. The design basis, criteria and analysis for any selected mitigation features should be provided.

PG&E Response:

The design basis criteria and analysis of potential slope instability mitigation features are discussed below. PG&E has evaluated the NRC-identified concerns and has concluded that: (1) the slope mitigation measures provide acceptable mitigation for any potential slope instability, and (2) the slope instability analyses presented in the Diablo Canyon ISFSI SAR were conducted with an appropriately conservative methodology. Furthermore, as suggested by the NRC, PG&E has recalculated the seismic coefficient time histories using the boundary force approach. The conclusion was that both the PG&E and NRC approaches produced similar results and the method used by PG&E provides slightly conservative results. The following sections and attachments address the NRC concerns in more detail.

Mitigation Design Criteria

PG&E's mitigation criteria for the ISFSI cutslope and hillslope are:

(1) The slope above the ISFSI pad is not expected to experience significant movement during the design basis earthquake.

(2) The established mitigation scheme would capture any dislodged rock of credible size from the slope before it could reach the ISFSI pad and adversely impact the safe operation of the structures, systems, and components for the ISFSI facility during the design basis earthquake.

(3) The mitigation design would be based on sound technical bases and its functions can be demonstrated through either computer simulations or proven experience.

Mitigation Design Basis

As presented in the SAR Section 4.2.1.1.9.2, potential rock mass displacements along clay beds in the hillslope during the design basis earthquake are calculated to range from 1 to 3 ft on the natural slope above the ISFSI cutslope, and from 1 to 2 ft on clay beds inferred to daylight in the cutslope. Based on the geologic characterization of the ISFSI site presented in GEO.DCPP.01.21, Revision 2, submitted by PG&E Letter DIL-01-004, dated December 21, 2001, seismically-induced slope movements would be localized along basal sliding planes formed by clay beds in the dolomite and sandstone bedrock.

The calculated earthquake-induced slope movements involve translation of the rock slope as a relatively coherent block over the clay beds with relatively little internal disruption and deformation of the sliding block itself. As a result, the rock mass movements would be localized along the sliding block margins, and would result in the formation of a linear zone of cracking and settlement at the headscarp tension crack, and overthrusting of rock at the toe of the sliding mass above the clay bed. The overthrust toe region would be susceptible to calving and progressive raveling, and represents the primary source of earthquake-generated rockfall and potential hazard to the ISFSI.

Calved/raveled rock blocks in the overthrust lip would detach from the rock mass along pre-existing steeply-inclined joints that sole out and daylight in the overthrust zone, or that exist immediately behind the overthrust lip. The size of the calved/raveled rock blocks from the overthrust toe region would therefore be controlled by the length of the overthrust lip (between 1 and 3 ft), and the joint spacing in the rock mass, which averages between 1 and 3 ft as described in the SAR Section 2.6.5.2.2. Based on the calculated ranges of displacements and rock mass joint spacing, probable maximum rock block sizes that could be dislodged from the clay bed overthrust regions are between 1 and 6 ft, with a most-credible range of between 1 and 3 ft.

The design basis evaluations and analyses show that the only significant slope stability hazard to the ISFSI from seismically-induced slope movements is rockfall from the overthrust toe region of probable rock masses sliding on clay beds. Based on the results of seismic displacement estimates of rock mass on clay beds, and also considering the geological information, the size of the rock that could dislodge from the ISFSI hillslope is 1 to 3 ft with maximum of about 6 ft. The mitigation design was conservatively designed based on rock block sizes of 10 ft.

Preliminary Rockfall Analyses

The final design for the mitigation system will be based on a detailed rockfall analysis and simulation, which will be performed during the ISFSI site construction phase.

As part of the feasibility assessment at this stage, a preliminary rockfall analysis for the hillslope above the ISFSI was made. The potential hazard to the ISFSI from rockfall was evaluated using standard rockfall evaluation methods that include development of topographic cross sections along the rockfall paths, evaluation of source rock characteristics, and iterative rockfall modeling using computer programs (e.g., Colorado Rockfall Simulation Program – CRSP, Rocscience Rocfall). The computer programs allow the user to estimate the rockfall trajectory path, bounce height, velocity, and impact force at selected analysis points along the slope profile. This information is used to evaluate adequacy of the design for rockfall mitigation measures such as catchment benches or ditches, fences, or walls.

The inclination of the hillslope above the ISFSI pad and cutslope is relatively gentle, on the order of about 15 to 21°. Based on Keefer (1984), rockfalls and rockslides typically need to have a minimum slope about 40°, suggesting that the ISFSI hillslope is not particularly prone to rockfalls. No significant rockfalls have occurred on the hillslope since the borrow cut excavation was made in 1971 (SAR Section 2.6.1.12.2), further suggesting that the slope is not prone to rockfall and rockslide failures. In addition, the tower access road (shown in SAR Figure 2.6-1), above the ISFSI, forms benches in the slope profile that would serve to slow and arrest most rockfalls generated above the road.

Based on the site geologic investigations (GEO.DCPP.01.21, Revision 2) dolomite and sandstone rock blocks are moderately hard to hard, and relatively angular. Rockfall blocks therefore would be relatively hard and tend to stay intact without significant breakage and disaggregation, but the angular shape of the blocks would tend to resist rolling. The slope surface between the potential clay bed slide mass rockfall source zones and the ISFSI pad is relatively rough, with a surface irregularity on the order of about 6 inches to 2 ft, and a thin cover of rock rubble. The surface irregularities serve to slow and arrest possible rockfalls, especially for angular blocks with relatively sharp corners and points.

Preliminary rockfall analyses, using the existing topographic cross sections, and the CRSP and Rocfall modeling programs, show that rocks dislodged at the various clay bed slide mass toe regions tend to only roll a few tens to about 100 ft downhill before becoming arrested either on the slope, or on the tower access road benches above the ISFSI pad and cutslope. The modeled rock blocks roll over the ground surface without bounding, exhibit low translational and rotational velocities, and low impact forces. The preliminary analyses results suggest that the rockfall hazard to the ISFSI is very low, and should not require mitigation. However, a defense-in-depth design approach was adopted and an ISFSI slope hazard mitigation system will be designed that incorporates several protection elements.

Mitigation Features

The following ISFSI cutslope design features provide mitigation against possible rockfall. These mitigation features include some of the possible mitigation approaches listed by the NRC in Request 4 and are described in SAR Section 4.2.1.1.9. Together, these mitigation features provide redundant measures against the already low potential rockfall hazard. The hillslope above the ISFSI cutslope is inclined between about 15 and 21°, and rockfall rarely occur during earthquakes on slopes less than about 40° (Keefer, 1984; California Division of Mines and Geology, 1997). Additionally, the preliminary rockfall modeling of the site shows that even if rockfall is triggered, it is not expected to travel more than several tens to about 100 ft downhill before becoming arrested on the slope or the existing tower access road. PG&E's detailed geologic and rock mass characterization of the site indicates that credible rockfall block sizes would be between 1 and 3 ft in maximum dimension, with a rare maximum size of 6 ft (GEO.DCPP.01.21, Revision 2). However, the rockfall mitigation design criteria accommodate possible rockfall blocks up to about 10 ft in maximum dimension. This provides a very substantial safety margin for the ISFSI.

The following elements comprise the rockfall mitigation system for the ISFSI.

- The existing 10- to 12-ft wide tower access road provides a very effective catchment bench for possible rockfall released above the road. The road bench will be maintained and periodically cleared to maintain its effectiveness as a rockfall catchment bench.

- A 2- to 6 ft-wide, 1-ft deep drainage ditch will be constructed at the top of the cutslope. This ditch would help catch small rockfall blocks generated on the slope above the cutslope.

- A rockfall barrier fence will be constructed at the top of the ISFSI cut that will be designed to absorb and dissipate the energy from possible rockfall generated on the slope above. The design criteria and supporting bases for the rockfall barrier fence are described immediately after the description of the mitigation features.

- The cutslope includes a 25-ft wide mid-slope horizontal bench. The significant width of the bench should effectively catch any rocks released from the upper part of the cutslope (above the bench), and also provides a wide buffer zone to accommodate the calculated 1- to 2-ft of displacement for the slide mass models No. 3b (SAR Figure 2.6-49) that toes-out in the vicinity of the bench location.

- The ISFSI pad is setback from the toe of the cutslope a distance of 41 ft. This setback provides a significant buffer zone to catch any possible rockfall from the lower part of the cutslope, and provides a substantial separation between the pad and zone of possible deformation at the toe-of-slope daylight of slide mass model No. 3a and 3c (SAR Figure 2.6-49).

The rockfall barrier fence to be constructed at the top of the ISFSI cutslope will be a commerically-available, rockfall fence system specifically designed for the possible site loading conditions. An example rockfall fence system under consideration is the Geobrugg rockfall fence system that has been installed at numerous locations throughout the United States, and locally along Highway 1 by Caltrans. PG&E's preliminary rockfall analysis suggests that the Geobrugg Very High Impact fence (design load of 295 ft-tons) would be suitable for the ISFSI installation. Such a system could easily withstand all foreseeable forces associated with rockfall blocks in the size range of about 1 to 3 ft that are most likely to be generated on the hillslope, and also could restrain rare larger blocks up to about 10 ft in dimension that are slowly rolling along the slope surface. The preliminary analysis suggests that dislodged rocks would slowly roll along the slope surface, without bounding. Therefore, a fence height on the order of about 8 ft should provide a substantial margin of safety against all possible rockfall block sizes and forces.

Computation of Seismic Coefficient Time Histories

The NRC has identified concerns regarding the methodology that was used to calculate the seismic coefficient time histories for the potential slide mass models. These seismic coefficient time histories form the bases of the displacement estimates of the postulated slide models. Although PG&E believes that the nodal acceleration averaging method is valid and would be slightly more conservative, PG&E recalculated the seismic coefficient time histories using the force averaging method as suggested by the NRC.

The seismic coefficient time histories for blocks 1b, 2c and 3c on Section I-I' in calculation GEO.DCPP.01.25, Revision 4, Attachment 9 (Attachment 4-1 to this response) were recalculated using the summation of boundary forces method as suggested by NRC using the appropriate algorithm described in QUAD4M (1994). The boundary force summation method is consistent with Kramer (1996). Figure 9-2 (in calculation GEO.DCPP.01.25, Revision 4, Attachment 9, shows the seismic coefficient time histories for blocks 1b, 2c, and 3c using ground motion Set 1 computed by averaging selected nodal points within the block. In calculation GEO.DCPP.01.25, Revision 4, Attachment 9, Figure 9-1, the seismic coefficient time histories computed by dividing the summation of boundary forces by the mass of the block are shown. For engineering purposes, it can be concluded that the seismic coefficient time histories computed by the two methods give the same results. Comparison of the time histories for Blocks 1b, 2c and 3c using ground motion Set 5 can be made between Figure 9-3 (force) and Figure 9-4 (nodal) in calculation GEO.DCPP.01.25, Revision 4, Attachment 9; the same conclusion can be reached.

The computed displacements using the boundary force-based seismic coefficient time histories are compared with those using nodal acceleration-based time histories as summarized in the following Table 4-1. It is clear that the seismic induced displacements computed using the two methods are close and the averaging of nodal acceleration approach used by PG&E produced slightly more conservative results.

Documentation of the computed seismic induced displacements with the boundary force based seismic coefficient time histories is provided in Calculation GEO.DCPP.01.26, Revision 4, Attachment 10 (Attachment 4-2 to this submittal).

Table 4-1

Comparisons of Seismic Induced Displacements for Potential Slide Masses

Sliding Mass Model	Input Motion	Displacements based on nodal accelerations[a] (ft)	Displacements based on boundary forces[b] (ft)
1b	Set 1	3.1	2.8
2c	Set 1	3.1	2.6
3c	Set 1	1.4	1.4
1b	Set 5	2.4	2.2
2c	Set 5	2.3	1.9
3c	Set 5	0.6	0.6

Note: (a) From SAR Section 2.6, Table 2.6-5 column no. 5
(b) From GEO.DCPP.01.26, Revision 4, Attachment 10, Table 10-1.

In PG&E Calculation 52.27.100.735 (GEO.DCPP.01.25, Revision 1), previously submitted in PG&E Letter DIL-01-004, dated December 21, 2001, the seismic coefficient time histories representing the response of the potential sliding masses during the design earthquakes were computed by averaging nodal time histories at selected nodal points located within the corresponding potential sliding masses. The reasons for PG&E's determination that the development of seismic coefficient time histories using the nodal acceleration averaging method was acceptable are:

(1) Compliance with Newmark (1965) method for simulating sliding rock mass movement. In the original derivation of the method, a rigid block placed on a moving support was used to simulate movement of a potential slide mass on a slope during earthquakes as shown on Figure 16 of Newmark (1965). The effect of an earthquake was simplified to a single rectangular pulse characterized by acceleration A_g and duration t_o as shown on Figure 17 of Newmark (1965). The resisting force at the base is represented by a resisting acceleration N_g which is the same as the yield acceleration (ky) used in GEO.DCPP.01.25, Revision 1. The velocity (V) of the block at time t_o was obtained by integrating the area above bounded by A_g and N_g between time zero and time t_o as follows:

$$V = A_g \times t_o \qquad (1)$$

After a time, the response acceleration (A) drops below the resisting acceleration (Ng) and the block is no longer accelerating, the block continues to move at the constant velocity (V) while the base is accelerating relative to the block until time tm, when the velocity of the block equals the velocity of the moving base and the net velocity becomes zero (the block comes to rest relative to the base). Integrating the velocity time history between time zero and time tm will then yield the displacement of the block during this pulse. In PG&E Calculation 52.27.100.736 (calculation GEO.DCPP.01.26, Revision 1) previously submitted in PG&E Letter DIL-01-004, dated December 21, 2001, this process is repeated for every pulse that exceeds the yield acceleration to come up with the cumulative displacement of the block throughout the duration. In Newmark (1965), acceleration was used as the main parameter and GEO.DCPP.01.26, Revision 1 implemented the Newmark procedure in the same manner.

(2) Coherency of Motion within Potential Slide Mass. Because of the high stiffness of the potential slide masses (as demonstrated by the high shear wave velocities of 3,500 ft/sec and above), the slide masses are expected to behave fairly rigidly with no significant relative movements within the blocks. In addition, no traveling waves were used in the two dimensional finite element dynamic analyses (calculation GEO.DCPP.01.25, Revision 1). With high material stiffness and no traveling waves, the ground motions developed with any potential slide masses are expected to be spatial coherent and thus averaging the time histories at representative points within the slide masses would be a good representation of seismic coefficient time history for the potential slide masses. If traveling waves were used, the incoherent motions developed within the fairly rigid block would encourage canceling at high frequencies (kinematic interaction) and the result would be a less conservative estimate of the seismic coefficient time history and in turn a lower estimate of the block movement.

To demonstrate the coherency of the time histories, ground motion Set 1 will be used as an example. The coherency of the motions can be demonstrated by the similarities between the input time history (calculation GEO.DCPP.01.25, Revision 1, Figure 4), and the average seismic coefficient time histories of blocks 1b, 2c and 3c (calculation GEO.DCPP.01.25, Revision 1, Figure 13). The comparison shows that the time histories are very similar in appearance, especially in the long period range that controls the seismic induced displacements. The comparison of the other time histories generated for the blocks to the corresponding input ground motion Set 5 also found them to be similar in appearance. High frequency portions of the two seismic coefficient time histories are slightly less than that of the input motion due to the canceling effect of averaging, observed both mathematically in the analysis and physically in the field. Similar effects were noticed in past earthquakes by comparing free-field stations with nearby recordings on

concrete slabs or in basements. The phenomenon is called kinematic interaction. Similar magnitude of this canceling effect would be encountered if averaging of the forces along the slide mass boundaries were performed. Under true field conditions with real earthquakes and traveling waves, the expected coherency of the ground motions would be less, i.e., more cancellation effects would be noticed resulting in lower seismic coefficient time histories and lower displacement estimates than those presented in the SAR.

(3) Newton's Second Law of Motion. For a rigid object sliding on a moving surface, Newton's Second Law of Motion states that the acceleration (a) the object would experience will be proportional to the force (F) exerted on the object and inversely proportional to the mass (M) of the object, or

$$F = M \times a \qquad (2)$$

In the case of the potential slide mass models for the ISFSI cut slope, there are very little spatial incoherent motions as discussed in (2), as such, the slide masses would move in a fairly rigid fashion. Under such conditions, obtaining the representative seismic coefficient time histories of the slide masses by averaging selected nodal force time histories (method used by PG&E) would be the same as dividing the averaging the force time histories by the constant mass of the potential slide mass (suggested by NRC).

Applicability of Pseudo-Static Stability Analysis Procedure

The NRC questioned why PG&E did not use the input motion directly into a pseudo-static slope stability analysis if the response acceleration is similar to the input acceleration. Rather, PG&E used the two dimensional response analyses results to estimate the seismic induced deformations for the potentially sliding masses.

PG&E did not use pseudo-static analysis as the design basis because it would not be in compliance with NUREG-1620 Section 2.2.3 Item (3) (d) which states that pseudo-static analysis is only acceptable if the design seismic coefficient is less than 0.2 g among other restrictions. For design seismic coefficients greater than 0.2 g, NUREG-1620 Section 2.2.3 Item (3) (g) stated that the dynamic stability investigation (Newmark, 1965) should be augmented by other appropriate methods (i.e., finite element method), depending on specific site conditions. The limited use of pseudo-static slope stability analysis for seismic coefficient of 0.2 g or less is also widely accepted by the profession (Seed, 1979) and by the California dam regulatory agency (Babbitt and Verigin, 1996).

The expected similarity between the computed block response acceleration and the input acceleration was used indirectly as a check to confirm the reasonableness of the two dimensional finite element analysis results. Specifically, if the slide mass and the underlying cut slope behave perfectly rigidly, then the slide mass response could be

represented by the input motion at the centroid of the mass, as the NRC reviewer has stated. However, the rock mass is not perfectly rigid (or infinitely stiff). Minor differences can be noticed by comparing the input time history (calculation GEO.DCPP.01.25, Revision 1, Figure 4 using ground motion Set 1 as an example), to the average seismic coefficient time histories of block 1b (calculation GEO.DCPP.01.25, Revision 1, Figure 13) as stated before.

The effect of the differences can be further quantified by performing a Newmark slide block analysis with these two time histories using the same yield acceleration to calculate the seismic induced displacements as summarized in Table 4-2 below.

Table 4-2

Comparisons of Seismic Induced Displacements Based on Input Time Histories and Generated Seismic Coefficient Time Histories

Sliding Mass Model	Yield Acceleration (g)	Input Motion	Displacements based input time history[a] (ft)	Displacements based on nodal accelerations[b] (ft)	Displacements based on boundary forces[c] (ft)
1b	0.2	Set 1	3.3	3.1	2.8
1b	0.2	Set 5	2.6	2.4	2.2

Notes:
(a) From SAR Section 2.6, Table 2.6-4, Set 1 and Set 5, negative polarity, I-I_{46}.
(b) From SAR Section 2.6, Table 2.6-5, Set 1 and Set 5 ground motion.
(c) From Table 10-1 in calculation GEO.DCPP.01.26, Revision 4 (Attachment 4-2)

The comparison shows that the displacement estimates using the input time histories directly are within 10 percent of that computed from the two-dimensional response analysis using either of the nodal acceleration based or boundary force based seismic coefficient time histories. The slightly lower results from the response analysis are reasonable because it includes some kinematic interaction. These comparisons also form the basis of the reasonableness of the two dimensional finite element analyses. Similar conclusions can be made when comparing SAR Tables 2.6-4 and 2.6-5 for slightly different yield accelerations.

Acceptable Seismically Induced Displacements

The NRC identified a concern regarding PG&E's use of the calculated Newmark displacements for estimating seismically induced displacements in a rock slope.

In evaluating the acceptability of the seismic-induced displacements, PG&E considered the amount of computed displacements are order-of-magnitude estimates. The conservatism built into the analytical model was tested by back analyzing geological-

based evidence. The amount of displacements were then further evaluated to identify potential impacts that they could have on the ISFSI facility, and whether these potential impacts could be mitigated by engineering measures, and then selected appropriate engineered components for the mitigation measures. The decision on acceptance of the computed displacements was made at this stage. The calculated displacements were determined to be acceptable based on the following:

(1) Planned mitigation measures:

As described in SAR Section 4.2.1.1.9.2, the rocks dislodged from displacements along any of the several clay beds will be prevented from reaching the ISFSI site by a rockfall barrier constructed at the top of the ISFSI cut slope. The barrier will be designed to absorb and dissipate the kinetic energy of the of the rock fall and will be constructed of articulated steel posts, bundled wire ring steel nets, friction brake elements anchoring, and retaining rope and rock anchors.

Rock offsets by displacements along clay beds daylighting in the cut slope will be prevented from dislodging from the cut slope face by wire-mesh-reinforced shotcrete facing and rock anchors.

In the improbable event of rock blocks becoming completely dislodged from the cut-slope face during a seismic event, the mid-slope bench width and offset distances from the slope base to the ISFSI pads are sufficient to accommodate a rock block of about 20 ft or more.

(2) Conservatism included in the seismic displacement calculations:

<u>In geology</u>, the base of all potential slide masses are assumed to be seated on clay beds and these clay beds are assumed to be infinitely continuous in the third direction (direction perpendicular to the cross sections). No contribution from interlocking of rock asperities was used within the thin clay beds across a distance of several hundred feet along the based of the slide mass models.

<u>In geotechnical engineering</u>, strength of the clay beds were determined on fully softened samples saturated under little or no confining pressure. All clay bed samples were taken from near surface trenches that have gone through many wet-dry cycles. Whereas the deep-seated clay bed materials, over which the potential slide masses slide, are very unlikely to reach a fully softened stage under the existing overburden pressure nor would they be likely to go through as many wet-dry cycles as the near surface samples did. The strength envelope for the clay bed samples was determined using post-peak strengths, thus neglecting the fact that the clay beds have to go through peak strength, which would be 10 to 30 percent higher than the post-peak strength, before they can reach the residual strength. The undrained strength envelope also

conservatively neglected the cohesive contribution to the strength by assuming no cohesion intercept.

In seismic ground motions, the design ground motions were developed based on an 84th percentile ground motion for a magnitude 7.2 earthquake with the long period motion further increased to include the maximum near fault effects.

The built-in conservatism can be validated with geological field evidence. In Section 2.6.5.1.3.6 of the SAR, it was pointed out that the topographic ridge upon which the ISFSI site is located has been stable for the past 500,000 years. During which period, at least 35 to 40 large earthquakes with the magnitude close to 7.2 on the Hosgri fault earthquake (recurrence interval of 11,350 years), would have occurred. Yet, there is no geological evidence to show seismic induced displacements in excess of 3 ft exist.

In conclusion, PG&E's interpretation of the computed displacement of 0.4 to 3.1 ft is that it represents a conservative estimate. Although geological evidence suggests that of the computed displacements did not occur in the past 500,000 years at the site, in the unlikely event that such displacements should occur, the adverse effect would be mitigated by engineering designed mitigation measures described above and in SAR Section 4.2.1.1.9.

Applicability of Newmark Displacement Calculation to Rock Slopes

The NRC identified a concern regarding applicability of the Newmark-type displacement estimation procedure for rock slopes and attributed the inapplicability to the difference between earth dams and embankments made of high damping material to low material damping of rocks in a rock slope.

Newmark (1965) deformation analyses are based on several simplifying assumptions. These include:

(1) the soil behaves in a rigid, perfectly plastic manner;

(2) displacements occur along a single well defined slip surface;

(3) the soil does not undergo strength loss as a result of shaking;

(4) the rigid soil model experiences only translation movement during shaking.

In the case of the ISFSI cut slope above the pads, the potential sliding masses are comprised of hard sandstone and dolomite, and their movements will occur along pre-existing and well-defined clay beds. With a post-peak strength assigned to the clay beds that is not expected to experience further reduction during shaking, the ISFSI sliding masses are in agreement with the model used in Newmark (1965).

Keefer (1984) identified 14 types of earthquake–induced landslides that fall into 3 general categories: coherent slides, disruptive slides and falls, and lateral spreads and flows. The coherent slide involves low to medium velocity "stick-slip" type displacement of coherent blocks of soils and rock. The coherent type slides are where Newmark type sliding analysis is most applicable (Wartman, Seed, and Bray, 2001), and it is also the form of movement expected of the potential slide mass above the ISFSI pads. Disrupted slide and falls generally apply to high velocity freefall failure of rock and soil and are therefore more amenable to factor-of-safety seismic slope stability analysis (Ashford, 1994). Based on Keefer (1984), rock falls and rockslides that fall into this category typically need to have a minimum slope of 40°. For the rock ridge above the ISFSI pads, the slope is about 20° and it is unlikely for such a form of failure to occur. Slow moving dislodged rock blocks on the relatively flat slope above the ISFSI pads are expected to be captured by the planned rock fall mitigation measures discussed earlier in this response and in SAR Section 4.2.1.1.9. The third form of failure is lateral spreading and flows that are typically associated with liquefaction of loose sands. This form of failure is not applicable to the ISFSI project site condition.

Wartman, Seed, and Bray (2001) performed shake table tests and centrifuge model tests to study seismically induced deformations on slopes. In the shake table test, the validity of Newmark-type slide block analysis model was verified by placing a 1- by 4-in square metal block on an inclined plane mounted on the shaker table (Figure 4.5). Figure 4.14 in the report shows the excellent agreement between the measured displacement and the computed displacement of the rigid metal block. To study the applicability of Newmark method for more flexible bodies, the metal rigid block was replaced with two 10-in diameter columns, constructed of a mixture of kaolinite and bentonite, to represent the more deformable body above the slide plane as shown in Figure 4.6 of their report. The results show that the displacement of this model is dependent on the frequency ratio between the predominant frequency of the shaking table excitation and the natural frequency of the deformable model representing the soil column above the slide plane. The shake table tests clearly show that the Newmark slide block analysis procedure is very suitable for rigid block sliding on top of a well defined slip plane. Also, using this procedure for more deformable bodies will depend on the vibration characteristics of the deformable mass and may not produce as good a result as the rigid block.

Although very limited documentation of rock mass movements on a gentle slope during an earthquake are available, because such case histories occur very rarely, rock mass movements on a gentle slope may be considered to be similar to a concrete dam sliding on rock foundation. In estimating the amount of lateral sliding of concrete dam during earthquake, the Newmark-type procedure is still the widely-accepted approach (Chopra and Zhang, 1991). A similar analytical approach was utilized by PG&E in SAR Section 8.2.1.2.3.2 to estimate the amount of sliding between the ISFSI concrete pad and the rock foundation.

To further demonstrate the applicability of Newmark sliding block analysis procedure for rock block sliding on clay beds, an independent check of the results was performed using the FLAC program (GeoPentech, 2002). The FLAC analysis summary and results were provided to the NRC in PG&E Letter DIL-03-001, dated February 7, 2003. In the FLAC analysis, the slide masses and the underlying rock mass were modeled as finite elements and the clay beds were modeled as interface elements (or slip elements). In this coupled analysis, displacements of the slide masses were directly obtained from solving the equation of motion and the results were compared with the decoupled Newmark-type analysis presented in SAR Table 2.6-5 for blocks 1b and 2c using ground motion Set 1 as summarized below.

Table 4-3

Comparisons of Newmark Displacements with FLAC Analysis Results

Slide Mass Model	Displacement estimate using Newmark decoupled procedure[a] (ft)	Displacement estimate using FLAC coupled analysis procedure[b] (ft)
1b	3.1	3.1
2c	3.1	2.3

Note: (a) From SAR Table 2.6-5
(b) From GeoPentech (2002) Table 2

It can be seen from the above table and the physical model tests that Newmark sliding block analysis is applicable for estimating rock translational movement on pre-defined failure surfaces, such as clay beds. Case history survey by Keefer (1994) also suggests that the coherent slide is the most likely form of movements of rock blocks on the gentle of about 20° slope above the Diablo Canyon ISFSI site.

Guidelines on Acceptable Seismic Deformation Estimates

The NRC reviewer cited "Guidelines for Evaluation and Mitigating Seismic Hazard in California" (Specially Publication (SP) No. 117 by CDMG, 1997) as a suggested guideline for classification of the seismic stability of a slope. The guideline provided a three-category classification for the seismic stability of a slope as (i) likely stable, (ii) likely unstable, and (iii) definitely unstable.

The CDMG SP-117 was developed in response to the passage of the Seismic Safety Mapping Act of 1990. The main objectives of the guidelines are: (1) to assist in the evaluation and mitigation of earthquake-related hazards for projects within designated zones and (2) promote uniform and effective implementation of the Seismic Hazard Mapping Act. The "Project" definition of the act is: (1) any subdivision of land, which contemplates the eventual construction of structures for human occupancy and

(2) structures for human occupancy. These guidelines are intended for residential and commercial developments. In order to promote seismic safety awareness, encourage site-specific investigation and mitigation activities, and provide safe codified rules, these guidelines were developed using a very conservative approach.

A more applicable guideline for determining acceptable seismic induced slope displacements would be that adopted by the California Department of Water Resources, Division of Safety of Dams (DSOD). In the publication by Babbitt and Verigin (1996) on the DSOD review process for embankment dams, the following statements were made:

- Deformations of 0 to 5 ft are sustainable provided the deformation is not too large a percentage of the total dam height and do not seriously compromise freeboard. Computations will almost always predict some deformation if a dam is subjected to peak ground acceleration exceeding about 0.35 g.

- Deformations of 5 to 10 ft are considered serious. As numbers approach 10 ft DSOD does not believe all related structural behavior is predictable. Freeboard, crest-width, zoning, remaining freeboard, and embankment slope would all be considered before a final decision on whether 5 to 10 ft deformations are acceptable without structural modifications.

- Deformation greater than 10 ft are considered to be in nearly the same class as embankments with post-seismic factors of safety less than unity. DOSD does not consider that there is precedent for predicting the final configuration or embankment integrity for dams sustaining deformations in excess of 10 ft.

In terms of the level of project importance, acceptable risk level, and consequences of failure, the Guidelines for dams are more applicable to the ISFSI than SP-117, which is for residential and commercially developments. Moreover, embankment dams are more sensitive to seismic induced deformation than ISFSI cut slope block movement for the following reasons: (1) embankment dams are extremely sensitive to transverse cracking which oftentimes occur with large deformations and (2) embankment dams can not withstand overtopping if the freeboard are lost with large deformations. As such, using the guidelines for dams as the basis for acceptable seismic induced deformations for the potential slide masses on ISFSI cut slopes would be applicable and conservative. On this basis and considering the implementation of rock slope stabilization measures (SAR Section 4.2.1.1.9), the seismic deformation of 0.4 to 3.1 ft of the potential slide masses on the ISFSI cut slope is considered acceptable by PG&E.

Conclusion

In conclusion, PG&E believes that the slope mitigation design described in this response and in the Diablo Canyon SAR provides acceptable mitigation for any potential slope instability.

NRC Request 5:

Provide an assessment of the long-term static stability of the subsurface materials under the transport route for sections of the transport route underlain by bedrock, considering the transporter loading superimposed on the long-term static loading.

PG&E Response:

In evaluating the stability along the transport route as presented in SAR Section 2.6.5.4, PG&E judged that the more critical sections along the route would be those underlain by surficial deposits where ground motion could be amplified by the softer surficial deposits. Seismic induced displacements for the transport route on rock were expected to be less than those computed for sections underlain by surficial deposits, which would control the design. On this basis, the static slope stability assessment for the transport route on rock presented in SAR Section 2.6.5.4.1 was based on kinematic analyses and qualitative assessment of portions of the transport route underlain by surficial deposits with the understanding that the computed displacements for portions of the transport route on rock would be bounded by those computed for sections constructed over surficial deposits.

As requested by the NRC, PG&E provided an additional static stability assessment for portions of the transport route on rock. Where the transport route is founded on rock begins at approximately Stations 34+50 and continues uphill to the CTF at station 53+50. Along the southern part of this section (station 34+50 to 46+10), the rock beddings dip into the slope and thus makes it kinematically unlikely for slope movements to daylight at the slope face. Along the northern section (station 46+10 to 53+50), the rock beddings show a gentle out-of-slope dip and thus it is kinematically feasible to have out-of-slope movement along possible clay beds that parallel bedding. PG&E developed a cross section with potential rock slide models to evaluate the static stability of the slope for potential movements along shallow dipping clay beds. The evaluation of static stability for the southern and northern sections is presented separately below.

Southern Section - Stations 34+50 to 46+10

The bedrock that underlies the portion of the transport route southeast of station 46+10 (to about 34+50, where the bedrock becomes buried by surficial deposits) is dolomite and sandstone (Tofb). Two potential failure modes for rock masses are considered: (1) displacement on clay beds and (2) displacement on low angle joints. Along this segment of the transport route the rock bedding dips into the slope generally between 20 to 50 degrees. Near the axis of the syncline, which crosses the transport route at station 46+10, the dips are shallower; one measurement is 10 degrees (Refer to calculation GEO.DCPP.01.21, Revision 2, Figure 21-3, submitted by PG&E Letter DIL-01-004, dated December 21, 2001. These dips are illustrated on two typical cross sections, D-D' and K-K' (Calculation GEO.DCPP.01.21, Revision 2, Figures 21-17

and 21-24). As shown in these cross sections, the steeply dipping bedding is not favorable to a rock mass failure along bedding planes, even if some bedding follows the irregular clay beds known elsewhere near the ISFSI site. Hence, failure of bedrock along bedding below the transport route is not possible.

The joint system in the area along the transport route is similar to that described in the slope above the ISFSI. These joints are generally discontinuous and short, and vary in space as well as in stratigraphic position, as discussed in GEO.DCPP.01.21, Revision 2, pages 47 and 49).

Mapping along Reservoir Road's (transport route's) cutslope documents only a few, minor, short joints. A kinematic stability analysis for the transport route cutslope was performed in calculation GEO.DCPP.01.22, Revision 1 (page 15), submitted by PG&E Letter DIL-01-004, dated December 21, 2001. The stereographic plots in calculation GEO.DCPP.01.22, Revision 1, Figure 22-8, shows that the planar sliding hazard as well as toppling for rock wedge failures is very low. Therefore, a rock mass failure below the transport route would not occur along an out-of-slope joint set based on the above information.

Northern Section - Stations 46+10 to 53+50

Kinematic analyses of the northerly trending portion of the transport route cutslope are shown in calculation GEO.DCPP.01.22, Revision 1, Figure 22-7. The north-trending slope shows moderate potential for toppling failure, as a large portion of set 1 plot within this failure envelope. There is low potential of planar sliding failure on joints, and very low potential for wedge sliding failure.

As part of the assessment, PG&E developed cross section M-M', which portrays potential clay beds and bedding orientation for the north trending part of the transport route using existing information. The development of cross section M-M' and the associated potential slide models are presented in a letter from Jeff Bachhuber to William Page, dated March 14, 2003, PG&E Diablo Canyon ISFSI Response to NRC Review Request No. 5 - Transport Route Rock Slope Stability, Rock Mass Models (Attachment 5-1 to this response). The location of this section is shown in plan on Attachment 5-1, Figure TR-1. The section is shown in Attachment 5-1, Figure TR-2.

A suite of potential rock mass models was considered for stability analyses based on evaluation of kinematically-permissible failure modes and geologic conditions. All rock mass slide block models involve failure surfaces controlled by bedding and inferred claybeds and also would involve movement of a substantial amount of rock below the transport route bed.

Attachment 5-1, Figures TR-3 and TR-4, show the slide mass models that were selected for stability analyses. These two models capture the reasonable range in size and uphill-downhill geometry that are feasible based on interpretation of the geology

and inspection of the kinematics for potential slope instability. Both models have basal sliding surfaces on clay beds that were interpreted from boring HLA-9, and are inferred to have a gentle downslope dip of about 9 degrees, similar to the nearest measured bedrock bedding measurement; the apparent dip on M-M' is 8 ½ degrees (Attachment 5-1, Figures TR-1 and TR-2). These developed alternative slide mass models capture the potential range of most-likely rock mass movements based on geologic and topographic conditions. These models are considered conservative and were used for stability analysis of the transport route on rock. The conservatisms built into these models include: (1) clay beds used to define the models based on clay filled fractures from old boring logs, which may or may not be true clay beds, (2) the continuity and lateral extent of the clay beds, and (3) the absence of geological evidence on this slope face to show such rock mass displacements on clay beds.

Static Slope Stability Analysis of Section M-M'

Static slope stability analyses were performed for the two postulated rock mass models shown on Section M-M' and included the mass of the transporter. These two models are assumed to slide on continuous clay beds and they represent the most likely failure scenarios based on geological evidence from surface mapping, trenching, exploratory boring, and conservative assumptions made.

The static slope stability was performed using UTEXAS4. The analysis procedure, assumptions, inputs, and results are documented in GEO.DCPP.01.28, Revision 3, (See Attachment 6-1 to PG&E Response to NRC Request 6). Table 5-1 summaries the factor of safety for static slope stability.

Table 5-1

Summary of Static Slope Stability Analysis for
Northern Section of Transport Route on Rock (Section M-M')

Rock Slide Model	Static FOS
Model 1	2.07
Model 2	2.14

Conclusion

The Diablo Canyon ISFSI transport route is founded on rock between station 34+50 and station 53+50.

The northern section of the transport route on rock, between stations 46+10 and 53+50, has bedding that dips gently out of the slope. Potential rock mass slide models on clay bed or rock discontinuities are kinematically feasible. Potential slide mass models were developed based on conservative interpretations of geological information from surfacing mapping, trenching, and exploratory boring as shown on Section M-M'. Static

slope stability analysis for the two rock slide models indicates that the minimum static factor of safety is 2.07, which is higher than the 1.5 that is typically required for static slope stability. This demonstrates the slope has ample safety factors against static slope failure.

The southern section of this alignment, between stations 34+50 and 46+10, has rock bedding that dips into the hillslope making slope failure on bedding not possible. Kinematic analysis of joints along the transport route also shows that failure of the bedrock below the transport route is not possible.

Based on the above evaluation and documentation provided in Attachments 5-1 and 6-1, PG&E concludes that the portions of transport route on rock have adequate static factor of safety against rock mass sliding on clay beds.

NRC Request No. 6:

Provide the technical bases for the engineering properties of the quaternary deposits under the transport route, which were used for stability evaluation of the sections of the transporter route underlain by Quaternary deposits.

PG&E Response:

The NRC has identified a concern that the material properties used for the calculation (shear strength and density) are provided, but the assignment of the properties to the various soil layers in the cross sections is not sufficiently explained.

The material properties used for the stability evaluation of the transport route are listed in Table 1 of PG&E Calculation GEO.DCPP.01.28, Revision 3 (Attachment 6-1). In this Table, the geological units for the material properties are identified. The same units are used to show the corresponding portions on the cross sections (Attachment 6-1, Figures 2 through 9). In PG&E Calculation GEO.DCPP.01.28, Revision 0, submitted in PG&E Letter DIL-01-004, dated December 21, 2001, figures showing the cross sections were complicated by showing the location of the slices used in the slope stability analyses and thus the assignment of geological units on these figures are not clear. Changes on the cross sections have been made to clarify this problem. Refer to Attachment 6-1, Figures 2 through 9.

The NRC also indicated that the technical basis for the property values was not provided in the calculation. In the INPUT Section of GEO.DCPP.01.28, Revision 3, the technical basis for the property values was provided as follows:

> *A summary of properties used for the stability and yield acceleration analyses for sections L-L', E-E', and D-D' is shown on Table 1. Soil properties for the Quaternary colluvial deposits (Qc, Qhf and Qpf), Pleistocene marine terrace deposit (Qptm), and Obispo Formation (Tof_b)*

were based on data reported in Harding Lawson, and Associates (1973), shown in Attachment B. The bi-linear undrained strength envelope for the clay beds in the Obispo Formation is described in GEO.DCPP.01.31, Rev 1.

Strength parameters for the deeper Pleistocene colluvial fan (Qpf) deposits were developed from the Unconsolidated-Undrained (UU) and Consolidated-Undrained (CU) triaxial compression data reported by Harding Lawson, and Associates (1973), shown in Attachment B and summarized in Figure 1. An undrained shear strength of 3000 psf was selected for the slope stability analysis. This value was selected based on the lower bound of the UU test data (below a depth of 10 feet) and the average of the three CU tests shown in Figure 1. The artificial fill (af) is described as a compacted fill derived from the native material underlying it, and was conservatively assigned the same properties as the Pleistocene colluvium (Qpf), as indicated in Attachment C. The artificial fill, however does not intersect any of the potential sliding surfaces analyzed and does not affect their stability.

Strength parameters for the shallow Quaternary colluvium (Qc) and Holocene colluvial fan (Qhf) deposits were based on test results from samples obtained from depths within 10 feet of the ground surface (Figure 1). A value of 1500 psf representing the lower-bound of the data shown on Figure 1 was selected for the analysis.

Conclusion

In response to the NRC concerns, PG&E has included revised calculation GEO.DCPP.01.28, Revision 3 to provide the technical basis for the material properties used in transport route stability analysis. The revised calculation also provides improved cross section presentations for which the geological units listed in Table 1 of the calculation can be more easily identified with the corresponding portions on the cross sections. Calculation GEO.DCPP.01.28, Revision 3 supercedes previous revisions and constitutes the material properties basis for the ISFSI transport route stability analysis.

NRC Request No. 7:

Provide an assessment of the seismic stability of the transport subsurface materials considering a potential simultaneous occurrence of the design-basis earthquake and the transport loading.

PG&E Response

PG&E has revised the stability analyses for the transport route incorporating the inertial mass of the transporter, a new section of the transport route with two slide mass models

and revised seismic coefficient time histories for the three slide masses in sections of the transport route underlain by surficial deposits. The results of the revised analyses support PG&E's previous results, that the transport route slope remains stable during and after a design basis earthquake.

In response to an NRC clarification request, PG&E has re-analyzed the three cross sections (D-D', E-E' and L-L') along the transport route with seismic coefficient time histories calculated using the boundary force approach as requested by NRC. The NRC also questioned the omission of a cross section in the portion of the transport route underlain by rock. Thus, a fourth section, M-M', to represent the northern section of the transport route was developed and analyzed. Additionally, the NRC suggested that the inertial loading of the transporter should be included in the stability analyses. In Table 7-1 under the title "Current Submittal", the displacements calculated for the 4 sections using the NRC recommended method in calculating the seismic coefficient time histories, with the inertial mass of the transporter included in the models are presented. Also shown in Table 7-1, under the header of "Previous Submittal", are the results from our previous submittal in which the seismic coefficient time histories were calculated using average nodal accelerations and the full transporter weight was modeled as two point loads on the section without distributing the transport load along its length.

Table 7-1

Comparison of Seismic Induced Displacements

Transporter Route Analytical Section	Ground Motion	Previous Submittal			Current Submittal		
		Yield Acc. without inertial force but with full transporter load modeled as point loads[a] (g)	Average Nodal Acceleration Approach[a]		Yield Acc. with inertial force modeled as distributed masses along transporter length[b] (g)	Summation of Boundary Force Approach[b]	
			Peak Seismic Coefficient (g)	Seismic Induced Displacement (ft)		Peak Seismic Coefficient (g)	Seismic Induced Displacement (ft)
L-L'	Set 5	0.46	1.15	1.3	0.48	1.01	0.8
	Set 6		0.97	0.9		0.88	0.5
E-E'	Set 5	0.57	1.07	0.5	0.50	0.94	0.6
	Set 6		0.91	0.32		0.81	0.3
D-D'	Set 5	0.45	1.07	1.1	0.63	0.94	0.2
	Set 6		0.91	0.85		0.81	0.1
M-M' Model 1	Set 5	--	--	--	0.33	0.93	1.4
	Set 6		--	--		0.88	1.5
M-M' Model 2	Set 5	--	--	--	0.44	0.95	0.5
	Set 6		--	--		0.90	0.8

(a) Based on GEO.DCPP.01.30, Revision 0, Table 2 (submitted in PG&E Letter DIL-01-004, dated December 21, 2001
(b) Based on GEO.DCPP.01.30, Revision 3, Table 2, Attachment 7-1

Based on Table 7-1, it can be seen that using the boundary force approach as recommended by NRC, the computed seismic coefficients (documented in calculation GEO.DCPP.01.29, Revision 3) (Attachment 7-2 to this submittal) are lower than those computed with time histories developed by averaging nodal point accelerations at selected nodal points (documented in calculation GEO.DCPP.01.29, Revision 0, previously submitted in PG&E Letter DIL-01-004, dated December 21, 2001). With the transporter modeled as distributed masses along its length to incorporate inertial load effects (in the current submittal), the resulting yield accelerations are not significantly different from those with the full transporter load modeled as point forces on the analytical section as PG&E did in its previous submittal. Only Section D-D' showed a more pronounced difference and the new calculation showed a higher yield acceleration than before for this section. The comparison shows that for the three sections

submitted previously (Sections L-L', D-D', and E-E'), the resulting displacements are lower than the previous submittal following the NRC recommended procedures as documented in our current submittal and calculation GEO.DCPP.01.30, Revision 3.

The computed displacement for Section M-M was the largest displacement of all sections and the displacement is estimated to be on the order of 1.5 ft. The transport route slope's estimated displacement magnitude is smaller than that computed for the ISFSI pads' slope (Section I-I' in calculation GEO.DCPP.01.26, Revision 4 (Attachment 4-2)). The estimated transporter route slope displacement is not indicative of an unstable slope.

The PG&E analysis of the transporter sliding on portions of the transport route underlain by surficial deposits (PG&E Calculation OQE-14, Revision 0, submitted in PG&E Letter DIL-02-009, dated October 15, 2002) was performed utilizing the ILP ground motion time histories amplified by a factor of two. This analysis would bound the impact of a 1.5 ft displacement of section M-M' as movement of this mass would reduce the peak ground acceleration at the transport route surface and cause a shift of the energy over a broader range of frequencies. The two times amplification of the ILP ground motions would produce a spectrum that is expected to envelope the effect of a shift of the surface response to a broader range of frequencies. On the above basis, it was concluded that the computed displacements are acceptable.

As stated above, PG&E developed a new cross section (Section M-M') along the northern end of the transport route. The bases for the development of this new cross section, including geological features and the two postulated slide mass models, are provided in Attachment 5-1 of the PG&E response to NRC Request 5. Static slope stability analysis and computation of yield accelerations for this new section are documented in GEO.DCPP.01.28, Revision 3. The two-dimensional finite element dynamic response analyses and the computation of seismic coefficient time histories using the boundary force approach for this section M-M' are documented in GEO.DCPP.01.29, Revision 3, Attachment 7-2. The seismic induced displacement for section M-M' is documented in GEO.DCPP.01.30, Revision 3. Table 7-1, presented above, summarizes the results of the analyses for two slide mass models of section M-M'.

The NRC requested that the documentation of the technical basis for the subsurface material properties used for the transport route slope stability analyses be provided. In response to this request, PG&E has provided the technical bases for the material properties used in the stability evaluation as Attachment 6-1 to PG&E Response to Request 6.

The NRC suggested that the inertial loading of the transporter should be included in the stability calculation. In calculation GEO.DCPP.01.28, Revision 0, previously submitted by PG&E Letter DIL-01-004, dated December 21, 2001, PG&E conservatively modeled the entire loading of a transporter as two point loads on the analytical sections instead

of distributing the gravitational load along the length of the transporter. This model is conservative because the entire weight of the transporter is placed on a one-foot-wide analytical section, and thus, the gravitational load was overestimated by a factor equivalent to its length. In responding to NRC suggestion to include inertial loading of the transporter, the mass of the transporter was distributed along the transporter length for each transport route section in the two-dimensional slope stability analyses. The effect of the inertial loading of the transporter is modeled in the stability analyses as a soil mass that has no strength contribution to the stability analyses. In this model, an assumption was made that the full distributed transporter inertial load for the section would be transferred to the potential sliding mass (i.e., the transporter does not slide on the road). This is a conservative assumption because once the transporter starts to slide, the amount of inertial load that can be transferred to the potential slide mass is limited by the frictional strength between transporter tracks and the road surface.

Based on PG&E's use of selected nodal accelerations in the slide mass to develop a representative seismic coefficient time history for the slide mass, the NRC questioned whether consideration of phase differences between the nodal time histories may lower the seismic coefficient time histories developed by PG&E. In response to this concern, PG&E re-calculated the seismic coefficient time histories for sections D-D', E-E', and L-L' and for section M-M', developed new seismic coefficient time histories, using the NRC suggested boundary force approach as documented in GEO.DCPP.01.29, Revision 3. The results are shown in Table 7-1 above. Comparison of the peak seismic coefficients computed using selected nodal time histories to the peak seismic coefficients based on boundary forces time histories, found that the peak seismic coefficients based on boundary forces were lower by an average of about 10 percent. Thus, the original seismic coefficient time histories developed by PG&E, using selected nodal time histories, resulted in a more conservative estimate of seismic induced displacements.

The differences between the two approaches for developing seismic coefficient time histories are less for stiffer materials as shown in Table 4-1 in the PG&E Response to NRC Request 4. The phase differences between the time histories at the different nodal points would be more pronounced in the softer colluvial material and the use of the boundary force approach to develop seismic coefficient time histories would appropriately account for the phase differences in the entire sliding body. On the other hand, it appears that using time histories at a few nodal points to calculate the average acceleration time history for the slide mass lessens any phase cancellation effect and assuming minor phase additive effects, results in a higher seismic coefficient time history. In addition, comparison of the seismic coefficient time history, created by using select nodal acceleration time histories, to the respective input ground motion time history, shows the latter to be generally higher.

While PG&E concurs with the NRC that using the boundary force approach would appropriately represent the response of the potential sliding masses, PG&E believes that selecting a few nodal accelerations and using their average to represent the

response of a slide mass would generally be very close to the response determined using the boundary force approach if the material is very stiff. For softer materials, the averaging nodal acceleration approach would generally overestimate the slide mass response because the full affect of the phase cancellation effect cannot be accounted for as in the boundary force approach.

Conclusion

PG&E has revised calculation packages GEO.DCPP.01.28 thru GEO.DCPP.01.30 for the transporter route stability evaluation to address all of the NRC concerns. The estimated maximum slope displacement along the transport route is very similar to what was previously submitted and designed for. These calculations packages supercede the previously submitted revisions and constitute the revised ISFSI transporter route stability evaluation.

List of Attachments

Attachment No.	TITLE
1-1	Hoek, E., February 10, 2003, [Review Letter] Review of Pacific Gas & Electric Company Diablo Canyon Nuclear Power Plant ISFSI Project Rock Mass Strength Analysis
1-2	RocLab Printouts
2-1	Determination of Earthquake-Induced Displacements of Potential Sliding Mass Beneath DCPP ISFSI Site Calculation GEO.DCPP.03.01, Revision 0
2-2	Evaluation of Potential Failure of Foundation Beneath DCPP ISFSI Pads PG&E, March 19, 2003, Revision 0
3-1	Letter report from Geomatrix to PG&E entitled "Request for Clarification 3. ISFSI Slope Stability Study. Diablo Canyon Power Plant ", dated March 6, 2003.
3-2	PG&E's Seismic Hazards Review Board letter to PG&E dated September 28, 2001.
3-3	Development of Strength Envelopes for Clay Beds at DCPP ISFSI Calculation GEO.DCPP.01.31, Revision 1 PG&E Calculation 52.27.100.741, Revision 0
4-1	Determination of Seismic Coefficient Time Histories for Potential Sliding Masses Above the Cutslope Behind the ISFSI Pads Calculation GEO.DCPP.01.25, Revision 4. (w/CD)
4-2	Determination of Earthquake-Induced Displacements of Potential Sliding Masses on DCPP ISFSI Slope Calculation GEO.DCPP.01.26, Revision 4. (w/CD)
5-1	Letter from Jeff Bachhuber to William Page, dated March 14, 2003, re: PG&E Diablo Canyon ISFSI Response to NRC Review Request No. 5 - Transport Route Rock Slope Stability, Rock Mass Models
6-1	Stability and Yield Acceleration Analysis of Potential Sliding Masses Along DCPP ISFSI Transport Route Calculation GEO.DCPP.01.28, Revision 3. (w/CD)

Attachment No.	TITLE
7-1	Determination of Earthquake-Induced Displacements of Potential Sliding Masses along DCPP ISFSI Transport Route Calculation GEO.DCPP.01.30, Revision 3. (w/CD)
7-2	Determination of Seismic Coefficient Time Histories for Potential Sliding Masses on DCPP ISFSI Transport Route Calculation GEO.DCPP.01.29, Revision 3. (w/CD)

ATTACHMENT

1-1

Evert Hoek

EVERT HOEK CONSULTING ENGINEER INC.

3034 EDGEMONT BOULEVARD
P.O. BOX 75516
NORTH VANCOUVER, B. C.
CANADA, V7R 4X1

TEL: 1 604 988 3064
FAX: 1 604 980 3512
EMAIL: ehoek@attglobal.net

10 February 2003

Mr Jeff Bachhuber
Principal Engineering Geologist
William Lettis and Associates
1777 Botelho Drive, Suite 262
Wallnut Creek, California 94596

Dear Mr Bachhuber:

Re: Review of Pacific Gas & Electric Company Diablo Canyon Nuclear Power Plant ISFSI Project Rock Mass Strength Analysis.

In response to your email dated 7 February 2003 and our follow-up telephone conversation this morning, I am writing to comment on the notes that you sent me.

I understand that the purpose of undertaking an evaluation of the rock mass properties of the proposed cut slope is to provide a background strength on which various structural features can be superimposed. In particular, for deep-seated failures, the features that control slope stability appear to be the shallow dipping clay seams associated with bedding or with contacts between different rock units. Typically, in these situations, the background strength of the rock mass is of secondary importance and the emphasis has to be placed on structurally controlled failures as you have done.

The selection of the Hoek-Brown m_i values given in your notes appears to be very reasonable. For relatively simple rock masses such as dolomites and sandstones, the values of m_i tend not to vary a great deal from those quoted in the various Hoek-Brown papers. Consequently, it is unusual to check these values by means of laboratory tests. In any case, m_i is the least important parameter in the determination of rock mass properties and even large variations in its value do not normally have a significant impact on the derived strength properties. I will comment further on a means of checking this later in this letter.

The calculation of the Hoek-Brown parameters has not changed for a long time and there is no difference between the spreadsheets that you have used and the latest RocLab program. What is different is the determination of equivalent Mohr-Coulomb parameters and the introduction of the blast damage factor D.

There is no correct way to calculate the exact equivalent Mohr Coulomb parameters corresponding to a given set of Hoek-Brown parameters. Over the years I have struggled with different ways of doing this and these are reflected in the various papers that I have published. In the RocLab program we set out to resolve this problem once and for all by carrying out a very large number of analyses of slopes and tunnels, using both the Hoek-Brown criterion and the Mohr Coulomb criterion. The methodology used for slopes was to find sets of parameters in the two criteria which gave the same factor of safety and failure surface geometry for any slope

configuration. We were able to establish relationships between these sets of parameters for both slopes and tunnels and these are described in the paper that comes with the program RocLab.

Hence, if you have a 200 foot high slope and you have an estimate of the Hoek-Brown input parameters, you can enter these into the RocLab program to find the equivalent Mohr Coulomb parameters. If you now do a slope stability analysis, using a program such as SLIDE that can accommodate both failure criteria, you will find that the failure surface geometries and the factors of safety are very close.

The estimate of $\phi = 50°$ provided by Skip Hendron can be approximated by putting in a slope height of about 60 m in for the RockLab analysis of dolomite. This may be a reasonable slope height for your problem but you will note that you also have a cohesion of 0.6 MPa. Hence Hendron's estimate is good, in terms of slope, but very conservative in terms of cohesion.

In terms of the blast damage factor and related stress relief, I fully agree that this will only penetrate for a relatively small distance in your slopes, which have been created by means of relatively gentle civil engineering blasting. Even if this blasting is badly done it does not come close to large open pit blasting where it is not uncommon to blast a million tons in one blast sequence and where the blast damage can extend 100 m or more behind the slope crest. Hence, for your problem, I consider that it is entirely appropriate to set D = 0 for deep-seated failures.

I hope that these comments are of some use to you.

With best wishes,

Dr Evert Hoek.

Reviewed documents:

1. Review request letter, J. Bachhuber, Feb. 7, 2003
2. ISFSI Calculation Package 01.19, Rev. 2, June 14, 2002

ATTACHMENT

1-2

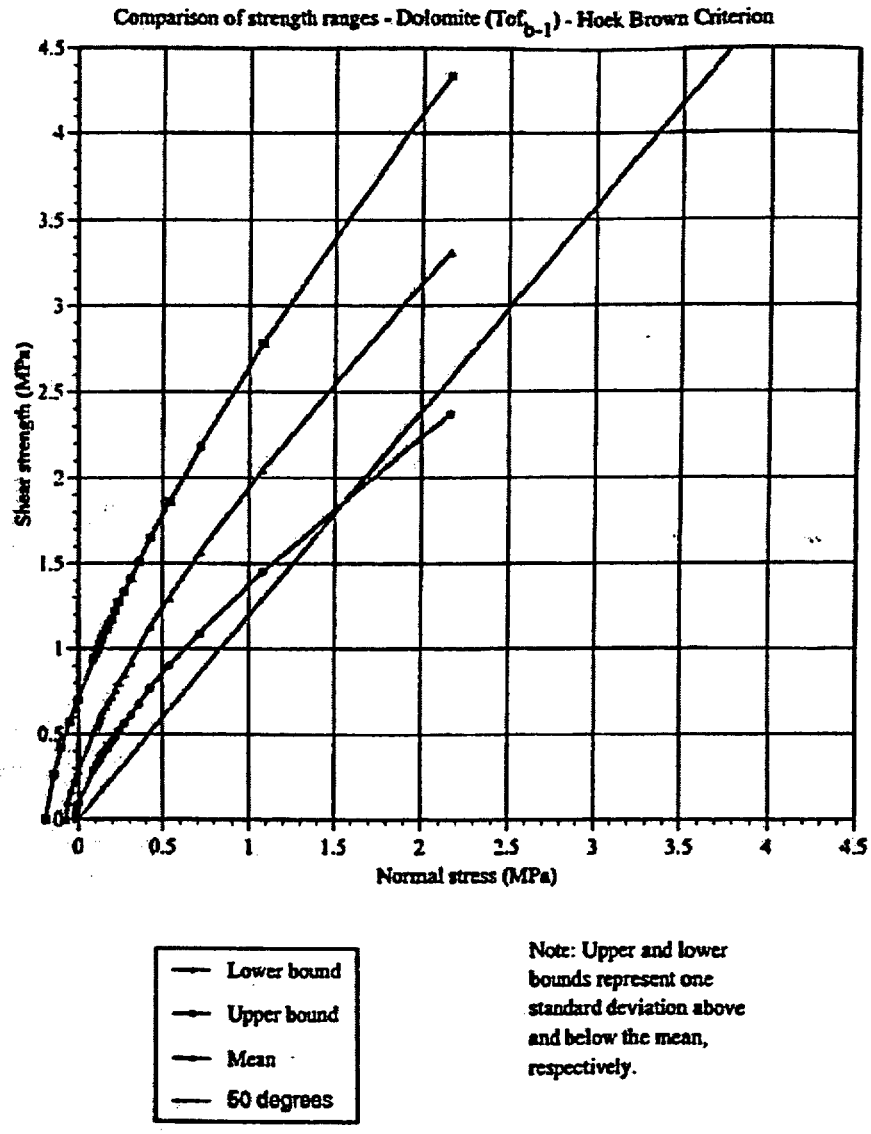

Note: Upper and lower bounds represent one standard deviation above and below the mean, respectively.

Figure 19-3. Curve D-1

DCPPre-analyses, Dolomite Low, D0

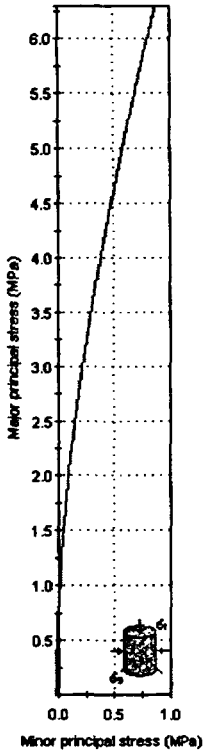

Hoek-Brown Classification
Intact uniaxial compressive strength = 18 MPa
GSI = 46 mi = 13 Disturbance factor = 0

Hoek-Brown Criterion
mb = 1.890 s = 0.0025 a = 0.508

Mohr-Coulomb Fit
cohesion = 0.315 MPa friction angle = 45.15 deg

Rock Mass Parameters
tensile strength = -0.024 MPa
uniaxial compressive strength = 0.856 MPa
global strength = 3.265 MPa
modulus of deformation = 3370.05 MPa

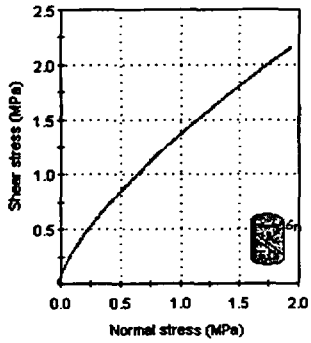

DCPPre-analyses, Dolomite Mean, D8

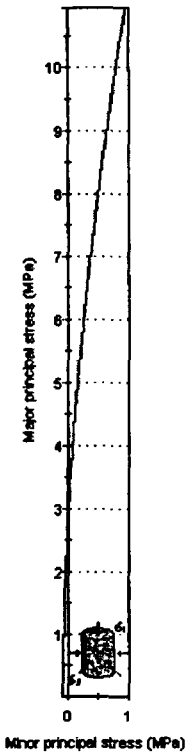

Hoek-Brown Classification
Intact uniaxial compressive strength = 32 MPa
GSI = 56 mi = 15 Disturbance factor = 0

Hoek-Brown Criterion
mb = 3.116 s = 0.0075 a = 0.504

Mohr-Coulomb Fit
cohesion = 0.545 MPa friction angle = 52.87 deg

Rock Mass Parameters
tensile strength = -0.077 MPa
uniaxial compressive strength = 2.726 MPa
global strength = 7.692 MPa
modulus of deformation = 7990.52 MPa

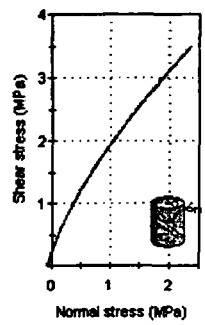

BCPPre-analyses, Dolomite High, D0

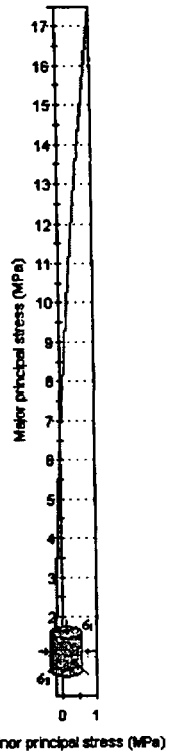

Hoek-Brown Classification
Intact uniaxial compressive strength = 47 MPa
GSI = 65 mi = 17 Disturbance factor = 0

Hoek-Brown Criterion
mb = 4.871 s = 0.0205 a = 0.502

Mohr-Coulomb Fit
cohesion = 0.944 MPa friction angle = 57.85 deg

Rock Mass Parameters
tensile strength = -0.198 MPa
uniaxial compressive strength = 6.673 MPa
global strength = 14.561 MPa
modulus of deformation = 16257.32 MPa

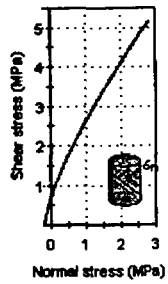

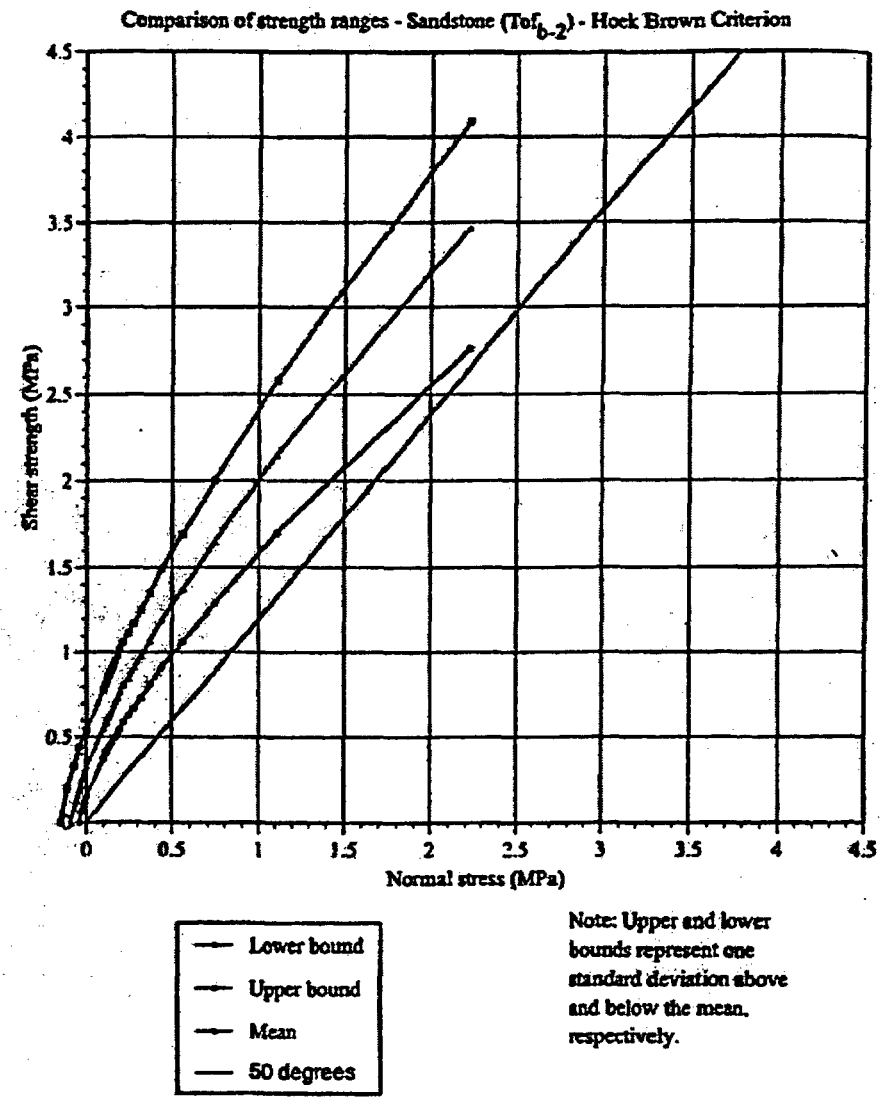

Figure 19-7. Curve SS-1

BCPPre-analyses, Sandstone Low, D0

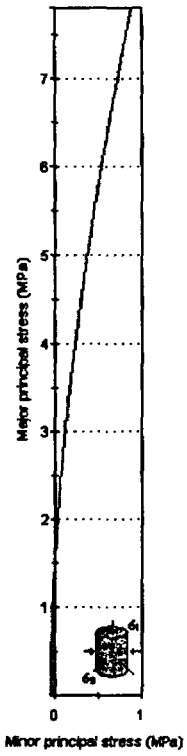

Hoek-Brown Classification
Intact uniaxial compressive strength = 12 MPa
GSI = 62 mi = 17 Disturbance factor = 0

Hoek-Brown Criterion
mb = 4.376 s = 0.0147 a = 0.502

Mohr-Coulomb Fit
cohesion = 0.391 MPa friction angle = 48.71 deg

Rock Mass Parameters
tensile strength = -0.040 MPa
uniaxial compressive strength = 1.438 MPa
global strength = 3.479 MPa
modulus of deformation = 6911.79 MPa

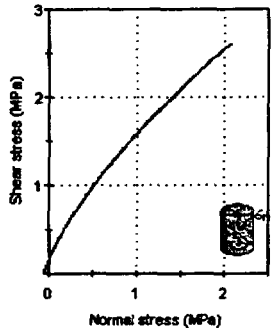

DCPPre-analyses, Sandstone Mean, 08

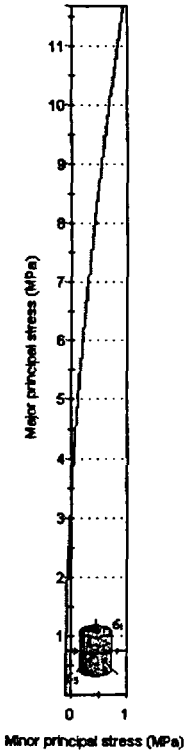

Hoek-Brown Classification
intact uniaxial compressive strength = 22 MPa
GSI = 65 mi = 18 Disturbance factor = 0

Hoek-Brown Criterion
mb = 5.157 s = 0.0205 a = 0.502

Mohr-Coulomb Fit
cohesion = 0.584 MPa friction angle = 53.90 deg

Rock Mass Parameters
tensile strength = -0.087 MPa
uniaxial compressive strength = 3.123 MPa
global strength = 6.993 MPa
modulus of deformation = 11122.73 MPa

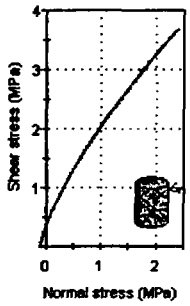

BCPPre-analyses, Sandstone High, D0

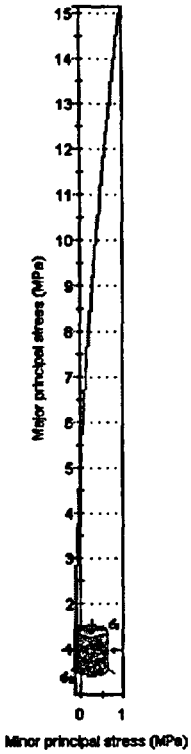

Hoek-Brown Classification
Intact uniaxial compressive strength = 30 MPa
GSI = 68 mi = 19 Disturbance factor = 0

Hoek-Brown Criterion
mb = 6.059 s = 0.0266 a = 0.502

***Mohr-Coulomb* Fit**
cohesion = 0.777 MPa friction angle = 55.76 deg

Rock Mass Parameters
tensile strength = -0.141 MPa
uniaxial compressive strength = 5.042 MPa
global strength = 10.450 MPa
modulus of deformation = 15436.92 MPa

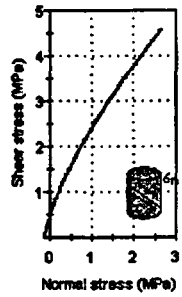

ATTACHMENT

2-1

PACIFIC GAS AND ELECTRIC COMPANY
GEOSCIENCES DEPARTMENT
CALCULATION DOCUMENT

Calc Number	GEO.DCPP.03.01
Revision:	0
Date:	318/03
Calc Pages:	11
Verification Method:	A

1.0 TITLE

Determination of earthquake-induced displacements of potential sliding mass beneath DCPP ISFSI Site

2.0 SIGNATURES

PREPARED BY: Robert K White DATE: 3/18/03

Robert White — Hydro Gen Department
Printed Name — Organization

VERIFIED BY: Robert K Green DATE: 19 March 2003

Robert Green — URS Corporation
Printed Name — Organization

APPROVED BY: Lloyd Cluff DATE: 3/21/03

Lloyd Cluff — Geosciences Department
Printed Name — Organization

REGISTERED GEOLOGIST
LLOYD S. CLUFF
No. EG567
CERTIFIED ENGINEERING GEOLOGIST
STATE OF CALIFORNIA

Exp. 9/30/03

3.0 RECORD OF REVISIONS

Rev. No.	Reason for Revision	Revision Date
0	Initial Issue	3/18/03

4.0 PURPOSE

As required by AR A0574914, this calculation package estimates the stability and earthquake-induced permanent displacement of a potential sliding mass beneath the proposed DCPP ISFSI site (hereinafter, "the site") using field and laboratory data, postulated design ground motions, and a displacement equation developed by Newmark, 1965.

5.0 ASSUMPTIONS

1. Clay beds beneath the potential sliding mass are continuous along the entire base of the mass. This is a very conservative assumption, as geologic evidence clearly indicates otherwise (e.g. Safety Analysis Report (SAR) Figs. 2.6-9 and 2.6-10 (PG&E, 2001)).
2. ISFSI pads are fully coupled to the underlying rock foundation and thus the horizontal inertial force imposed by the pads fully contributes to the sliding potential of the underlying rock mass. This is a conservative assumption, as SAR section 8.2.1.2.3.2, pp. 8.2-18 through 8.2-21 indicates some decoupling potential due to one or more ground motions.
3. The coefficient of lateral earth pressure at rest, k_o, for faults bounding the potential sliding mass is assumed equal to 1.0. This is a reasonable assumption, as rock mass overconsolidation ratios vary from 2 to 20 for rock at depths of 5 to 50 feet (due to significant removal of overburden as shown on page 4 and Table 4 of calculation GEO.DCPP.01.31), and for an OCR range of 2 to 10, k_o values vary from 0.55 to 1.65, irrespective of soil type (as shown in Clough and Duncan, 1991).
4. The Newmark equation used to estimate displacement of the potential sliding mass (input 10) is a conservative estimate, as the equation was developed to bound the displacements calculated from a number of large-magnitude earthquakes, especially for those values of (maximum resistance coefficient / maximum earthquake acceleration) > 0.5, as described in Newmark, 1965.

6.0 INPUTS

1. The dimensions of the potential sliding mass (50 feet deep by 490 feet wide by 510 feet long) are determined from Geosciences calculation package GEO.DCPP.01.21, figure 21-22, and SAR figure 4.1-1 (PG&E, 2001), as described in step 1 of the Body of the Calculation.
2. Rock types within the proposed sliding mass consist of sandstone and non-jointed (altered) rock, from SAR figures 2.6-9 and 2.6-10 (PG&E, 2001).
3. The friction angle for sandstone rock and altered rock of 50 degrees is obtained from Geosciences calculation package GEO.DCPP.01.19 and GEO.DCPP.01.26, respectively.
4. The friction angle for faults assumed bounding the lateral boundaries of the potential sliding mass of 16 degrees is the lower bound value obtained from Geosciences calculation package GEO.DCPP.01.20, figure 20-7.
5. The undrained shear strength parameters of either 29 degrees and 0 psf cohesion or 15 degrees and 800 psf cohesion (whichever is lower for a given normal stress) for clay beds are from Geosciences calculation package GEO.DCPP.01.31.
6. The rock unit weight of 140 pcf for the rock mass is obtained from Witter, 11/5/01, Data Report I.
7. The weight of casks and each pad of 15,500 kips is obtained from page 7 of Geosciences calculation package GEO.DCPP.01.04.
8. The pseudostatic acceleration coefficient factor of 0.50 used to assess stability of the potential sliding mass is obtained from Kramer, 1996, pg. 436.
9. The 84th percentile site specific peak ground acceleration of 0.83g used with the pseudostatic acceleration coefficient factor to obtain a pseudostatic acceleration coefficient is obtained from PG&E, 1988, figure 4-36.
10. The equation used to estimate displacement of the potential sliding mass is obtained from Newmark, 1965, pg. 157.
11. The ratio of peak velocity to peak acceleration of 36 in/sec/g used in the part to estimate potential displacement is obtained from Newmark and Hall, 1978.

7.0 METHODOLOGY AND EQUATION SUMMARY

1. Determine dimensions and weight of the potential sliding mass encompassing all fully-loaded ISFSI pads.
2. Determine the average normal stress along the base of the potential sliding mass.

3. Calculate the average undrained shear strength and the resulting sliding resistance along the base of the potential sliding mass using clay bed strength parameters.
4. Calculate the sliding resistance within the sandstone and altered rock along the rear of the potential sliding mass using rock mass strength parameters.
5. Calculate the sliding resistance within the faults assumed bounding the sides of the potential sliding mass using fault strength parameters.
6. Calculate the equivalent friction factor (also the yield acceleration) of the potential sliding mass by dividing the sum of the sliding resistance forces by the weight of the mass.
7. Calculate the pseudostatic acceleration coefficient to be imposed on the potential sliding mass by multiplying the coefficient factor obtained from input 8 by the peak ground acceleration obtained from input 9.
8. Calculate the safety factor against sliding of the potential sliding mass by dividing the yield acceleration by the pseudostatic acceleration coefficient.
9. Calculate displacement of the potential sliding mass using the equation from input 10 and the various parameters defined above.

8.0 SOFTWARE

No software is used to perform calculations in this calculation package.

9.0 BODY OF CALCULATION

1. The dimensions and weight of the potential sliding mass encompassing all fully-loaded ISFSI pads are determined as follows. Clay beds identified approximately 50 feet beneath the site, as shown on Figure 21-22 of GEO.DCPP.01.21 (Figure 1, attached), define the depth of the mass. The width (490 feet) and length (510 feet) of the mass are defined by the length of the pads and the proximity of the canyon wall, respectively, as shown on SAR Figure 4.1-1 (Figure 2, attached). The unit weight of the rock of 140 pcf, from input 6, is used to determine the mass weight:

   $W = 50\text{ ft} \cdot 510\text{ ft} \cdot 490\text{ ft} \cdot 0.140\text{ kcf} = 1{,}749{,}300\text{ k}$

   The weight of the seven pads from input 7 is:

$W = 15{,}500\ k \cdot 7 = 108{,}500\ k$

2. The average normal stress along the base of the potential sliding mass is determined as follows:

$\sigma_{v(avg)} = (1{,}749{,}300\ k + 108{,}500\ k) / (510\ ft \cdot 490\ ft) = 7.434\ ksf$

3. The average undrained shear strength and the resulting sliding resistance along the base of the potential sliding mass, using the clay bed shear undrained strength parameters from input 5 are determined as follows:

$\tau_{avg} = \sigma_v \cdot \tan\varphi_u + c_u = 7.434 \cdot \tan 15 + 0.8\ ksf = 2.792\ ksf$

and

$R_b = \tau_{avg} \cdot \text{base area} = 2.792\ ksf \cdot 510\ ft \cdot 490\ ft = 697,700\ k$

4. The sliding resistance within the sandstone and altered rock along the rear of the potential sliding mass is calculated using rock mass strength parameters. The failure is modeled as a stepwise failure at about the same orientation as slide masses modeled on the hillside above the ISFSI site, that is at about 2 vertical to 1 horizontal (e.g. SAR figure 2.6-43), and the shear resistance along the horizontal planes of the failure surface is a function of the normal (vertical) stress, as follows:

$R_r = \Sigma\, \sigma_v \cdot \tan\varphi_{rock} \cdot L_h \cdot W,$

where $\Sigma\, \sigma_v = 0.5 \cdot 50\ ft \cdot 0.140\ kcf = 3.5\ ksf$
$\tan\varphi_{rock} = \tan 50 = 1.19$
$L_h = 0.5 \cdot 50\ ft\ (\text{depth of mass}) = 25\ ft$
$W = 490\ ft$

$R_r = 3.5\ ksf \cdot 1.19 \cdot 25\ ft \cdot 490\ ft = 51{,}000\ k$

5. The sliding resistance within the faults assumed bounding the sides of the potential sliding mass is calculated using fault strength parameters. The shear resistance is a function of the normal (horizontal) stress on the fault planes, as follows:

$R_s = 2 \Sigma \sigma_h \cdot \tan\varphi_{fault} \cdot H \cdot L$

where $2 \Sigma \sigma_h = 2 \Sigma k_o 0.5 \gamma h = 2 \cdot 1.0 \cdot 0.5 \cdot 0.140$ kcf $\cdot$ 50 ft = 7.0 ksf

k_o = coefficient of lateral earth pressure = 1.0 (Assumption 3)

$\tan\varphi_{fault} = \tan 16 = 0.29$

H = 50 ft

L = 510 ft

R_s = 7.0 ksf $\cdot$ 0.29 $\cdot$ 50 ft $\cdot$ 510 ft = 51,800 k

6. The equivalent friction factor (also the yield acceleration) of the potential sliding mass is calculated by dividing the sum of the sliding resistance forces by the weight of the mass, as follows:

$R = R_b + R_r + R_s$ = 697,700 + 51,000 + 51,800 = 800,500 k

The equivalent friction factor = R / W = 800,500 / 1,857,800 = 0.43

7. The pseudostatic acceleration coefficient to be imposed on the potential sliding mass is calculated by multiplying the coefficient factor obtained from input 8 by the peak ground acceleration obtained from input 9, as follows:

$k_h = 0.5 \cdot 0.83g = 0.42g$

8. The safety factor against sliding of the potential sliding mass is calculated by dividing the yield acceleration by the pseudostatic acceleration coefficient, as follows:

SF = 0.43 / 0.42 = 1.02.

9. Displacement of the potential sliding mass is calculated using the equation from input 10 and the various parameters defined above, as follows:

$u = [v^2 / 2gN] \cdot [1 - N / A] \cdot A / N$

where $v = 0.83g \cdot 36$ inc/sec/g (from input 11) = 30 in/sec

$g = 386$ in/sec^2

$N = 0.43g$ from step 6, above

$A = 0.83g$

$u = [30^2 / 2 \cdot 386 \cdot 0.43] \cdot [1 - 0.43 / 0.83] \cdot [0.83 / 0.43]$

$= 2.71 \cdot 0.48 \cdot 1.93 = 2.5$ inches

10.0 RESULTS AND CONCLUSIONS

Results of stability analyses of the potential sliding mass beneath the ISFSI site indicate a pseudostatic safety factor of 1.02. Results of the simple Newmark equation displacement analysis indicate displacement of the potential sliding mass due to a 0.83g pga earthquake of 2.5 inches.

According to Kramer, 1996, page 436, earth structures with safety factors greater than 1.0 using $k_h = 0.5\ a_{max}$ will not develop "dangerously large" deformations. Therefore, it is concluded that the potential sliding mass modeled will not fail. The calculated displacement of 2.5 inches is similar to the range of displacements calculated for pad sliding of between 0.4 and 1.2 inches as presented in SAR pages 8.2-18 through 8.2-21, thus it is concluded that the calculated displacement of the sliding mass is acceptable in light of the acceptability of the range of pad sliding values calculated elsewhere.

11.0 LIMITATIONS

This calculation is intended only to provide a conservative estimate of the displacement of a potential sliding mass beneath the ISFSI pads. The assumptions and methods used herein differ from those used in other displacement calculations for the hillside above the ISFSI site, and are therefore not applicable for use in those calculations.

12.0 IMPACT EVALUATION

The results of this calculation are not used in any other calculation and do not impact the results and conclusions previously determined.

13.0 REFERENCES

1. Kramer, S. L., 1996, Geotechnical Earthquake Engineering, Prentice-Hall.
2. Newmark, N.M., 1965, Effects of earthquakes on dams and embankments: Geotechnique, v. 15, no. 2, p. 139-160.
3. Newmark, N. M., and Hall, W. J., 1978, Development of criteria for seismic review of selected nuclear power plants: Nuclear Regulatory Commission, Report NUREG/CR-0098, 49 p., May.
4. PG&E, 1988, Final Report of the Diablo Canyon Long Term Seismic Program, July.
5. PG&E, 2001, Diablo Canyon ISFSI Safety Analysis Report, April.
6. GEO.DCPP.01.04, Methodology for determining sliding resistance along the base of DCPP ISFSI pads, rev. 1.
7. GEO.DCPP.01.19, Development of strength envelopes for jointed rock mass at DCPP ISFSI using Hoek-Brown equations, rev. 2.
8. GEO.DCPP.01.20, Development of strength envelopes for shallow discontinuities at DCPP ISFSI using Barton equations, rev. 2
9. GEO.DCPP.01.21, Analysis of bedrock stratigraphy and geologic structure at the DCPP ISFSI site, rev. 2.
10. GEO.DCPP.01.26, Determination of earthquake-induced displacements of potential sliding masses on DCPP ISFSI slope, rev. 3.
11. GEO.DCPP.01.31, Development of strength envelopes for clay beds at DCPP ISFSI, rev. 1.
12. Witter, R., 11/5/01, Data Report I, Rock Laboratory Test Data, rev. 1.
13. Clough, G.W., and Duncan, J.M., 1991, "Foundation Engineering Handbook," 2nd Edition, edited by H.Y. Fang, Van Nostrand Reinhold, New York, pp. 223-235.

14.0 ATTACHMENTS

There are no attachments to this calculation.

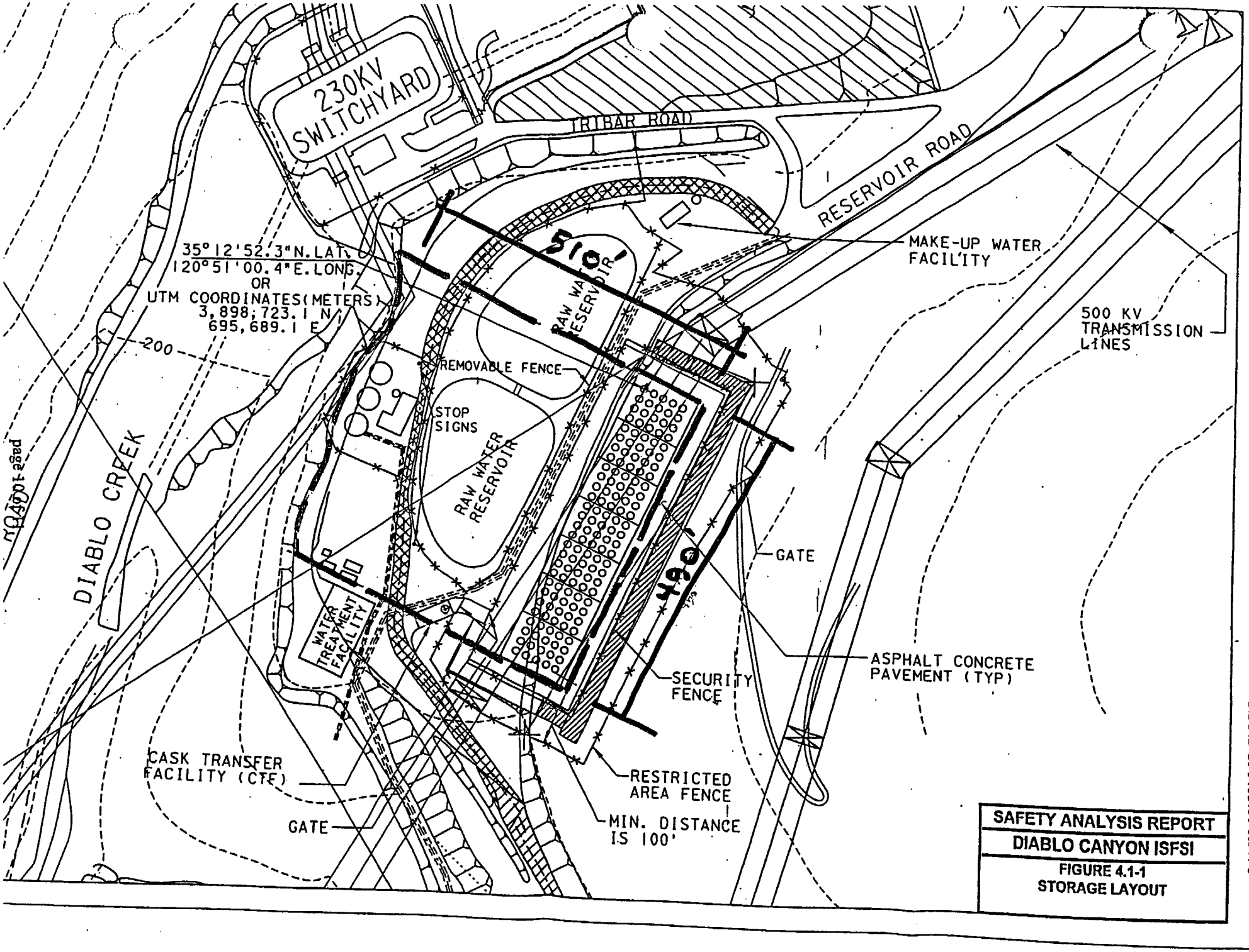

SAFETY ANALYSIS REPORT
DIABLO CANYON ISFSI
FIGURE 4.1-1
STORAGE LAYOUT

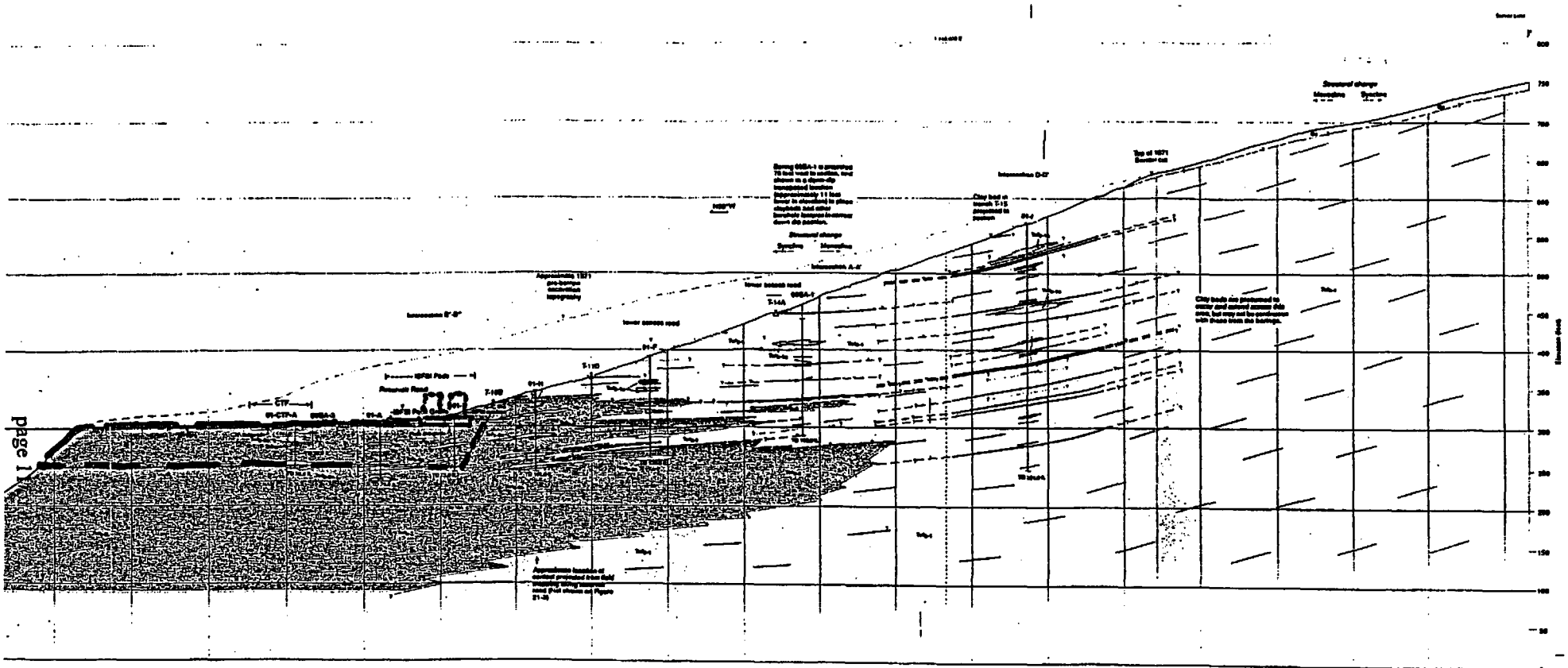

Notes

1. Location of cross section shown on Figures 21-3 and 21-4. Nearby borings are projected to cross section.
2. See Figure 21-13 for explanation of geologic units.
3. Horizontal scale = vertical scale.

0 25 50 75 100 feet
Scale

DIABLO CANYON ISFSI

FIGURE 21-22
CROSS SECTION I-I'

GEO.DCPP.01.21 REV 2 December, 2001

ATTACHMENT

2-2

PACIFIC GAS AND ELECTRIC COMPANY
GEOSCIENCES DEPARTMENT
NON-QUALITY RELATED DOCUMENT

Document Number:
Revision: 0
Date: 19 March 2003
Quality Related: No
Review Method:

1.0 TITLE: Evaluation of Potential Rotational Failure of Foundation beneath DCPP ISFSI Pads

2.0 SIGNATORIES

PREPARED BY:	Robert K. Green	DATE:	19 March 2003
	Robert K. Green, PE, GE		URS Corporation
	Printed Name		Organization
REVIEWED BY:	Rob White	DATE:	3/19/03
	Robert K. White		Geosciences
	Printed Name		Organization

URS

3.0 RECORD OF REVISIONS

Rev. No.	Reason for Revision	Revision Date
0	Initial issue	19 March 2003

TABLE OF CONTENTS

1.0 TITLE: EVALUATION OF POTENTIAL ROTATIONAL FAILURE OF FOUNDATION BENEATH DCPP ISFSI PADS 1

2.0 SIGNATORIES 1

3.0 RECORD OF REVISIONS 2

4.0 PURPOSE 5

5.0 ASSUMPTIONS 5

6.0 INPUTS 5

6.1 Geometry 6
6.1.1 Geometry and Weight of Foundations and Casks 6
6.1.2 Geometry of subsurface materials 6
6.2 Properties of the subsurface materials 6
6.2.1 Non-jointed (altered) rock 6
6.2.2 Jointed rock mass 6
6.2.3 Rock Joints 6
6.2.4 Clay beds 6
6.3 Potential earthquake motions 7
6.4 Induced loads on the foundations 7

7.0 METHOD AND EQUATION SUMMARY 7

7.1 Bearing Capacity 7
7.2 Slope Stability 8

8.0 SOFTWARE 8

8.1 Bearing Capacity 8
8.2 Slope Stability – UTEXAS3 8

9.0 BODY OF CALCULATION 8

9.1 Bearing Capacity Approach 8
9.2 Slope Stability Approach 9

10.0 RESULTS AND CONCLUSIONS 10

10.1 Results 10
10.2 Conclusions 10

11.0 LIMITATIONS 10

12.0 IMPACT EVALUATION 10

13.0 REFERENCES 10

14.0 ATTACHMENTS 13

14.1 Attachment 1 – Geologic Cross Sections beneath the ISFSI foundation pads 13
14.2 Attachment 2 – UTEXAS3 Computer Input and Output Files 13

4.0 PURPOSE

The purpose of this document is to respond to Request 2 – Seismic Stability of the ISFSI foundation for the potential rotational failure mode presented in Figure 2-1(b) of the Clarification of the Request for Additional Information regarding slope stability issues dated January 16, 2003, from the U.S. Nuclear Regulatory Commission, Office of Nuclear Material Safety and Safeguards, Spent Fuel Project Office. Figure 2-1(b) is copied below from the Clarification of RAIs.

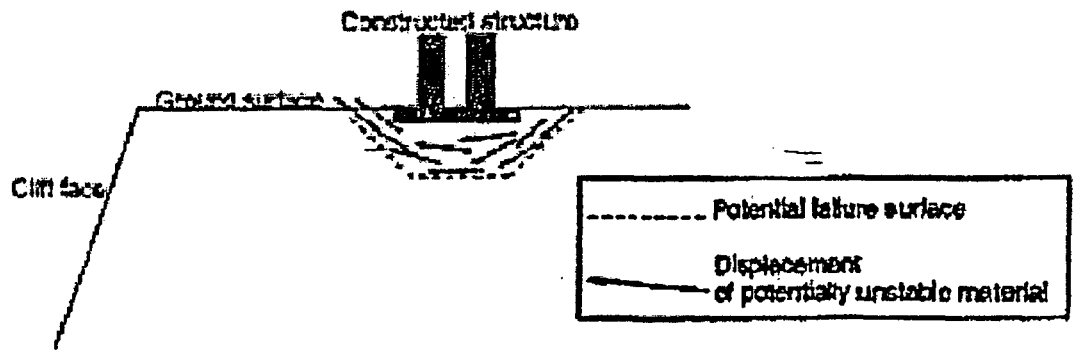

(b) Potential rotational failure along a combined surface consisting of inclined joints and horizontal bedding

5.0 ASSUMPTIONS

Several assumptions are made in this evaluation. Key assumptions include the following:

1. Potential failure surfaces capable of developing beneath the cask foundations are assumed to occur along inclined joints and sub-horizontal bedding planes. This is a reasonable assumption, as these are inherently weaker elements within the overall rock mass.
2. The strength of the subsurface materials can be represented by Mohr-Coulomb strength envelopes. This is a reasonable assumption, as demonstrated in the several supporting calculations referenced herein.

6.0 INPUTS

The inputs to the evaluation include the geometry of the subsurface materials, the strengths and unit weights of the subsurface materials, the potential earthquake ground motions, and the induced loads on the foundation from the casks as a result of the earthquake shaking. Each of these inputs is discussed in the following sections:

6.1 Geometry

6.1.1 Geometry and Weight of Foundations and Casks

The geometry and weight of the foundation and casks are from PGE-009-CALC-003. The pads are 105 feet by 68 feet by 7.5 feet thick (from page 10). The total cask weight for 20 casks is 7200 kips, and the total pad weight is 8033 kips (from page 39). The center of gravity of the casks is 118.5 inches (9.875 feet) above the pad (from page 14).

6.1.2 Geometry of subsurface materials

The geometry of the subsurface materials has been evaluated by Ms. Eliza Nemser of URS working under the direction of Dr. William Page of PG&E. The resulting cross-sections under the cask foundations are included as Attachment 1 to this document. Based on a visual review of the cross sections and the location and extent of the clay beds and faults, the most critical cross section was judged to be geologic cross-section Y-Y' for Pad 3 (intersection with cross-section T-T'). This section had a clay bed under most of the width of the pad and a fault near one edge of the pad.

6.2 Properties of the subsurface materials

The properties of the subsurface materials were evaluated in previous calculations and are adopted for use in this evaluation.

6.2.1 Non-jointed (altered) rock

The shear strength of the non-jointed rock is based on Calculation No. GEO.DCPP.01.16, Development of strength envelopes for non-jointed rock at DCPP ISFSI based on laboratory data. The recommended shear strength is a friction angle of 50 degrees.

6.2.2 Jointed rock mass

The shear strength of the jointed rock mass is based on Calculation No. GEO.DCPP.01.19, Development of Strength Envelopes for Jointed Rock Mass at DCPP ISFSI Using Hoek-Brown Equations. The shear strengths were all above a friction angle of 50 degrees, so 50 degrees will be used to conservatively represent the strength of the altered sandstone.

6.2.3 Rock Joints

The shear strength of the rock joints is based on Calculation No. GEO.DCPP.01.23, Pseudostatic Wedge Analysis of DCPP ISFSI Cutslope (SWEDGE Analysis). The recommended shear strengths from Table 23-1 of this calculation are 30.5 degrees for sub-horizontal joints and 26.5 degrees for fault related or more vertically oriented joints. The joints in the cross-sections under the pads are associated with faults, so 26.5 degrees will be assigned for the rock joint materials.

6.2.4 Clay beds

The shear strength of the clay beds is based on Calculation No. GEO.DCPP.01.31, Development of strength envelopes for clay beds at DCPP ISFSI. The recommended

undrained shear strength is the lower of c = 0 and ϕ = 29 degrees or c = 800 psf and ϕ = 15 degrees.

6.3 Potential earthquake motions

The potential earthquake motions are based on Calculation Number GEO.DCPP.01.11, Development of ISFSI Spectra. The peak horizontal acceleration is 0.83g for the horizontal motions in both the fault normal and fault parallel directions.

6.4 Induced loads on the foundations

The induced loads on the foundations were taken from Calculation No. PGE-009-CALC-003 by Enercon Systems, Inc., dated 30 November 2001.

The maximum vertical load combination from that calculation is 6.95 ksf for the Hosgri load case (page 68). This load case is for the very hard rock analyses. The maximum load in their analysis occurs along the edge of the long dimension of the foundation. The loading causes the opposite edge of the pad to lift off the underlying material. Based on the stress distribution plot for Load Step 6 shown in Figures 35 and 36 of the calculations, approximately 42 feet of the width of the pad has compressive stresses under it. This means that about 26 feet of the width of the pad (68 feet – 42 feet) is tending to lift off of the foundation, or about 62% of the pad is still in contact with the underlying rock. The loading on the foundation will therefore be assumed to vary linearly from 0 at a point 26 feet from one edge of the pad to a maximum value of 6.95 ksf at the opposite edge.

7.0 METHOD AND EQUATION SUMMARY

The potential for rotational type failures through the rock under the foundation pads are evaluated as potential bearing capacity failures and as potential slope stability failures.

7.1 Bearing Capacity

Bearing capacity is calculated using standard geotechnical procedures developed by Meyerhof (1955) and summarized in Calculation No. GEO.DCPP.01.03, Development of allowable bearing capacity for DCPP ISFSI pad and CTF stability analyses.

The ultimate bearing capacity is given by the following equation:

$$q_u = c\,N_c + \tfrac{1}{2}\,B\,\gamma_h\,N_\gamma$$

where: c = cohesion for material in the potential failure wedge
N_c = bearing capacity factor for cohesion dependent on friction angle
B = footing width (but no greater than 6 feet)
γ_h = unit weightN_γ = bearing capacity factor for material in the failure wedge dependent on the friction angle

7.2 Slope Stability

Slope stability is evaluated using standard slope stability methods commonly used in geotechnical engineering practice. The method developed by Spencer (1967) was selected for use on the analyses in this document. Spencer's method is a limit equilibrium method of slices, where the soil or rock within the potential sliding mass is divided into slices and the forces acting on the slices are calculated so that the forces are in equilibrium. Spencer's method assumes that the forces between the slices are parallel. The factor of safety is calculated as the factor that the strength would need to be multiplied by to put the slope in equilibrium, or commonly referred to as the resisting forces divided by the driving forces.

8.0 SOFTWARE

8.1 Bearing Capacity

No software used. The bearing capacity was calculated by hand using a hand held calculator.

8.2 Slope Stability – UTEXAS3

The computer program UTEXAS3 was developed by Dr. Stephen G. Wright (Wright, 1991) to calculate the stability of slopes. The program has options to calculate the factor of safety against sliding using several methods including those developed by Spencer (1967), Bishop (1955), and Lowe and Karafiath (1960). The program has been verified and approved for use on the Diablo Canyon Power Plant Project in Calculation GEO.DCPP.01.33.

9.0 BODY OF CALCULATION

9.1 Bearing Capacity Approach

The allowable bearing capacity cited in the Enercon Services calculation is 52 ksf (page 68, which cited Section 6.4.3.5 of PG&E Specification, 10012-N-NPG, Rev. 2). This is consistent with Calculation No. GEO.DCPP.01.03, Development of allowable bearing capacity for DCPP ISFSI pad and CTF stability analyses, which is based on a material with a friction angle of 50 degrees for mat foundations with widths in excess of 6 feet.

The clay bed is at a minimum depth of about 26 feet. The strength of the clay beds is the lower of c = 800 psf, ϕ = 15 degrees or c = 0, ϕ = 29 degrees. At a depth of 26 feet, the shear strength, τ = 800 psf + 26 feet * 140 pcf * tan (15°) = 1776 psf or τ = 0 + 26 feet * 140 pcf * tan (29°) = 2018 psf. At this depth, the strength envelope c = 800 psf, ϕ = 15 degrees gives a lower strength, so will be used.

Assuming that the pad was founded entirely on material with the strength of the clay seam would result in the following ultimate bearing capacity:

$$q_u = c\,N_c + \tfrac{1}{2}\,B\,\gamma_h\,N_\gamma$$
$$c = 800 \text{ psf}$$

N_c = 10.97 (based on ϕ = 15 degrees from Bowles, 1988, Table 4-4)
B = 6 feet (maximum value to be used in calculation)
γ_h = 140 pcf
N_γ = 1.1 (based on ϕ = 15 degrees from Bowles, 1988, Table 4-4)

$q_u = c\,N_c + \frac{1}{2} B\,\gamma_h\,N_\gamma$
= 800 psf * 10.97 + ½ * 6 ft * 140 pcf * 1.1
= 8776 + 462
= 9238 psf
= 9.24 ksf

The allowable bearing capacity for static loading is 1/3 of this value or 3.08 ksf. For earthquake loading this can be increased by 33% to 4.11 ksf. The clay bed is at a minimum depth of about 26 feet. The stresses can conservatively be spread out over a wider area equal to the width of the foundation plus 1.16 times the depth (assuming area increases by 30 degrees from edges of foundation). Using the loading foundation width of 42 feet and increasing the area results in a reduction in the loading pressure to 45% of the surface pressure as shown below:

Pressure at 26 feet depth = Surface Pressure * B/(B+1.16H) * L/(L+1.16H)
= Surface Pressure * 42/(42+1.16*26)*105/(105+1.16H)
= Surface Pressure * 0.454
= 6.95 * 0.454
= 3.15 ksf

This is less than the allowable capacity for earthquake loading of 4.11 ksf. It should be noted that this is an extremely conservative approach because it assumes that the peak load is applied over the entire 42-foot width of the contact area and that the bearing capacity failure surface passes entirely through clay with these properties as it propagates to the surface. The average pressure over this width is about half of the peak value.

9.2 Slope Stability Approach

The vertical loading from the Enercon Services analyses was applied as a linearly varying surface load over geologic cross-section Y-Y' for Pad 3 (intersection with cross-section T-T'). The loading on the rock surface from the adjacent pads was not included, which is conservative because those pressures act on the rock surface. The geometry of the clay bed and fault beneath and near the foundation were modeled in UTEXAS3. A search was performed for the critical failure surface. Spencer's method was used to calculate the factor of safety, which is the recommended method in the program user guide. The minimum factor of safety found was 3.34. Input and output files are found in Attachment 2. The geometry of the failure surface is shown in the following figure:

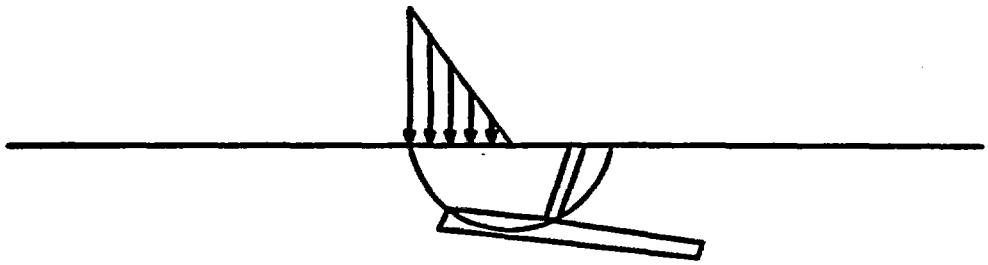

The critical circle passes through the clay bed, and exits beneath the adjacent foundation pad, which was not modeled. It should be noted that the clay bed was conservatively modeled as a continuous thick feature, which is not indicated in the geologic information. The critical circle did not stay within the fault due to geometrical constraints of the depth of the clay bed and location of the pad.

10.0 RESULTS AND CONCLUSIONS

10.1 Results

The bearing capacity calculation was made using extremely conservative assumptions regarding the foundation conditions and was found to show an adequate capacity. The calculated factors of safety for rotational failure surfaces beneath the IFSFI foundation pads are greater than 3.

10.2 Conclusions

The analyses contained in this document show that rotational failure through the rock beneath the ISFSI foundation pads is unlikely.

11.0 LIMITATIONS

The calculations described in this document are for the express purpose of evaluating the potential for rotational type of failures through the rock beneath the ISFSI foundation pads, and should not be used for any other purpose. The assumptions used in this calculation are conservative, and should not be used in other analyses without evaluating the impact of the degree of conservatism on the particular problem being evaluated.

12.0 IMPACT EVALUATION

The impact of the calculations within this document support the conclusion that failure of the rock under the foundations of the ISFSI pads is unlikely, which is consistent with other Geosciences calculations.

13.0 REFERENCES

Bishop, A. W., 1955, The use of the slip circle in the stability analysis of slopes: Géotechnique, Vol. 5, No. 1, pp. 7-17, March.

Bowles, J. E., 1988, Foundation Analysis and Design: McGraw-Hill, Inc., Fourth Edition, 1004 p.

Enercon Services, Inc., 2002, ISFSI Cask Storage Pad Seismic Analysis: Calculation No. PGE-009-CALC-003, Rev. 1, prepared by S.C. Tumminelli, November 30.

Lowe, J., and Karafiath, L., 1960, Stability of earth dams upon drawdown: Proceedings of the First PanAmerican Conference on Soil Mechanics and Foundation Engineering, Mexico City, Vol. 2, pp. 537-552.

Meyerhof, G.G., 1955, Influence of roughness of base and ground water conditions on the ultimate bearing capacity of foundations: Géotechnique, Vol. 5.

Pacific Gas and Electric Company, 2001, Development of allowable bearing capacity for DCPP ISFSI pad and CTF stability analyses: Calculation No. GEO.DCPP.01.03, Rev. 1, prepared by Robert White, November 5.

Pacific Gas and Electric Company, 2001, Methodology for determining sliding resistance along the base of DCPP ISFSI pads: Calculation No. GEO.DCPP.01.04, Rev. 1, prepared by Robert White, November 5.

Pacific Gas and Electric Company, 2001, Development of ISFSI Spectra: Calculation No. GEO.DCPP.01.11 (Tables 6-13 & 6-14 only), Rev. 1, prepared by Norman Abrahamson, September 5.

Pacific Gas and Electric Company, 2002, Development of strength envelopes for non-jointed rock at DCPP ISFSI based on laboratory data: Calculation No. GEO.DCPP.01.16, Rev. 2, prepared by Joseph Sun, June 27.

Pacific Gas and Electric Company, 2001, Determination of basic friction angle along rock discontinuities at DCPP ISFSI based on laboratory tests: Calculation No. GEO.DCPP.01.18, Rev. 2, prepared by Robert White, November 19.

Pacific Gas and Electric Company, 2001, Development of Strength Envelopes for Jointed Rock Mass at DCPP ISFSI Using Hoek-Brown Equations: Calculation No. GEO.DCPP.01.19, Rev. 2, prepared by Jeffrey Bachhuber of William Lettis & Associates, June 14.

Pacific Gas and Electric Company, 2002, Pseudostatic Wedge Analysis of DCPP ISFSI Cutslope (SWEDGE Analysis), Calculation No. GEO.DCPP.01.23, Rev. 1, prepared by Jeffrey Bachhuber of William Lettis & Associates, June 18.

Pacific Gas and Electric Company, 2002, Development of Strength Envelopes for Clay Beds at DCPP ISFSI: Calculation No. GEO.DCPP.01.31, Rev. 1, prepared by Karthik Narayanan of Geomatrix, June 25.

Pacific Gas and Electric Company, 2002, Verification of program UTEXAS3: Calculation No. GEO.DCPP.01.33, Rev. 2, prepared by Karthik Narayanan of Geomatrix, Nov. 14.

Spencer, E., 1967, A method of analysis of the stability of embankments assuming parallel inter-slice forces: Géotechnique, Vol. 17, No. 1, pp. 11-26, March.

U.S. Nuclear Regulatory Commission, 2003, Clarification of RAIs regarding slope stability issues, Office of Nuclear Material Safety and Safeguards, Spent Fuel Project Office, fax to PG&E, January 16.

Wright, S. G., 1991, UTEXAS3 — A computer program for slope stability calculations: Shinoak Software, Austin, Texas, 158 p., revised September.

14.0 ATTACHMENTS

14.1 Attachment 1 – Geologic Cross Sections beneath the ISFSI foundation pads

The geologic section beneath the ISFSI pads were prepared by Ms. Eliza Nemser of URS under the direction of Dr. William Page of PG&E.

14.2 Attachment 2 – UTEXAS3 Computer Input and Output Files

Memorandum

Date: March 7, 2003 **File #:**

To: Joseph Sun, Manager DCPP IFSI Project for Geosciences

From: William D. Page, Senior Project Geologist

Subject: RESPONSE TO NRC REQUEST 2
Assessment of seismic stability under the pads considering inertial loading

Pacific Gas and Electric Company

NRC REQUEST 2 - Provide an assessment of the seismic stability of the cask-storage pad considering the effects of earthquake loading (inertial loading from the structures superimposed on the loading associated with the free-field ground motion), the occurrence of clay beds underneath the storage pad site, and the failure modes illustrated in Figure 2-1.

William Page prepared this response. Eliza Nemzer, Staff Geologist at URS Corporation, prepared the diagrams and sections for the potential rotational failures.

RESPONSE TO REQUEST 2

The response to request 2 is broken into two parts: analysis of the potential for lateral sliding along clay beds and analysis of potential rotational failure.

Analysis of Lateral Sliding along Clay Beds beneath the Pads (Figure R2-1a)

The diagram illustrating the question is reproduces as Figure R2-1a. Other than the small inertial lateral displacements 0.4 to 1.2 inches calculated for the pads during the postulated earthquake that are discussed in SAR pages 8.2-18 through 8.2-21, lateral displacements of the pads under earthquake loading along clay beds are not possible because of the following reasons:

1. The clay beds beneath the ISFSI pads are discontinuous and limited in extent. In the ISFSI site area the lateral extent of the clay beds as measured in the field is 160 feet and as interpreted from the borings is 400 feet (200 feet on either side of the location encountered in the boring) for the thickest clay beds and shorter for the thinner beds, as discussed in Calculation Package 21 (page 24). These relationships are shown in the area beneath the pads and in the slope above the ISFSI as illustrated in cross sections A-A', B-B', C-C', G-G', H-H', K-K', and I-I' (Figures 21-14 to 21-16 and 21-20 to 21-24).

2. The continuity of the strata beneath the pads is disrupted by the several faults that displace the beds in this area. These faults extend into the area to the north between the pads and the canyon wall of Diablo Creek

3. Any lateral displacement from inertial loads on the pads would have to be transferred along near horizontal beds for a distance of over 400 feet as illustrated in cross sections A-A' and I-I' (Figures 21-14 and 21-24).

4. A potential model that illustrates possible geometry of inferred clay beds between the pads and the canyon wall of Diablo Creek is shown on Figure R2-2-1. The inferred beds are drawn by postulating the existence of clay beds in the area between the pads and the canyon wall using a typical sequence found in boring 01-I sown on cross section I-I' (Figure 21-24). The potential failure surface is sketched as stepping along clay beds from known clay beds at the pads to the canyon wall using the criteria explained in CP-21 (page 56). Inspection shows that the geometry is very different than that shown in the NRC Figure 2-1 and does not appear conducive to any displacement.

5. Between 65 and 110 feet of rock has been removed from the area between the pads and the canyon wall during the 1971 borrow cut for the construction of the the Raw Water Reservoir as shown on Section A-A' (Figure 21-14) and discussed in CP-21 (page 9). The natural pre-construction slope showed no evidence of any large landslide in this area (CP-21, page 56 and 57) under earthquake loading during prehistoric events in the more than 300,000 years the slope has been at or near its present form. The incision of Diablo Creek that created the small canyon north of the Raw Water Reservoir is younger, but the canyon was at approximately its current position by the time the marine terrace Q-2 formed its shoreline angle at elevation 105 feet some 120,000 years ago (Figures 21-2, 21-13, 21-17 to 21-19; Hanson and others, 1992, listed in SAR references). The current condition of the slope at the ISFSI pads has much less mass than during the geologic past, and hence any inertial conditions from weight of the casks and the pads during a large earthquake will not cause significant lateral displacements.

For the above reasons the potential for deep-seated rock mass failure along clay beds that cause lateral displacement of the pads is not possible. This conclusion is confirmed by a simple stability analysis of this configuration documented in an URS calculation report entitled "Evaluation of Potential Rotational Failure of Foundation beneath DCPP ISFSI Pads", dated March 2003.

Analysis of Potential Rotational Failure beneath the Pads (Figure 2-1b)

The schematic diagram illustrating the potential rotational failures (NRC Figure 2-1) is reproduced as Figure R2-1b. To assess the potential rotational failure of the pads and casks from inertial loading during an earthquake, models of the potential rotational

failures have been drawn for each pad by plotting the geology on 8 cross sections that transect the ISFSI pads. The map showing the cross sections through the pads is Figure R2-2. For each pad, two mutually perpendicular cross sections were constructed to illustrate the subsurface geology underlying each pad. These are shown as the "a" part on Figures 2-3 to 2-10. The information for these cross sections was compiled from existing maps, cross sections, borings, and trenches in the site (Calculation Package 21, Figures 21-4, 21-15, 21-20 to 21-22, and 21-41). A separate cross section in the northwest-southeast direction illustrates the geology for each of the 7 pads (Figures 2-3a to 2-9a); a long cross section in the southwest-northeast direction includes information about the geology beneath all of the pads (Figure 2-10a). Besides fractured sandstone and dolomite, the cross sections indicate the distribution and extent of all relatively weak geologic units and discontinuities (altered rock, clay beds, joint sets, and faults) that could potentially accommodate failure initiated by either a southwest-northeast or a northwest-southeast rocking motion.

On each cross section, a reference semi-circle is drawn to represent the potential curvilinear failure plane with the optimal geometry to accommodate failure caused by a rocking motion. These potential failure models are shown as the "b" part of Figures 2-3 to 2-10. Up to 3 model scenarios are drawn for each cross section to illustrate different potential failure planes. One is the semicircular 'theoretical' failure mode. The others are modified models based on the premise that the geometry of the failure planes may deviate from the optimal geometry, if a nearby weak layer facilitates the failure. For each of these failure scenarios, the percentages of different rock units - fractured rock and altered rock - and discontinuities – clay beds, faults, and joints - that would accommodate failure has been calculated; these percentages are indicated on each of the "b" cross sections. Fractured rock dominates the models and ranges between 35% to 90% of the postulated failure plane in the models. Altered rock is locally present and ranges between 5% to 55% in the models, for example below Pad 1 (Figure 2-3b). In several failure scenarios, some of the failure may occur along clay beds that are above the semicircular potential failure plane and in the case at Pad 5 is about 50% of the postulated failure plane (Figure 2-7b). Because the average orientation of the dominant joint set in the area beneath the pads dips steeply southwest (N29W, 54SW), the joints would not be significant to failure models in the northwest-southeast direction, across the short axis of the pads. However, in the southwest-northeast direction, along the long axis of the pads, joints may accommodate part of the failure plane. For the failure scenarios in this direction on section Y-Y', the percentage of the total failure that would occur sub-parallel to the dominant joint set ranges between 20% to 40%, for example, at pad 6, scenario #3 (Figure 2-10).

In conclusion, the geologic constraints of the potential failure planes require breakage through significant amounts of rock and shows that the potential for rotational failure below the pads from inertial forces during an earthquake is not likely.

List of Figures

R2-1	Schematic failure modes from inertial forces on casks and pads (from NRC Figure 2-1)
R2-2	Map of ISFSI Pads showing cross sections
R2-3a	Cross Section R-R' through Pad 1.
R2-3b	Potential failure models on Cross Section R-R' through Pad 1.
R2-4a	Cross Section S-S' through Pad 2.
R2-4b	Potential failure models on Cross Section S-S' through Pad 2.
R2-5a	Cross Section T-T' through Pad 3.
R2-5b	Potential failure models on Cross Section T-T' through Pad 3.
R2-6a	Cross Section U-U' through Pad 4.
R2-6b	Potential failure models on Cross Section U-U' through Pad 4.
R2-7a	Cross Section V-V' through Pad 5.
R2-7b	Potential failure models on Cross Section V-V' through Pad 5.
R2-8a	Cross Section W-W' through Pad 6.
R2-8b	Potential failure models on Cross Section W-W' through Pad 6.
R2-9a	Cross Section X-X' through Pad 7.
R2-9b	Potential failure models on Cross Section X-X' through Pad 7.
R2-10a	Cross Section Y-Y' through Pads 1 to 7.
R2-10b	Potential failure models on Cross Section Y-Y' through Pads 1 to 7.

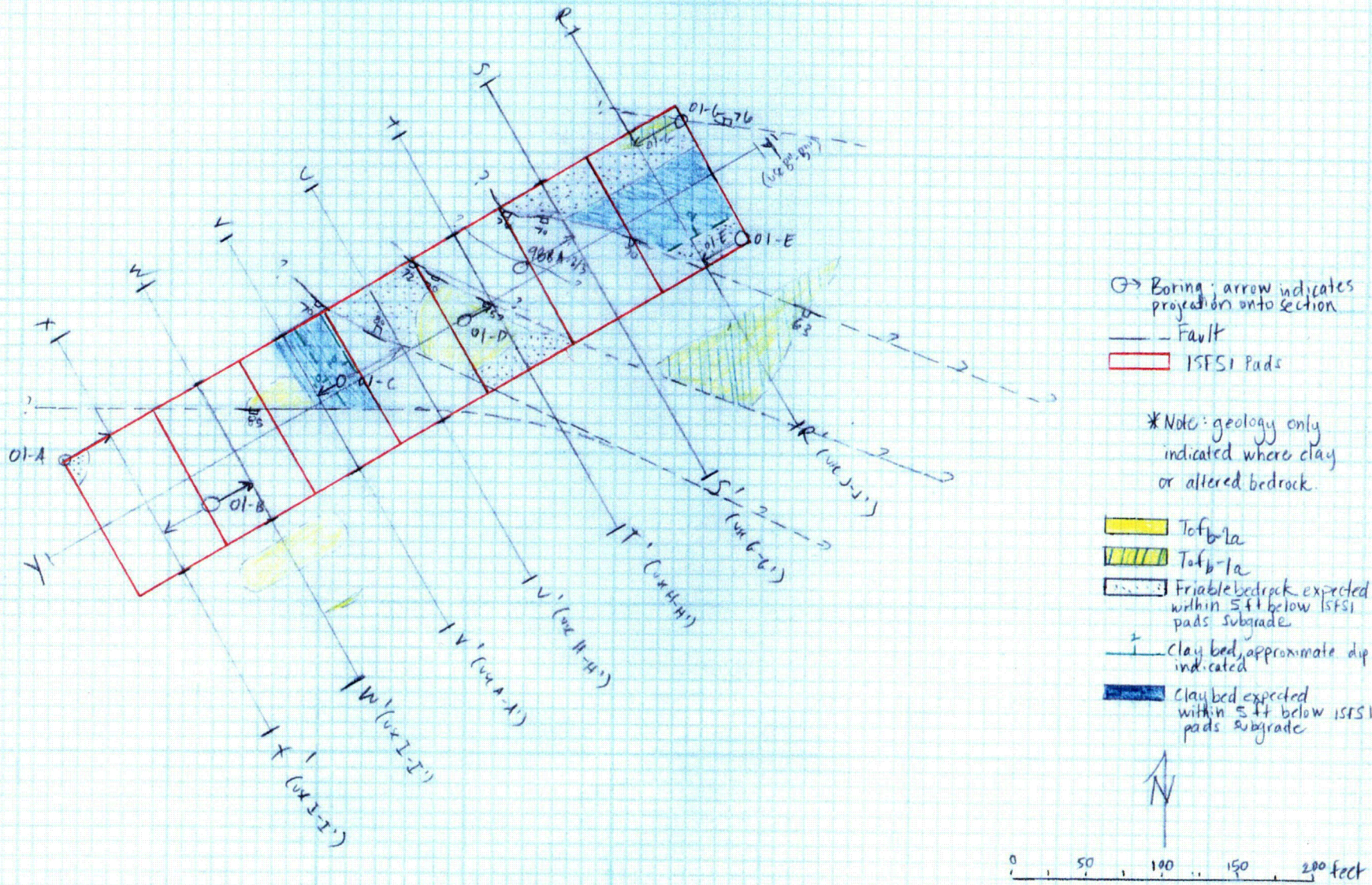
Boring; arrow indicates projection onto section
Fault
ISFSI Pads
*Note: geology only indicated where clay or altered bedrock.
Tofb-1a
Tofb-1a
Friable bedrock expected within 5 ft below ISFSI pads subgrade
Clay bed, approximate dip indicated
Clay bed expected within 5 ft below ISFSI pads subgrade
N
0 50 100 150 200 feet
01-A
01-B
01-C
01-D
01-E
01-G
X'
Y'
R'
S'
T'
U'
V'
W'
X'

C-01

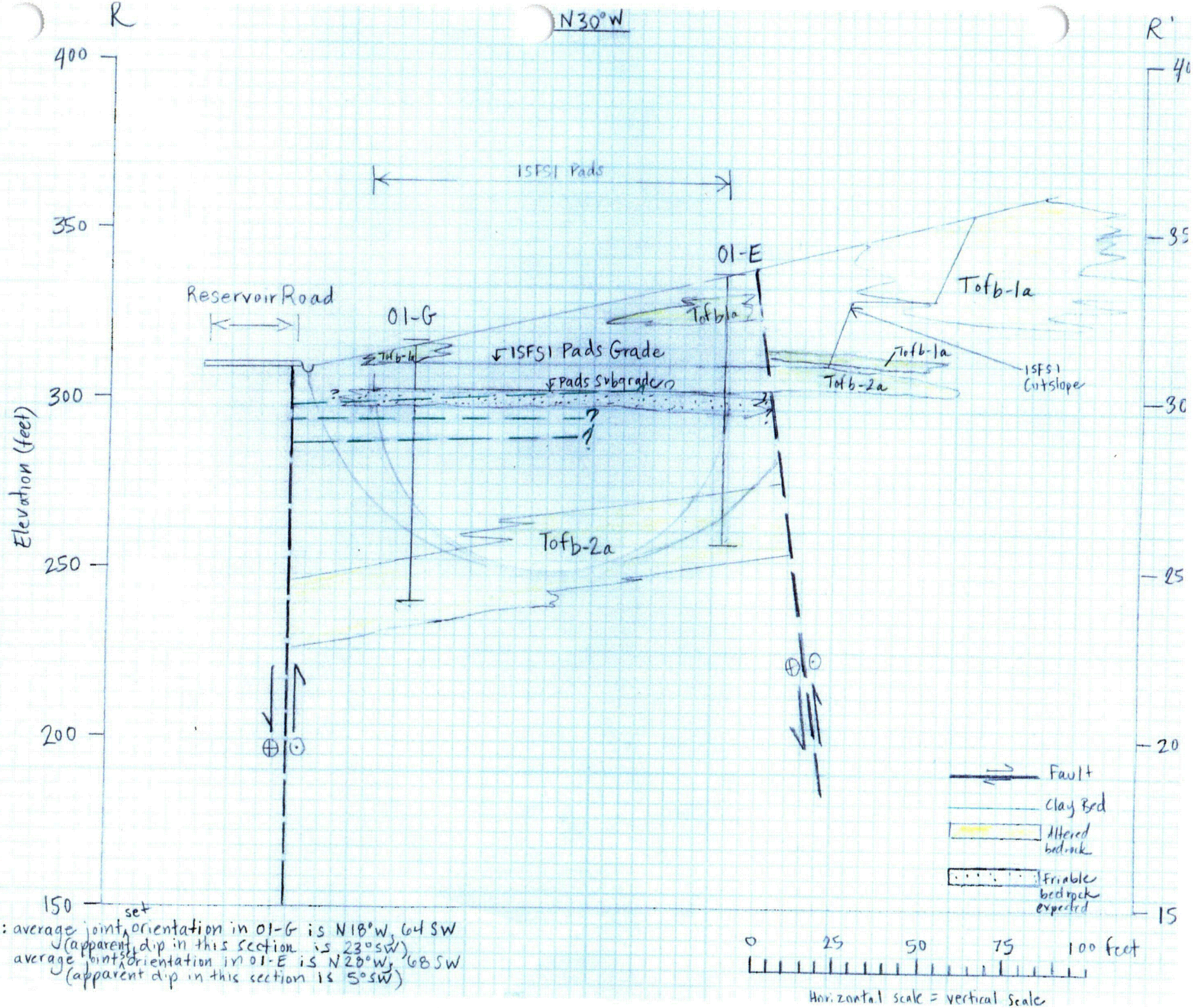

*Note: average joint set orientation in 01-G is N18°W, 64 SW (apparent dip in this section is 23°SW)
average joint set orientation in 01-E is N28°W, 68 SW (apparent dip in this section is 5°SW)

20-7

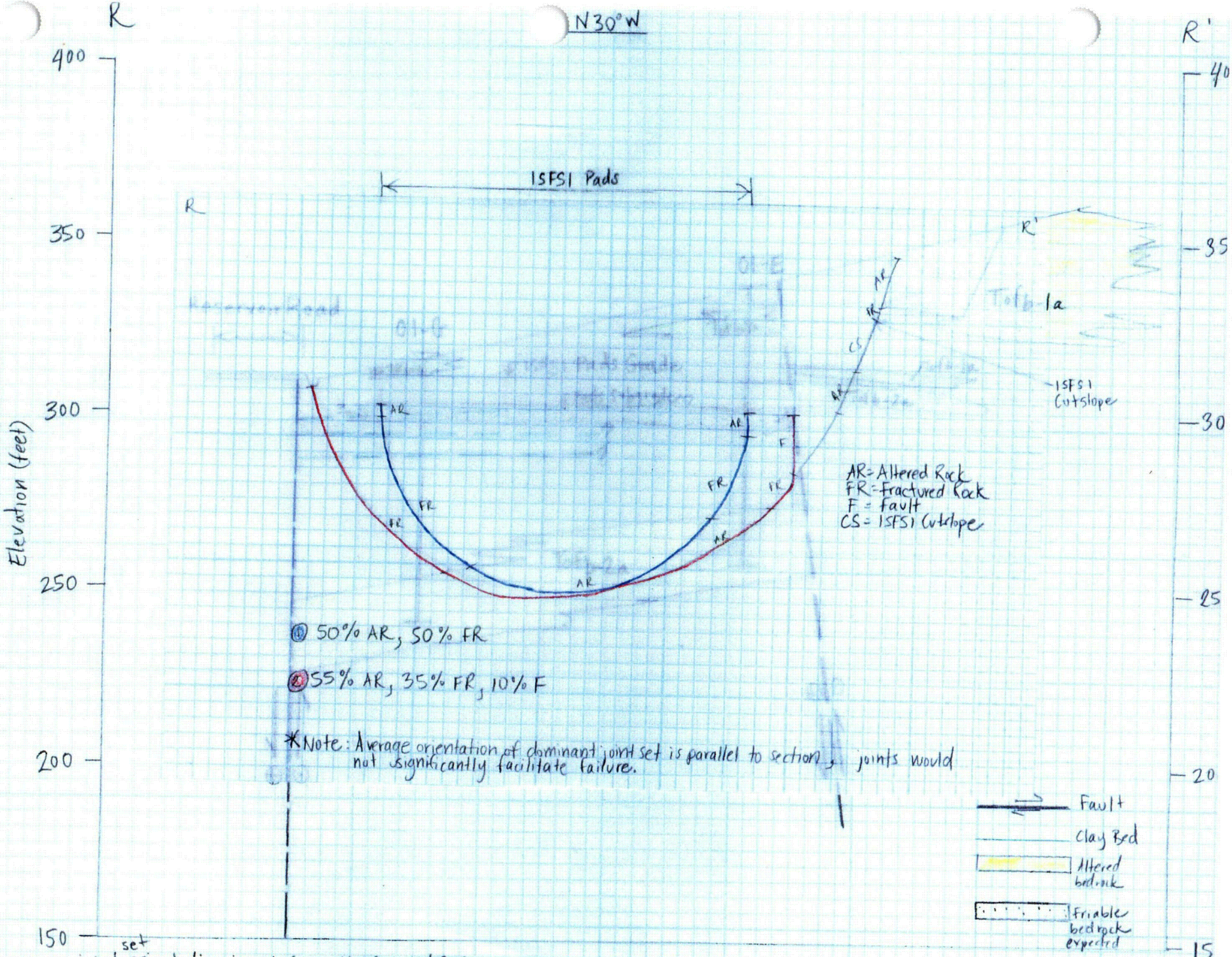

*Note: average joint set orientation in 01-G is N18°W, 64 SW (apparent dip in this section is 23°SW)
average joint set orientation in 01-E is N28°W, 68 SW (apparent dip in this section is 5°SW)

C-03

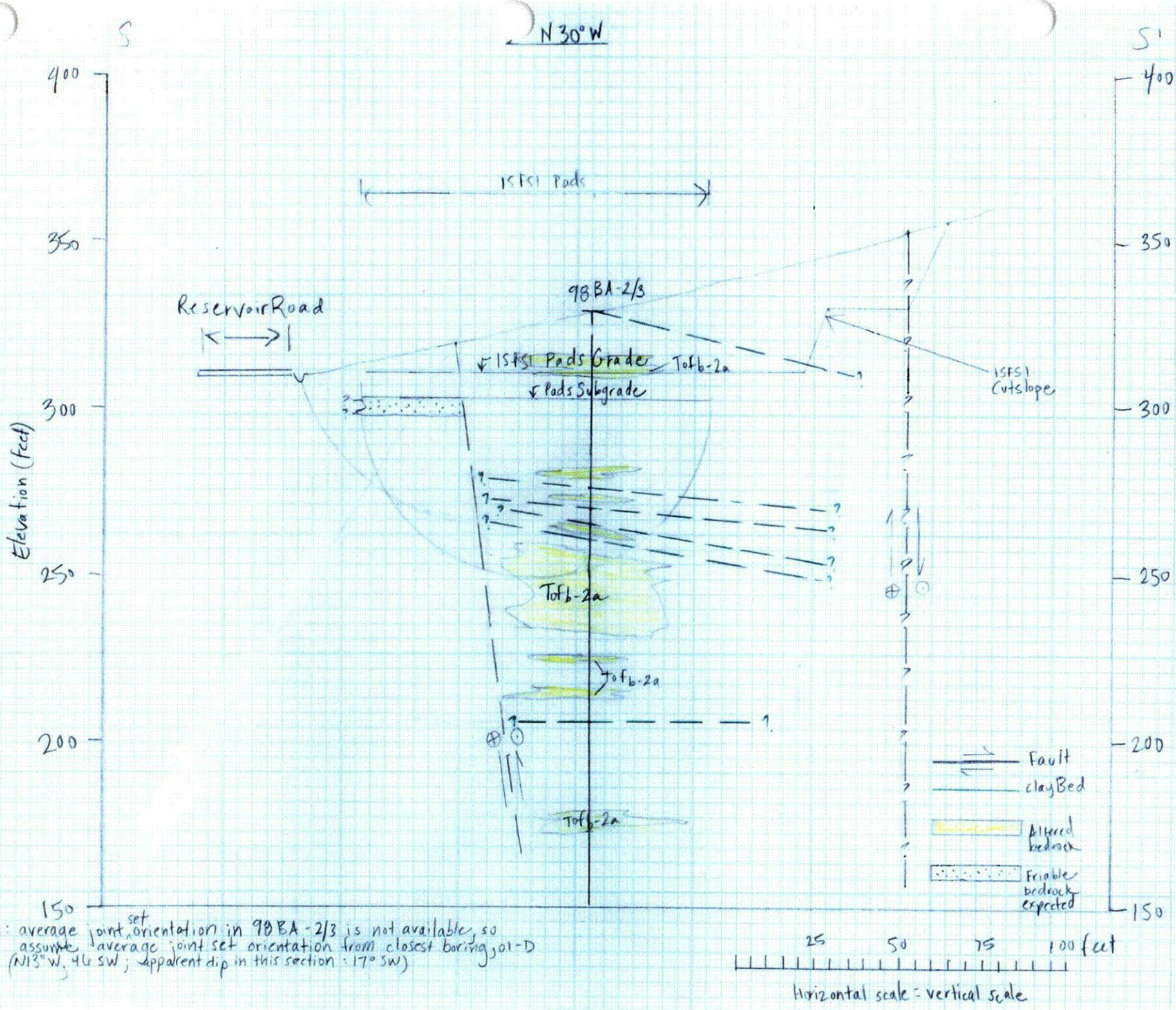

* Note: average joint set orientation in 98BA-2/3 is not available, so assume average joint set orientation from closest boring, 01-D (N13°W, 46 SW; apparent dip in this section: 17° SW)

C-04

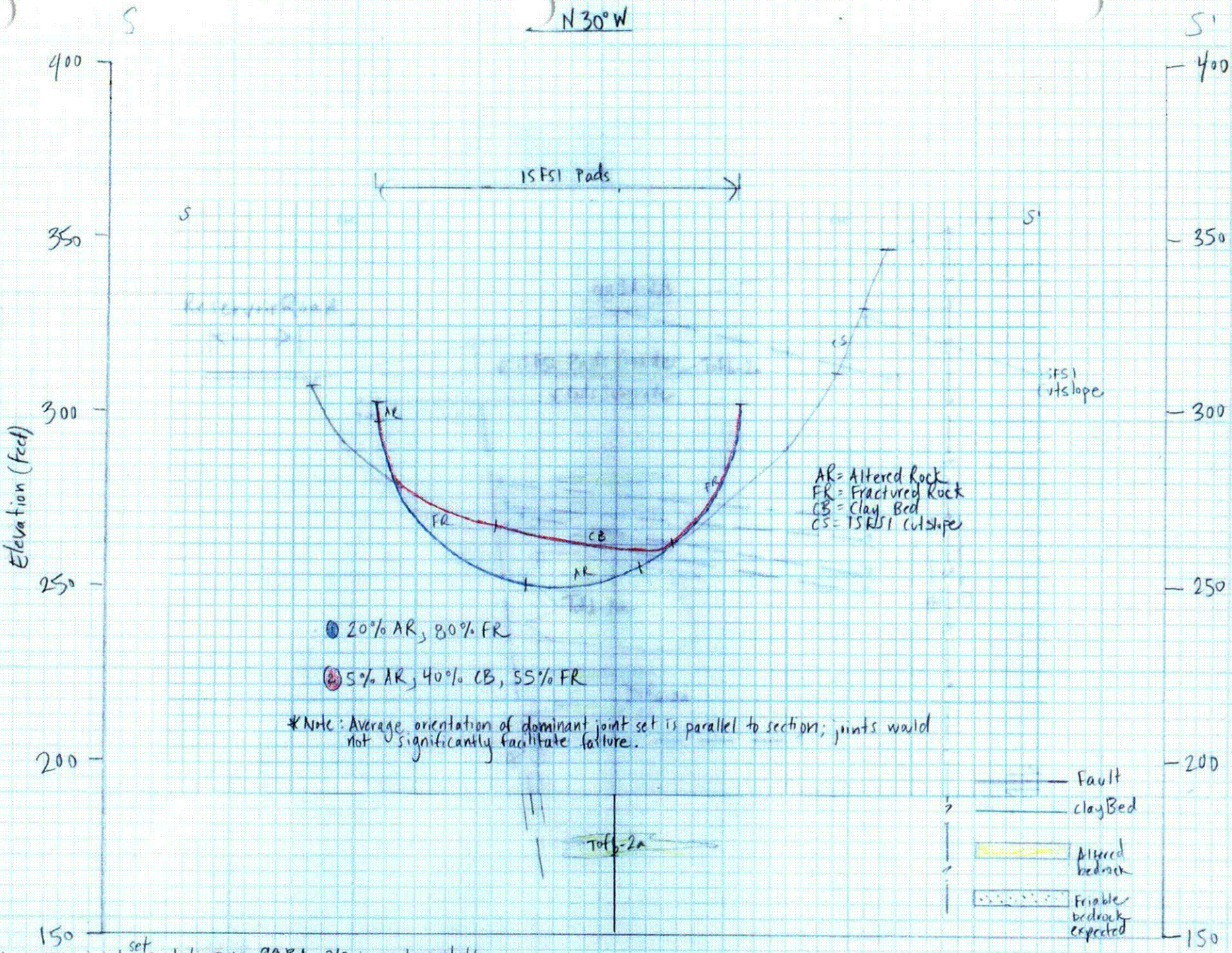

* Note: Average orientation of dominant joint set is parallel to section; joints would not significantly facilitate failure.

* Note: average joint set orientation in 98BA-2/3 is not available, so assume average joint set orientation from closest boring, 01-D (N13°W, 46 SW; apparent dip in this section: 17° SW)

C-05

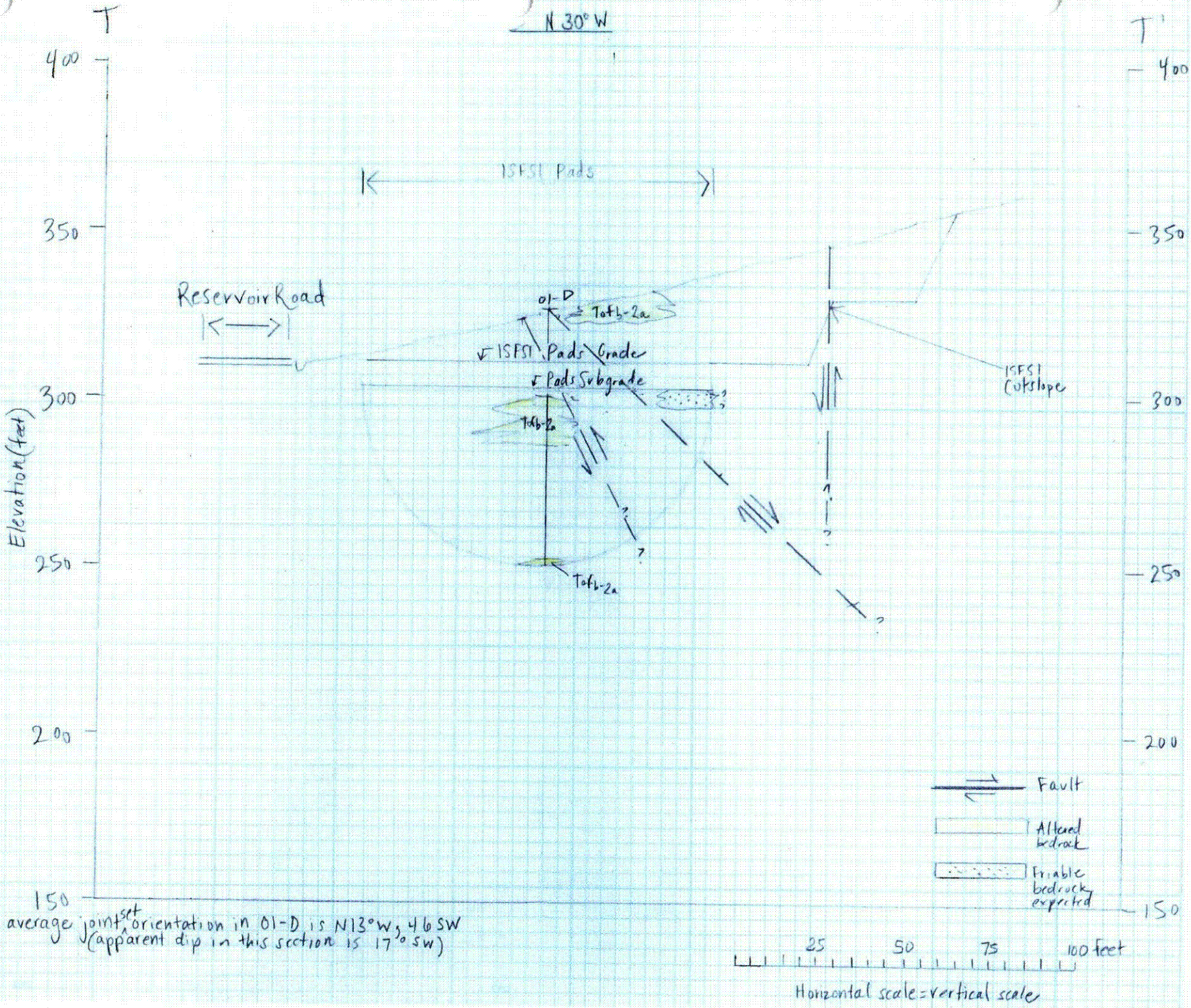

* Note: average joint set orientation in 01-D is N13°W, 46 SW (apparent dip in this section is 17° SW)

C-06

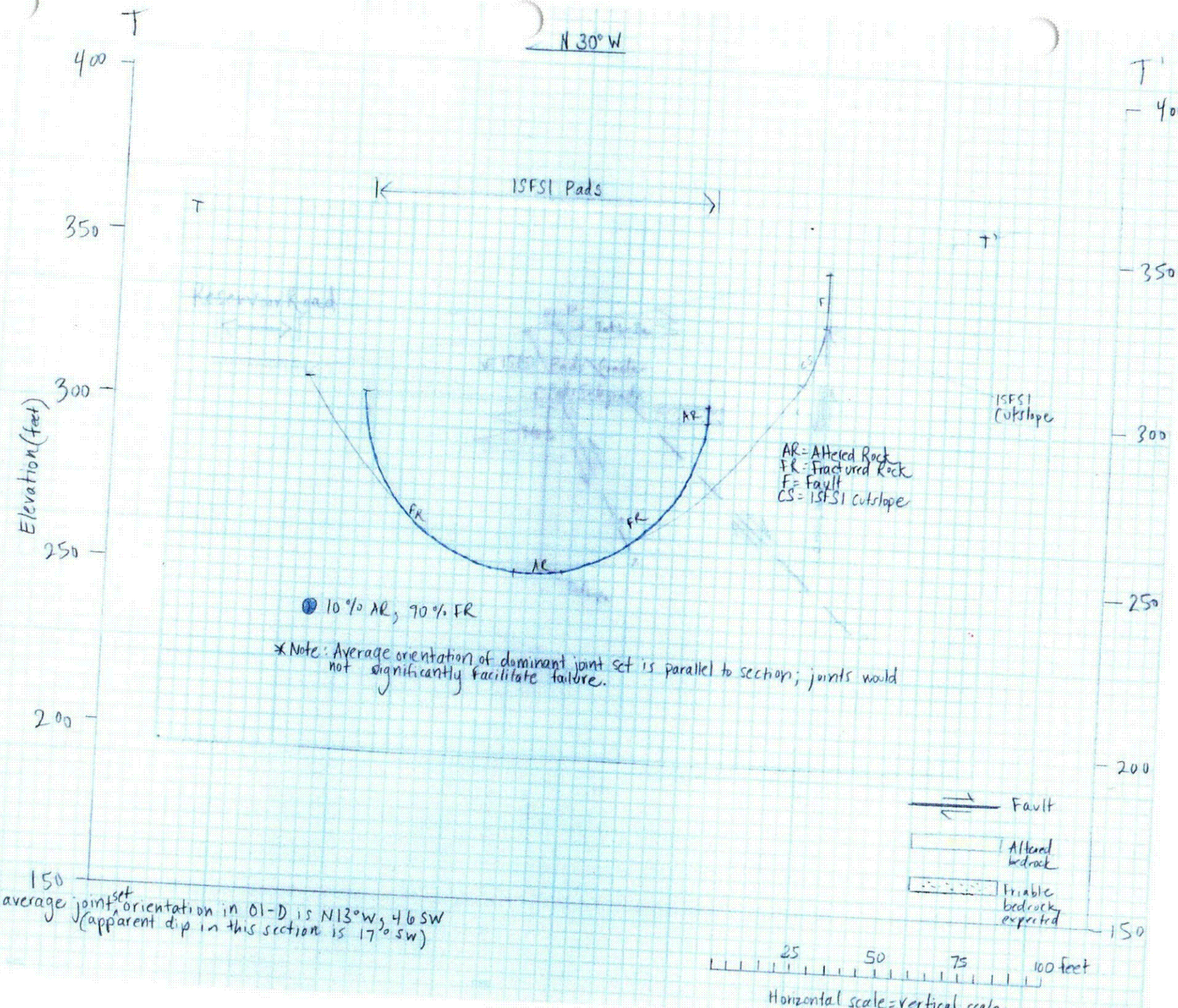

* Note: average joint set orientation in 01-D is N13°W, 46 SW (apparent dip in this section is 17° SW)

C-07

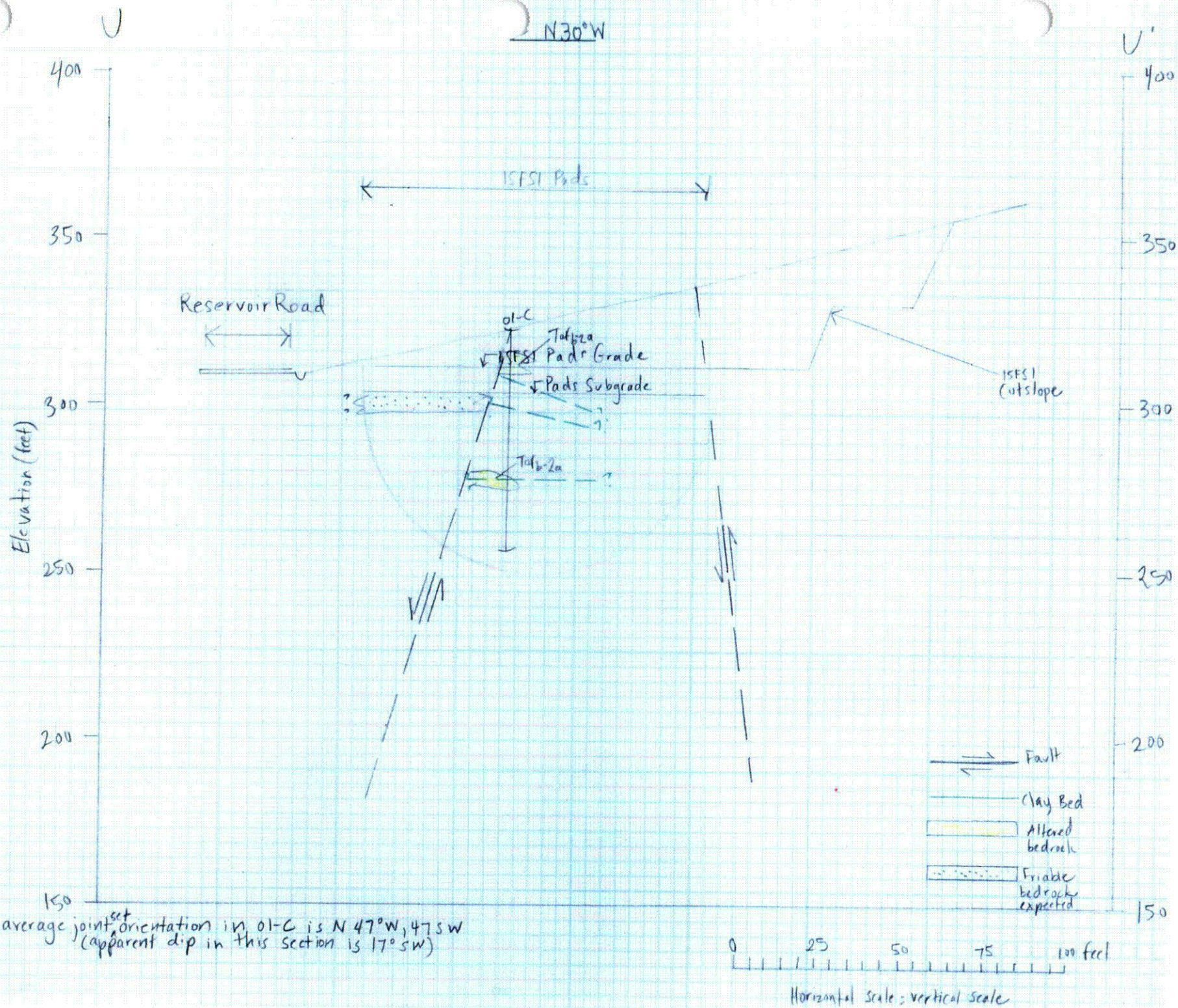

*Note: average joint set orientation in 01-C is N 47°W, 47 SW (apparent dip in this section is 17° SW)

C-08

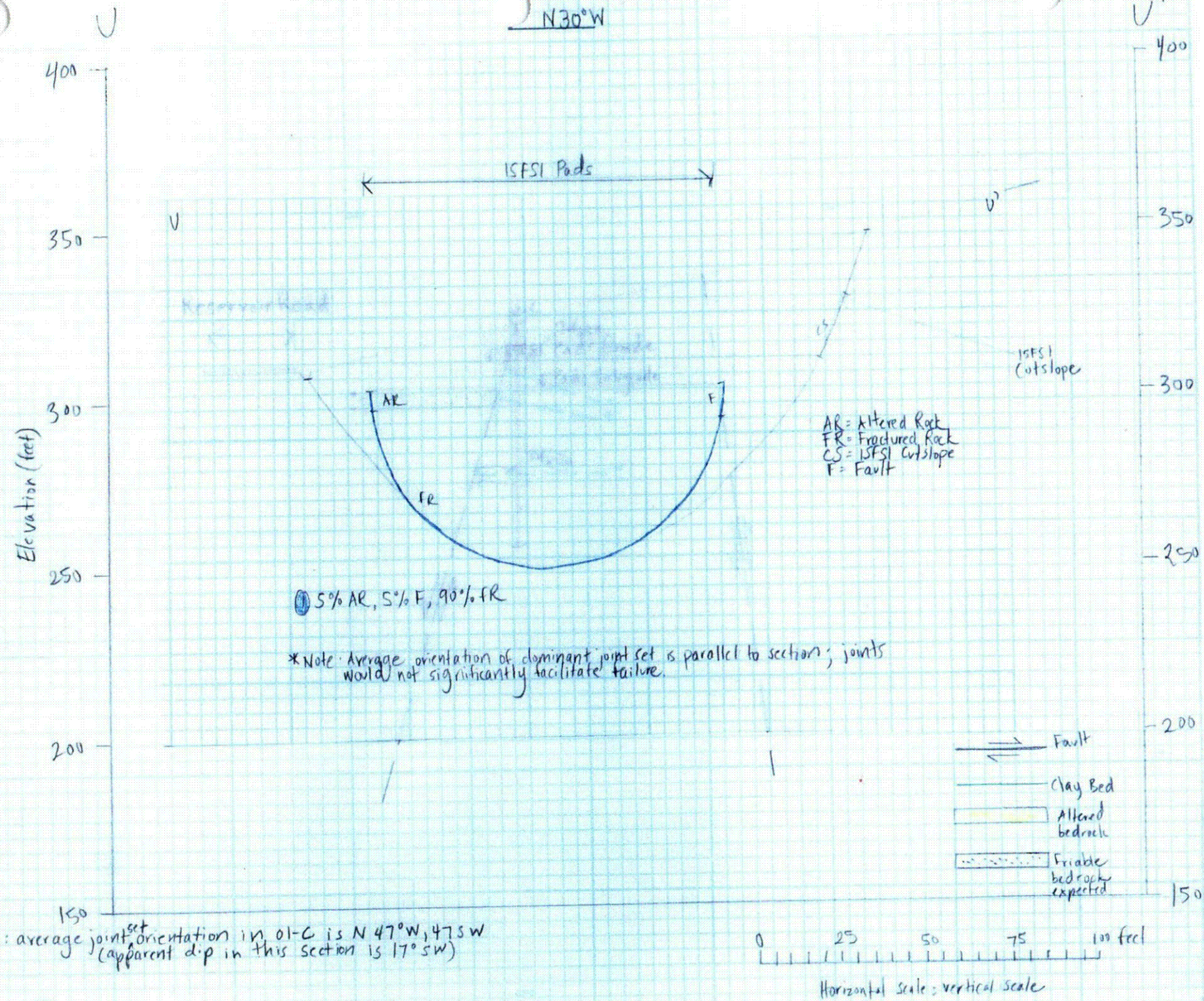

*Note: Average joint set orientation in 01-C is N 47°W, 47 SW (apparent dip in this section is 17° SW)

*Note: Average orientation of dominant joint set is parallel to section; joints would not significantly facilitate failure.

C-09

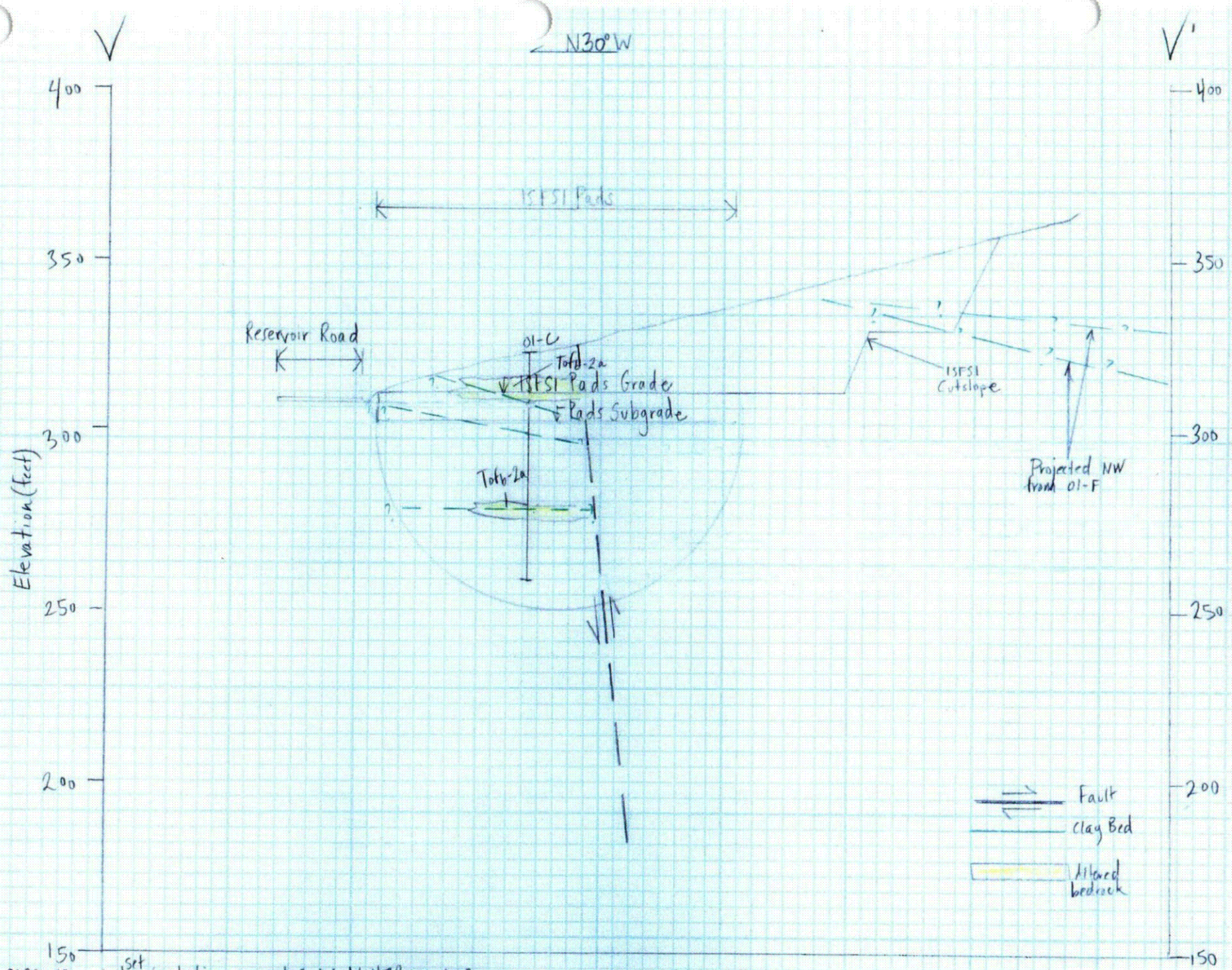

* Note: average joint set orientation in 01-C is N 47°W, 47SW (apparent dip in this section is 17°SW)

0 25 50 75 100 feet

Horizontal scale = vertical scale

C-10

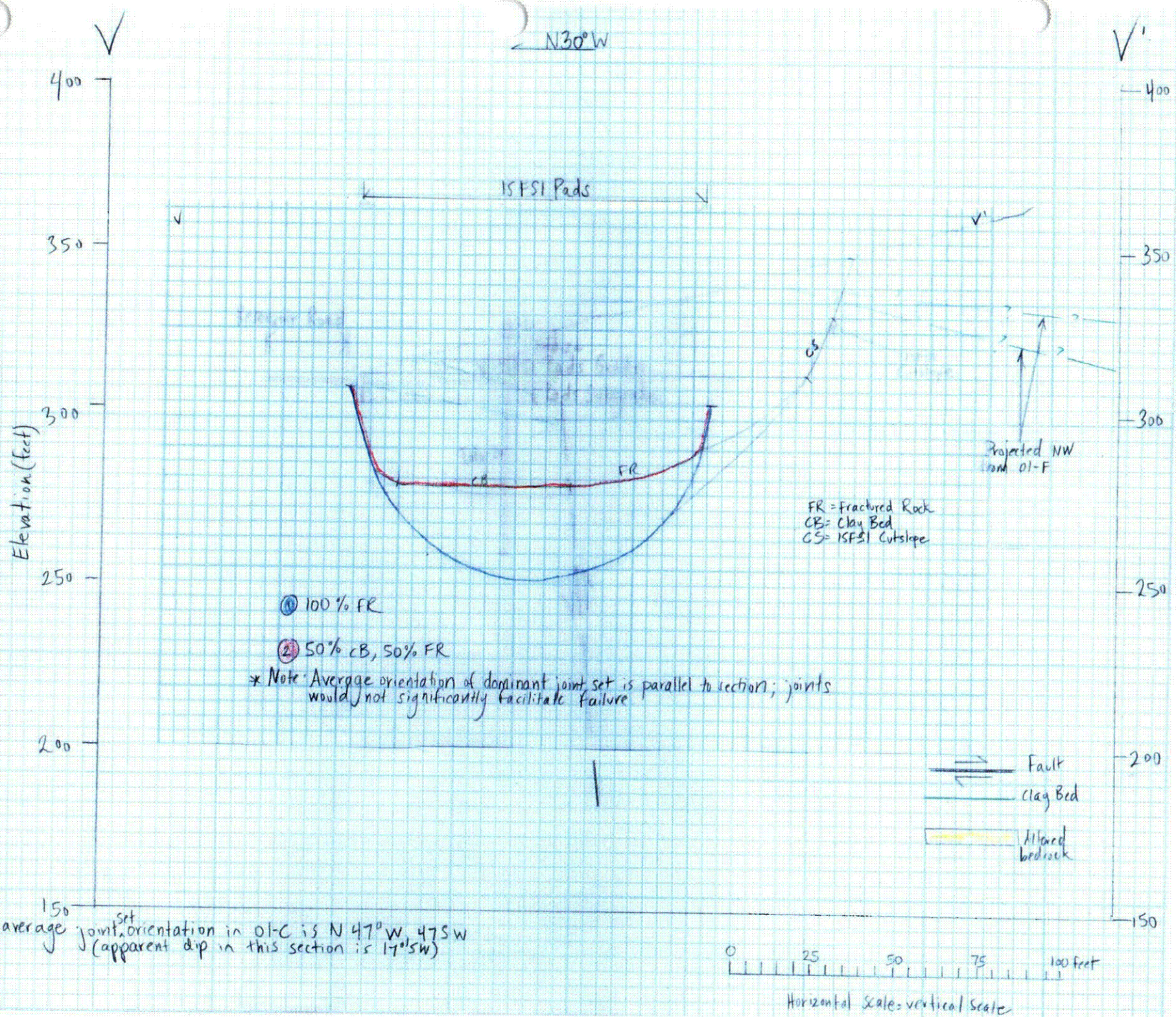
V
V'
N30°W
400
350
300
250
200
150
Elevation (feet)
ISFSI Pads
CB
FR
CS
Projected NW trend 01-F
FR = Fractured Rock
CB = Clay Bed
CS = ISFSI Cutslope
1 100% FR
2 50% CB, 50% FR
* Note: Average orientation of dominant joint set is parallel to section; joints would not significantly facilitate failure
Fault
Clay Bed
Altered bedrock
* Note: average 1st joint orientation in 01-C is N 47° W, 47 SW (apparent dip in this section is 17° SW)
0
25
50
75
100 feet
Horizontal scale = vertical scale

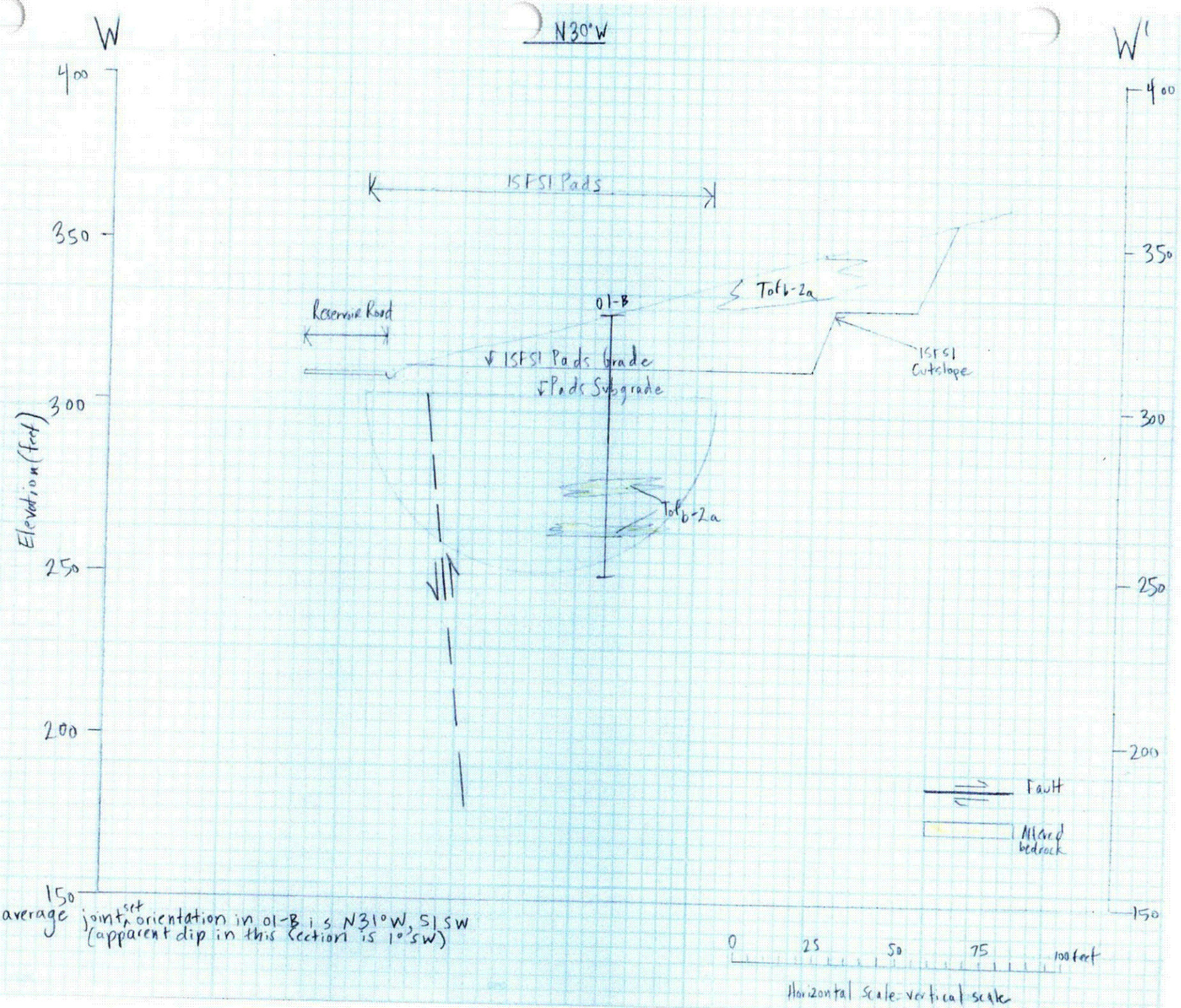

*Note: average joint set orientation in 01-B is N31°W, 51 SW (apparent dip in this section is 1° SW)

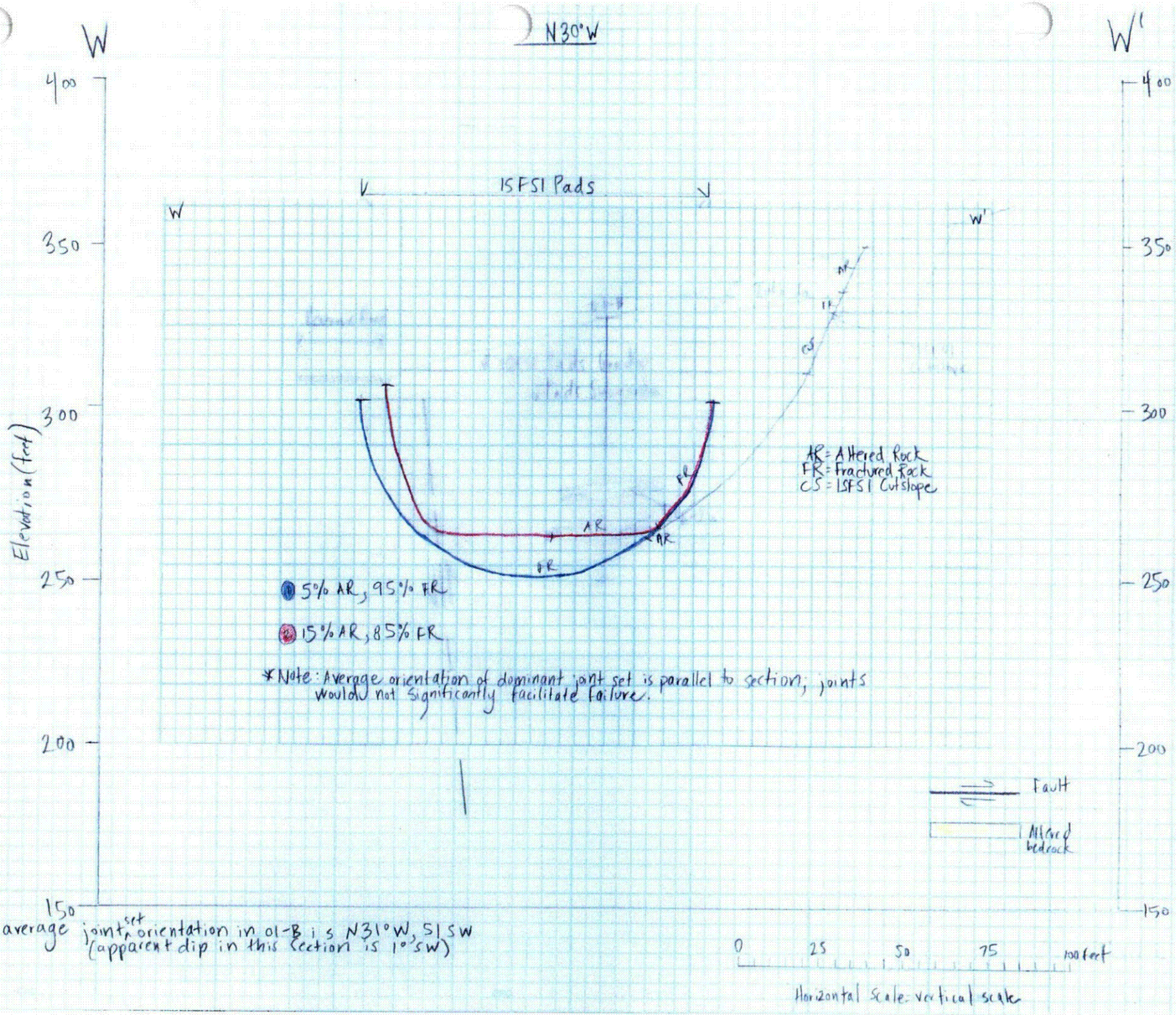

*Note. average joint set orientation in 01-B is N31°W, 51 SW (apparent dip in this section is 1° SW)

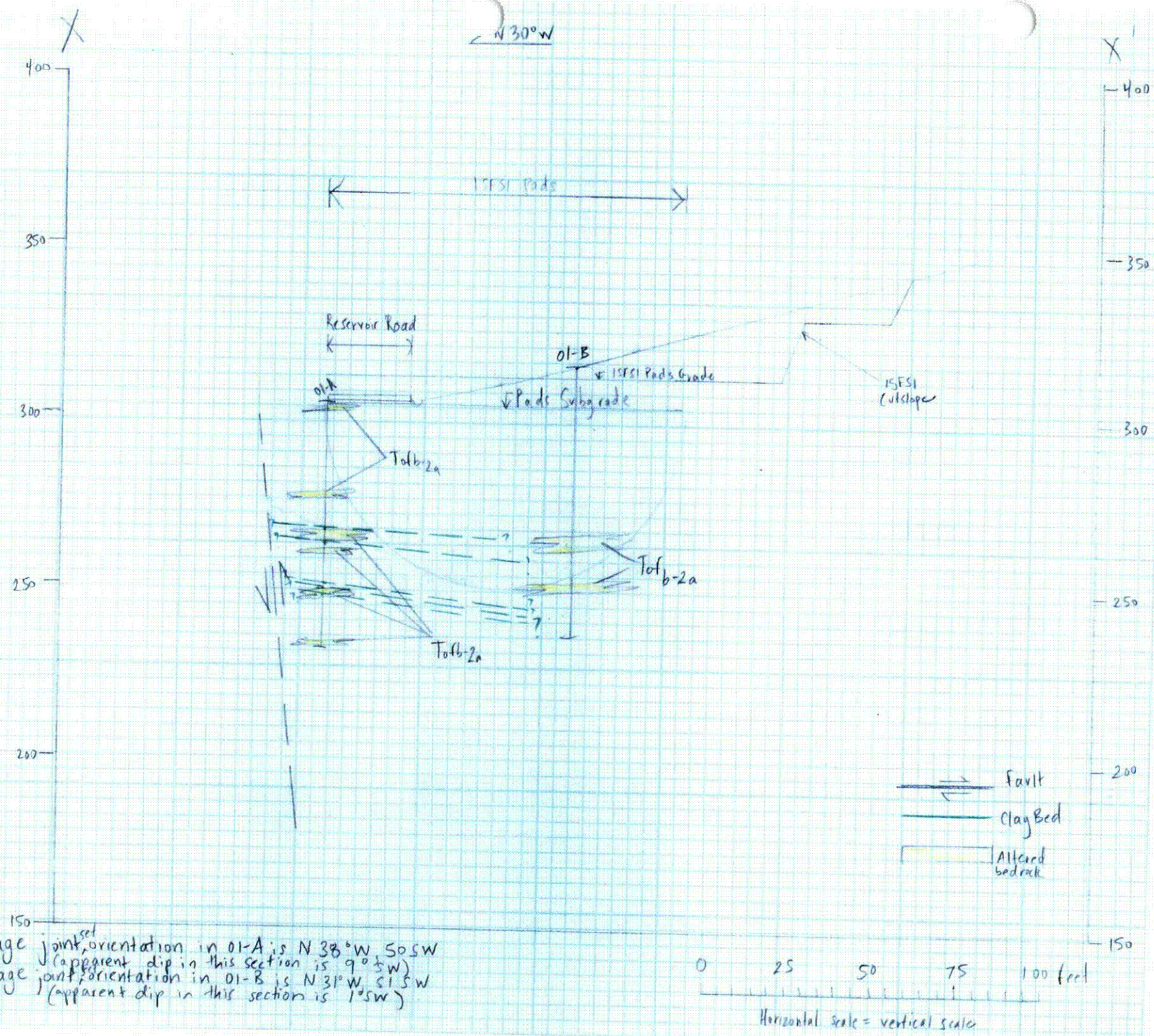

* Note: average joint set orientation in 01-A is N 38° W 50 SW (apparent dip in this section is 9° SW)
average joint set orientation in 01-B is N 31° W 51 SW (apparent dip in this section is 1° SW)

C-14

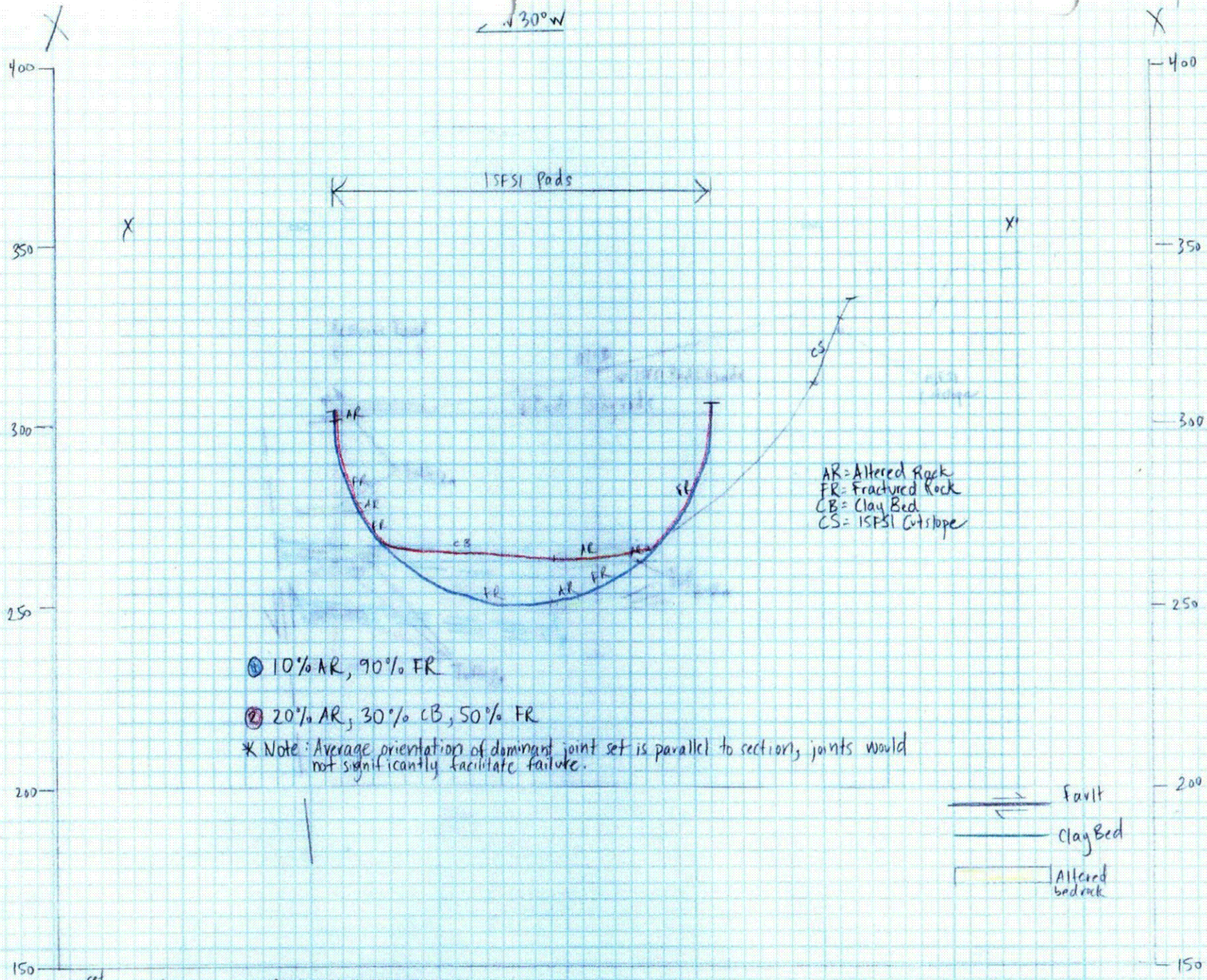

(1) 10% AR, 90% FR

(2) 20% AR, 30% CB, 50% FR

* Note: Average orientation of dominant joint set is parallel to section, joints would not significantly facilitate failure.

* Note: average joint set orientation in 01-A is N 38° W 50 SW (apparent dip in this section is 9° SW)
average joint orientation in 01-B is N 31° W 51 SW (apparent dip in this section is 1° SW)

C-15

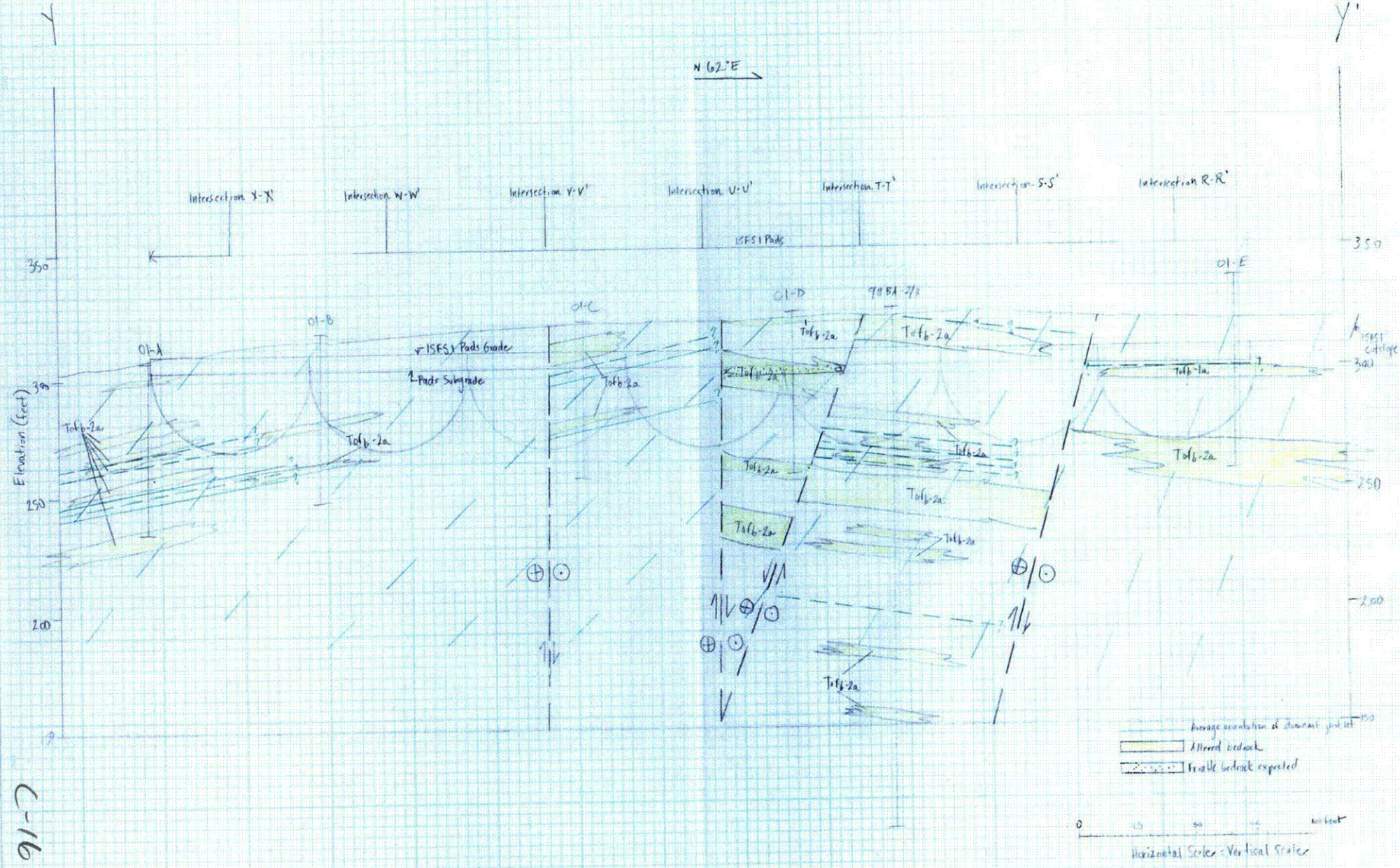
Y
Y'
N 62° E
Intersection X-X'
Intersection W-W'
Intersection V-V'
Intersection U-U'
Intersection T-T'
Intersection S-S'
Intersection R-R'
ISFS I Pads
01-A
01-B
01-C
01-D
01-E
ISFS I Pads Grade
Pads Subgrade
ISFS I cutslope
Tofb-2a
Tofb-1a
Elevation (feet)
350
300
250
200
150
Average orientation of dominant joint set
Altered bedrock
Fractured bedrock expected
0
50
100 feet
Horizontal Scale = Vertical Scale

C-16

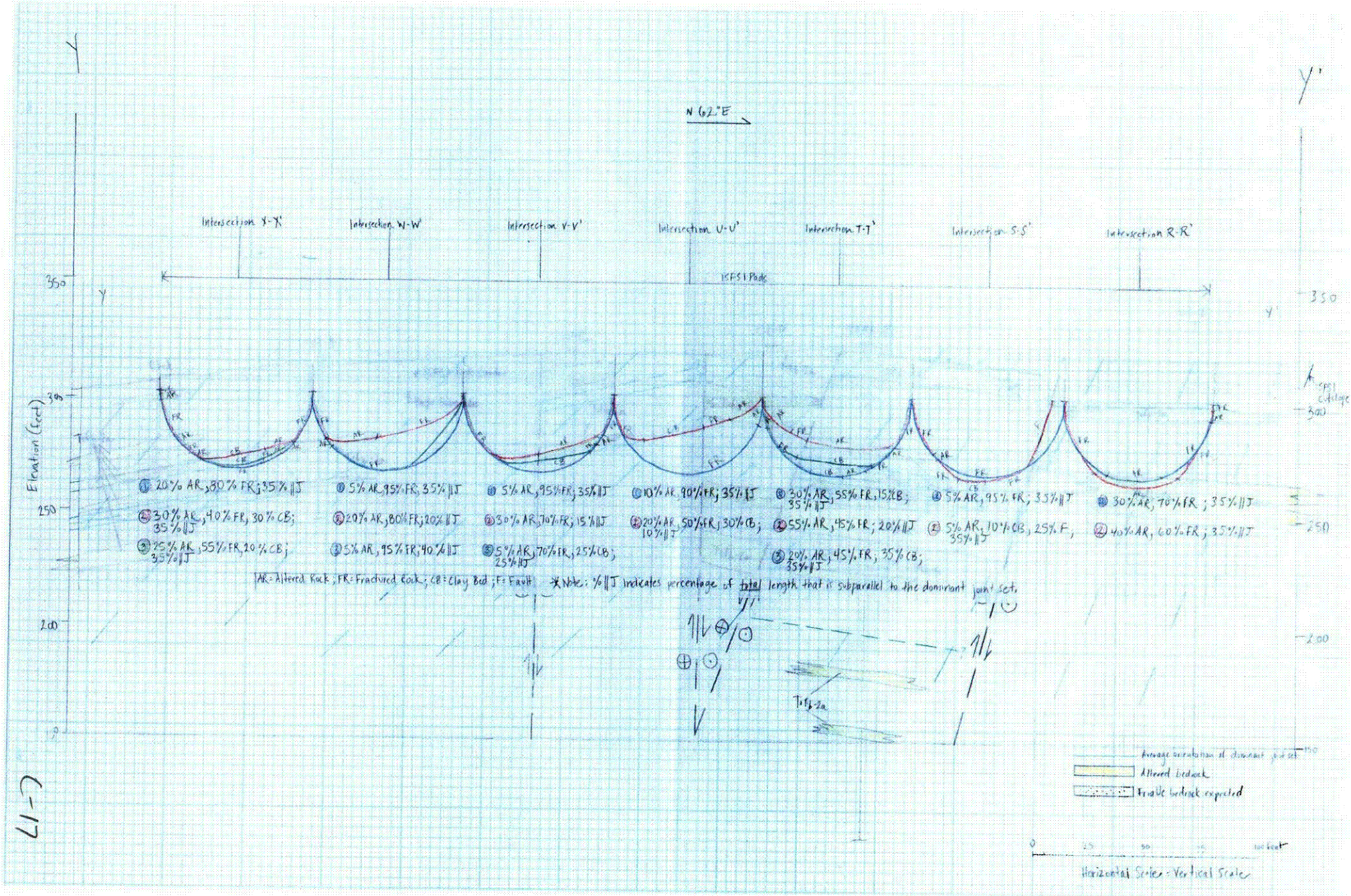
N 62.°E
Intersection X-X'
Intersection W-W'
Intersection V-V'
Intersection U-U'
Intersection T-T'
Intersection S-S'
Intersection R-R'
KFS1 Pad
Elevation (feet)
350
300
250
200
150
Y
Y'
① 20% AR, 80% FR; 35% ∥J
② 30% AR, 40% FR, 30% CB; 35% ∥J
③ 25% AR, 55% FR, 20% CB; 35% ∥J
④ 5% AR, 95% FR; 35% ∥J
⑤ 20% AR, 80% FR; 20% ∥J
⑥ 5% AR, 95% FR; 40% ∥J
⑦ 5% AR, 95% FR; 35% ∥J
⑧ 30% AR, 70% FR, 15% ∥J
⑨ 5% AR, 70% FR, 25% CB; 25% ∥J
⑩ 10% AR, 90% FR; 35% ∥J
⑪ 20% AR, 50% FR, 30% CB; 10% ∥J
⑫ 30% AR, 55% FR, 15% CB; 35% ∥J
⑬ 55% AR, 45% FR; 20% ∥J
⑭ 20% AR, 45% FR, 35% CB; 35% ∥J
⑮ 5% AR, 95% FR; 35% ∥J
⑯ 5% AR, 10% CB, 25% F, 35% ∥J
⑰ 30% AR, 70% FR; 35% ∥J
⑱ 40% AR, 60% FR; 35% ∥J
AR = Altered Rock; FR = Fractured Rock; CB = Clay Bed; F = Fault
*Note: % ∥J indicates percentage of total length that is subparallel to the dominant joint set.
Tuff-2a
Average orientation of dominant joint set
Altered bedrock
Fractured bedrock expected
Horizontal Scale = Vertical Scale

C-17

14.2 Attachment 2 – UTEXAS3 Computer Input and Output Files

14.2.1 UTEXAS3 Input File

```
PLOt output activated
HEADING ---------------------------------------------------
Diablo Canyon Power Plant ISFSI
Stability Analysis - Case 1

PROFILE LINE ----------------------------------------------
1 1 Rock
-200 .1
31.5 0

2 2 Clay Bed
-22 -34
-18 -26
21 -30
26 -31
85 -40

3 1 Rock
-22 -34
83 -46
85 -40

4 3 Joint
21 -30
31 0
37 0

5 3 Rock
26 -31
37 0
200 -1


MATERIAL -------- >>>> first stage <<< ---------------------
     1 Rock
         150 = unit weight
         Conventional shear strengths
         0  50
         No pore pressure
     2 Clay Bed
         150 = unit weight
         Conventional shear strengths
         800  15
         No pore pressure
     3 Joint
         150 = moist unit weight
         Conventional shear strengths
         0  26.5
         No pore pressure
```

```
Surface Pressures
-34    0      6950  0
8      0      0     0

ANAlysis/Computation
CIRCULAR Search
5      5   1   -100
Point
-34    0
stop

COMpute/Results
```

14.2.2 UTEXAS3 Output File

```
1          UTEXAS3 - VER. 1.200 - 12/16/92 - (C) 1985-1992 S. G. WRIGHT
           Date:  3: 7:2003   Time: 10:29:15   Input file: Casel.inp


           TABLE NO. 1
           ****************************************
           * COMPUTER PROGRAM DESIGNATION - UTEXAS3 *
           * Originally Coded By Stephen G. Wright  *
           * Version No. 1.200                      *
           * Last Revision Date 12/16/92            *
           * (C) Copyright 1985-1992 S. G. Wright   *
           * All Rights Reserved                    *
           ****************************************

           ************************************************************
           *                                                          *
           *      RESULTS OF COMPUTATIONS PERFORMED USING THIS COMPUTER *
           * PROGRAM SHOULD NOT BE USED FOR DESIGN PURPOSES UNLESS THEY *
           * HAVE BEEN VERIFIED BY INDEPENDENT ANALYSES, EXPERIMENTAL   *
           * DATA OR FIELD EXPERIENCE. THE USER SHOULD UNDERSTAND THE   *
           * ALGORITHMS AND ANALYTICAL PROCEDURES USED IN THE COMPUTER  *
           * PROGRAM AND MUST HAVE READ ALL DOCUMENTATION FOR THIS      *
           * PROGRAM BEFORE ATTEMPTING ITS USE.                         *
           *                                                            *
           *      NEITHER THE UNIVERSITY OF TEXAS NOR STEPHEN G. WRIGHT *
           * MAKE OR ASSUME LIABILITY FOR ANY WARRANTIES, EXPRESSED OR  *
           * IMPLIED, CONCERNING THE ACCURACY, RELIABILITY, USEFULNESS  *
           * OR ADAPTABILITY OF THIS COMPUTER PROGRAM.                  *
           *                                                            *
           ************************************************************
1          UTEXAS3 - VER. 1.200 - 12/16/92 -   1985-1992 S. G. WRIGHT
           Date:  3: 7:2003   Time: 10:29:1   Input file: Casel.inp
           Diablo Canyon Power Plant ISFSI
           Stability Analysis - Case 1


           TABLE NO.  2
           *************************
           * NEW PROFILE LINE DATA *
           *************************

           PROFILE LINE  1 - MATERIAL TYPE =  1
           Rock

                Point      X              Y
```

```
        1       -200.000          .100
        2         31.500          .000

PROFILE LINE  2 - MATERIAL TYPE =  2
Clay Bed

     Point       X              Y

        1       -22.000       -34.000
        2       -18.000       -26.000
        3        21.000       -30.000
        4        26.000       -31.000
        5        85.000       -40.000

PROFILE LINE  3 - MATERIAL TYPE =  1
Rock

     Point       X              Y

        1       -22.000       -34.000
        2        83.000       -46.000
        3        85.000       -40.000

PROFILE LINE  4 - MATERIAL TYPE =  3
Joint

     Point       X              Y

        1        21.000       -30.000
        2        31.000          .000
        3        37.000          .000

PROFILE LINE  5 - MATERIAL TYPE =  3
Rock

     Point       X              Y

        1        26.000       -31.000
        2        37.000          .000
        3       200.000        -1.000

All new profile lines defined - No old lines retained
1       UTEXAS3 - VER. 1.200 - 12/16/92 - (C) 1985-1992 S. G. WRIGHT
Date:  3: 7:2003   Time: 10:29:15   Input file: Case1.inp
Diablo Canyon Power Plant ISFSI
Stability Analysis - Case 1


TABLE NO.  3
**********************************************************************
* NEW MATERIAL PROPERTY DATA - CONVENTIONAL/FIRST-STAGE COMPUTATIONS *
**********************************************************************

DATA FOR MATERIAL TYPE  1
Rock

     Unit weight of material =  150.000

     CONVENTIONAL (ISOTROPIC) SHEAR STRENGTHS
     Cohesion - - - - - - - -        .000
```

```
     Friction angle - - - - -  50.000 degrees

     No (or zero) pore water pressures

DATA FOR MATERIAL TYPE  2
Clay Bed

     Unit weight of material =  150.000

     CONVENTIONAL (ISOTROPIC) SHEAR STRENGTHS
     Cohesion - - - - - - - -     800.000
     Friction angle - - - - -  15.000 degrees

     No (or zero) pore water pressures

DATA FOR MATERIAL TYPE  3
Joint

     Unit weight of material =  150.000

     CONVENTIONAL (ISOTROPIC) SHEAR STRENGTHS
     Cohesion - - - - - - - -        .000
     Friction angle - - - - -  26.500 degrees

     No (or zero) pore water pressures

All new material properties defined - No old data retained
1    UTEXAS3 - VER. 1.200 - 12/16/92 - (C) 1985-1992 S. G. WRIGHT
Date:  3: 7:2003   Time: 10:29:15   Input file: Case1.inp
Diablo Canyon Power Plant ISFSI
Stability Analysis - Case 1


TABLE NO. 10
*********************************************************************
* NEW SURFACE PRESSURE DATA - CONVENTIONAL/FIRST-STAGE COMPUTATIONS *
*********************************************************************

ALL NEW DATA INPUT - NO OLD DATA RETAINED

Surface Pressures -
                                   Normal       Shear
Point       X           Y        Pressure      Stress

   1     -34.000        .000     6950.000        .000
   2       8.000        .000         .000        .000
1    UTEXAS3 - VER. 1.200 - 12/16/92 - (C) 1985-1992 S. G. WRIGHT
Date:  3: 7:2003   Time: 10:29:15   Input file: Case1.inp
Diablo Canyon Power Plant ISFSI
Stability Analysis - Case 1


TABLE NO. 15
*********************************
* NEW ANALYSIS/COMPUTATION DATA *
*********************************

Circular Shear Surface(s)

Automatic Search Performed
```

```
Starting Center Coordinate for Search at -
                                          X =       5.000
                                          Y =       5.000

Required accuracy for critical center (= minimum
spacing between grid points) =       1.000

Critical shear surface not allowed to pass below Y =    -100.000

For the initial mode of search
all circles pass through the point at -
                                          X =     -34.000
                                          Y =        .000

Search terminated after initial mode completed

-----------------------------------------------------------------------
THE FOLLOWING REPRESENT EITHER DEFAULT OR PREVIOUSLY DEFINED VALUES:

Initial trial estimate for the factor of safety =   3.000

Initial trial estimate for side force inclination =  15.000 degrees
(Applicable to Spencer's procedure only)

Maximum number of iterations allowed for
calculating the factor of safety =   40

Allowed force imbalance for convergence =     100.000

Allowed moment imbalance for convergence =     100.000

Initial trial values for factor of safety (and side force inclination
for Spencer's procedure) will be kept constant during search

Maximum subtended angle to be used for subdivision of the
circle into slices =   3.00 degrees

Depth of crack =        .000

Depth of water in crack =        .000

Unit weight of water in crack =    62.400

Seismic coefficient =  .000

Conventional (single-stage) computations to be performed

Procedure used to compute the factor of safety: SPENCER
1       UTEXAS3 - VER. 1.200 - 12/16/92 - (C) 1985-1992 S. G. WRIGHT
Date:  3: 7:2003   Time: 10:29:15   Input file: Case1.inp
Diablo Canyon Power Plant ISFSI
Stability Analysis - Case 1


TABLE NO. 16
***************************
* NEW SLOPE GEOMETRY DATA *
***************************

NOTE - NO DATA WERE INPUT, SLOPE GEOMETRY DATA
WERE GENERATED BY THE PROGRAM
```

```
Slope Coordinates -

     Point       X           Y

        1    -200.000        .100
        2      31.500        .000
        3      37.000        .000
        4     200.000      -1.000
1    UTEXAS3 - VER. 1.200 - 12/16/92 - (C) 1985-1992 S. G. WRIGHT
     Date:  3: 7:2003   Time: 10:29:15   Input file: Case1.inp
     Diablo Canyon Power Plant ISFSI
     Stability Analysis - Case 1


     TABLE NO. 17
     INFORMATION FOR CURRENT MODE OF SEARCH - All Circles Pass Through
     the Fixed Point at   X =   -34.000  and Y =      .000
     ----------------------------------------------------------------
                                      1-Stage
     Center Coordinates               Factor  Side Force
                                        of    Inclination
          X         Y       Radius   Safety   (degrees)   Iterations


        -25.00    -25.00     26.57 Center of circle is below lowest
                                   point of slope - CIRCLE REJECTED
          5.00    -25.00     46.32 Center of circle is below lowest
                                   point of slope - CIRCLE REJECTED
         35.00    -25.00     73.39 Center of circle is below lowest
                                   point of slope - CIRCLE REJECTED
        -25.00      5.00     10.30  17.530     -33.95        38
     Message on the following line(s) applies to the above circle
     DENOMINATOR IN EQUATIONS FOR F WAS SMALL FOR   8 SLICES
     FIRST AND LAST SLICES WHERE DENOMINATOR WAS LOW -    37    44
          5.00      5.00     39.32   3.397     -14.44         4
     Message on the following line(s) applies to the above circle
     DENOMINATOR IN EQUATIONS FOR F WAS SMALL FOR   8 SLICES
     FIRST AND LAST SLICES WHERE DENOMINATOR WAS LOW -    55    62
         35.00      5.00     69.18  13.188     -22.83        23
     Message on the following line(s) applies to the above circle
     DENOMINATOR IN EQUATIONS FOR F WAS SMALL FOR   8 SLICES
     FIRST AND LAST SLICES WHERE DENOMINATOR WAS LOW -    55    62
        -25.00     35.00     36.14 See Message on Next Line(s)
     Last Trial Values =             22.000     -36.59        41
     (Last Trial Values Shown Above Are Not Correct Final Values)
     FATAL ERROR IN CALCULATING FACTOR OF SAFETY
     SOLUTION DID NOT CONVERGE WITHIN  40 ITERATIONS
          5.00     35.00     52.40   4.896      -7.86         7
         35.00     35.00     77.37   6.778      -5.96        10

           .00       .00     34.00   4.002     -16.68         6
     Message on the following line(s) applies to the above circle
     DENOMINATOR IN EQUATIONS FOR F WAS SMALL FOR   8 SLICES
     FIRST AND LAST SLICES WHERE DENOMINATOR WAS LOW -    54    61
          5.00       .00     39.00   5.136     -19.76         9
     Message on the following line(s) applies to the above circle
     DENOMINATOR IN EQUATIONS FOR F WAS SMALL FOR   9 SLICES
     FIRST AND LAST SLICES WHERE DENOMINATOR WAS LOW -    54    62
         10.00       .00     44.00   6.742     -19.74        10
     Message on the following line(s) applies to the above circle
```

```
DENOMINATOR IN EQUATIONS FOR F WAS SMALL FOR   8 SLICES
FIRST AND LAST SLICES WHERE DENOMINATOR WAS LOW -    55    62
      .00      5.00     34.37   4.723     -19.00        11
Message on the following line(s) applies to the above circle
DENOMINATOR IN EQUATIONS FOR F WAS SMALL FOR   9 SLICES
FIRST AND LAST SLICES WHERE DENOMINATOR WAS LOW -    51    59
    10.00      5.00     44.28   4.965     -19.01         6
Message on the following line(s) applies to the above circle
DENOMINATOR IN EQUATIONS FOR F WAS SMALL FOR   8 SLICES
FIRST AND LAST SLICES WHERE DENOMINATOR WAS LOW -    54    61
      .00     10.00     35.44   5.550     -18.03         8
Message on the following line(s) applies to the above circle
DENOMINATOR IN EQUATIONS FOR F WAS SMALL FOR   8 SLICES
FIRST AND LAST SLICES WHERE DENOMINATOR WAS LOW -    48    55
     5.00     10.00     40.26   4.011     -17.36         4
Message on the following line(s) applies to the above circle
DENOMINATOR IN EQUATIONS FOR F WAS SMALL FOR   8 SLICES
FIRST AND LAST SLICES WHERE DENOMINATOR WAS LOW -    52    59
    10.00     10.00     45.12   3.491     -14.18         9
Message on the following line(s) applies to the above circle
DENOMINATOR IN EQUATIONS FOR F WAS SMALL FOR   7 SLICES
FIRST AND LAST SLICES WHERE DENOMINATOR WAS LOW -    52    58

     2.00      2.00     36.06   3.641     -14.64         7
Message on the following line(s) applies to the above circle
DENOMINATOR IN EQUATIONS FOR F WAS SMALL FOR   9 SLICES
FIRST AND LAST SLICES WHERE DENOMINATOR WAS LOW -    57    65
     5.00      2.00     39.05   4.026     -15.26        10
Message on the following line(s) applies to the above circle
DENOMINATOR IN EQUATIONS FOR F WAS SMALL FOR   8 SLICES
FIRST AND LAST SLICES WHERE DENOMINATOR WAS LOW -    58    65
     8.00      2.00     42.05   5.395     -19.50         7
Message on the following line(s) applies to the above circle
DENOMINATOR IN EQUATIONS FOR F WAS SMALL FOR   8 SLICES
FIRST AND LAST SLICES WHERE DENOMINATOR WAS LOW -    55    62
     2.00      5.00     36.35   3.973     -15.81         5
Message on the following line(s) applies to the above circle
DENOMINATOR IN EQUATIONS FOR F WAS SMALL FOR   8 SLICES
FIRST AND LAST SLICES WHERE DENOMINATOR WAS LOW -    55    62
     8.00      5.00     42.30   3.821     -17.61         5
Message on the following line(s) applies to the above circle
DENOMINATOR IN EQUATIONS FOR F WAS SMALL FOR   8 SLICES
FIRST AND LAST SLICES WHERE DENOMINATOR WAS LOW -    52    59
     2.00      8.00     36.88   4.587     -18.22         6
Message on the following line(s) applies to the above circle
DENOMINATOR IN EQUATIONS FOR F WAS SMALL FOR   9 SLICES
FIRST AND LAST SLICES WHERE DENOMINATOR WAS LOW -    51    59
     5.00      8.00     39.81   3.660     -15.91         4
Message on the following line(s) applies to the above circle
DENOMINATOR IN EQUATIONS FOR F WAS SMALL FOR   8 SLICES
FIRST AND LAST SLICES WHERE DENOMINATOR WAS LOW -    52    59
     8.00      8.00     42.76   3.424     -14.15         7
Message on the following line(s) applies to the above circle
DENOMINATOR IN EQUATIONS FOR F WAS SMALL FOR   9 SLICES
FIRST AND LAST SLICES WHERE DENOMINATOR WAS LOW -    54    62

     4.00      4.00     38.21   3.377     -15.20         4
Message on the following line(s) applies to the above circle
DENOMINATOR IN EQUATIONS FOR F WAS SMALL FOR   8 SLICES
FIRST AND LAST SLICES WHERE DENOMINATOR WAS LOW -    55    62
     5.00      4.00     39.20   3.434     -14.33         6
```

```
Message on the following line(s) applies to the above circle
DENOMINATOR IN EQUATIONS FOR F WAS SMALL FOR   8 SLICES
FIRST AND LAST SLICES WHERE DENOMINATOR WAS LOW -    55    62
      6.00      4.00     40.20   3.426     -15.59         4
Message on the following line(s) applies to the above circle
DENOMINATOR IN EQUATIONS FOR F WAS SMALL FOR   8 SLICES
FIRST AND LAST SLICES WHERE DENOMINATOR WAS LOW -    55    62
      4.00      5.00     38.33   3.439     -15.61         4
Message on the following line(s) applies to the above circle
DENOMINATOR IN EQUATIONS FOR F WAS SMALL FOR   8 SLICES
FIRST AND LAST SLICES WHERE DENOMINATOR WAS LOW -    54    61
      6.00      5.00     40.31   3.391     -15.67         4
Message on the following line(s) applies to the above circle
DENOMINATOR IN EQUATIONS FOR F WAS SMALL FOR   8 SLICES
FIRST AND LAST SLICES WHERE DENOMINATOR WAS LOW -    53    60
      4.00      6.00     38.47   3.568     -16.22         4
Message on the following line(s) applies to the above circle
DENOMINATOR IN EQUATIONS FOR F WAS SMALL FOR   8 SLICES
FIRST AND LAST SLICES WHERE DENOMINATOR WAS LOW -    53    60
      5.00      6.00     39.46   3.360     -14.61         5
Message on the following line(s) applies to the above circle
DENOMINATOR IN EQUATIONS FOR F WAS SMALL FOR   8 SLICES
FIRST AND LAST SLICES WHERE DENOMINATOR WAS LOW -    54    61
      6.00      6.00     40.45   3.358     -15.79         3
Message on the following line(s) applies to the above circle
DENOMINATOR IN EQUATIONS FOR F WAS SMALL FOR   8 SLICES
FIRST AND LAST SLICES WHERE DENOMINATOR WAS LOW -    54    61

      7.00      5.00     41.30   3.403     -16.41         4
Message on the following line(s) applies to the above circle
DENOMINATOR IN EQUATIONS FOR F WAS SMALL FOR   8 SLICES
FIRST AND LAST SLICES WHERE DENOMINATOR WAS LOW -    54    61
      7.00      6.00     41.44   3.372     -16.50         4
Message on the following line(s) applies to the above circle
DENOMINATOR IN EQUATIONS FOR F WAS SMALL FOR   8 SLICES
FIRST AND LAST SLICES WHERE DENOMINATOR WAS LOW -    55    62
      5.00      7.00     39.62   3.501     -15.23         4
Message on the following line(s) applies to the above circle
DENOMINATOR IN EQUATIONS FOR F WAS SMALL FOR   8 SLICES
FIRST AND LAST SLICES WHERE DENOMINATOR WAS LOW -    53    60
      6.00      7.00     40.61   3.344     -16.00         3
Message on the following line(s) applies to the above circle
DENOMINATOR IN EQUATIONS FOR F WAS SMALL FOR   8 SLICES
FIRST AND LAST SLICES WHERE DENOMINATOR WAS LOW -    53    60
      7.00      7.00     41.59   3.340     -16.62         5
Message on the following line(s) applies to the above circle
DENOMINATOR IN EQUATIONS FOR F WAS SMALL FOR   8 SLICES
FIRST AND LAST SLICES WHERE DENOMINATOR WAS LOW -    54    61

      8.00      6.00     42.43   3.397     -16.83         7
Message on the following line(s) applies to the above circle
DENOMINATOR IN EQUATIONS FOR F WAS SMALL FOR   8 SLICES
FIRST AND LAST SLICES WHERE DENOMINATOR WAS LOW -    53    60
      8.00      7.00     42.58   3.452     -14.04         7
Message on the following line(s) applies to the above circle
DENOMINATOR IN EQUATIONS FOR F WAS SMALL FOR   8 SLICES
FIRST AND LAST SLICES WHERE DENOMINATOR WAS LOW -    53    60
      6.00      8.00     40.79   3.389     -16.38         4
Message on the following line(s) applies to the above circle
DENOMINATOR IN EQUATIONS FOR F WAS SMALL FOR   8 SLICES
FIRST AND LAST SLICES WHERE DENOMINATOR WAS LOW -    52    59
```

```
      7.00      8.00      41.77   3.432     -13.97          8
Message on the following line(s) applies to the above circle
DENOMINATOR IN EQUATIONS FOR F WAS SMALL FOR   8 SLICES
FIRST AND LAST SLICES WHERE DENOMINATOR WAS LOW -    54    61

At the end of the current mode of search the most critical
circle which was found has the following values -
X-center =      7.00     Y-center =      7.00     Radius =     41.59
Factor of Safety =   3.340     Side Force Inclination = -16.62
1       UTEXAS3 - VER. 1.200 - 12/16/92 - (C) 1985-1992 S. G. WRIGHT
Date:  3: 7:2003   Time: 10:29:15   Input file: Case1.inp
Diablo Canyon Power Plant ISFSI
Stability Analysis - Case 1


TABLE NO. 21
*****  1-STAGE FINAL CRITICAL CIRCLE INFORMATION  *****
X Coordinate of Center - - - - - - -     7.000
Y Coordinate of Center - - - - - - -     7.000
Radius - - - - - - - - - - - - - - -    41.593
Factor of Safety - - - - - - - - - -     3.340
Side Force Inclination - - - - - - -    -16.62

Number of circles tried  - - - - - -   42
No. of circles F calc. for - - - - -   38
1       UTEXAS3 - VER. 1.200 - 12/16/92 - (C) 1985-1992 S. G. WRIGHT
Date:  3: 7:2003   Time: 10:29:15   Input file: Case1.inp
Diablo Canyon Power Plant ISFSI
Stability Analysis - Case 1


TABLE NO. 26
*************************************************************
*  Coordinate, Weight, Strength and Pore Water Pressure     *
*  Information for Individual Slices for Conventional       *
*  Computations or First Stage of Multi-Stage Computations. *
*  (Information is for the Critical Shear Surface in the    *
*  Case of an Automatic Search.)                            *
*************************************************************
```

Slice No.	X	Y	Slice Weight	Matl. Type	Cohesion	Friction Angle	Pore Pressure
	-34.0	.0					
1	-34.0	.0	.0	1	.00	50.00	.0
	-34.0	.0					
2	-33.8	-1.1	69.5	1	.00	50.00	.0
	-33.6	-2.1					
3	-33.3	-3.2	257.8	1	.00	50.00	.0
	-33.0	-4.2					
4	-32.7	-5.3	513.1	1	.00	50.00	.0
	-32.4	-6.3					
5	-32.0	-7.3	831.6	1	.00	50.00	.0
	-31.6	-8.4					
6	-31.2	-9.4	1208.9	1	.00	50.00	.0
	-30.8	-10.4					
7	-30.3	-11.4	1640.0	1	.00	50.00	.0
	-29.8	-12.3					
8	-29.3	-13.3	2119.3	1	.00	50.00	.0
	-28.8	-14.2					
9	-28.2	-15.1	2640.5	1	.00	50.00	.0

	-27.6	-16.1					
10	-27.0	-17.0	3197.3	1	.00	50.00	.0
	-26.4	-17.9					
11	-25.7	-18.7	3782.6	1	.00	50.00	.0
	-25.0	-19.6					
12	-24.3	-20.4	4389.3	1	.00	50.00	.0
	-23.6	-21.2					
13	-22.8	-22.0	5010.0	1	.00	50.00	.0
	-22.1	-22.8					
14	-22.0	-22.8	188.9	1	.00	50.00	.0
	-22.0	-22.8					
15	-21.2	-23.6	5659.2	1	.00	50.00	.0
	-20.4	-24.3					
16	-19.6	-25.0	6285.0	1	.00	50.00	.0
	-18.7	-25.7					
17	-18.4	-25.9	2478.9	1	.00	50.00	.0
	-18.1	-26.2					
18	-18.0	-26.2	345.0	2	800.00	15.00	.0
	-18.0	-26.2					
19	-17.1	-26.9	7156.4	2	800.00	15.00	.0
	-16.2	-27.5					
20	-15.3	-28.1	7748.1	2	800.00	15.00	.0
	-14.4	-28.7					
21	-13.4	-29.2	8313.4	2	800.00	15.00	.0
	-12.5	-29.7					

1 UTEXAS3 - VER. 1.200 - 12/16/92 - (C) 1985-1992 S. G. WRIGHT
Date: 3: 7:2003 Time: 10:29:15 Input file: Case1.inp
Diablo Canyon Power Plant ISFSI
Stability Analysis - Case 1

TABLE NO. 26

```
*************************************************************
*  Coordinate, Weight, Strength and Pore Water Pressure     *
*  Information for Individual Slices for Conventional       *
*  Computations or First Stage of Multi-Stage Computations. *
*  (Information is for the Critical Shear Surface in the    *
*  Case of an Automatic Search.)                            *
*************************************************************
```

Slice No.	X	Y	Slice Weight	Matl. Type	Cohesion	Friction Angle	Pore Pressure
	-12.5	-29.7					
22	-11.5	-30.2	8845.8	2	800.00	15.00	.0
	-10.5	-30.7					
23	-9.5	-31.1	9338.8	2	800.00	15.00	.0
	-8.5	-31.6					
24	-7.5	-32.0	9786.7	2	800.00	15.00	.0
	-6.5	-32.3					
25	-5.5	-32.7	10184.2	2	800.00	15.00	.0
	-4.4	-33.0					
26	-3.4	-33.3	10526.6	2	800.00	15.00	.0
	-2.3	-33.5					
27	-1.3	-33.8	10809.9	2	800.00	15.00	.0
	-.2	-34.0					
28	.9	-34.1	11030.8	2	800.00	15.00	.0
	2.0	-34.3					
29	3.1	-34.4	11186.7	2	800.00	15.00	.0
	4.1	-34.5					
30	5.2	-34.5	11275.8	2	800.00	15.00	.0

	6.3	-34.6					
31	6.7	-34.6	3563.3	2	800.00	15.00	.0
	7.0	-34.6					
32	7.5	-34.6	5189.6	2	800.00	15.00	.0
	8.0	-34.6					
33	9.1	-34.5	11266.5	2	800.00	15.00	.0
	10.2	-34.5					
34	11.3	-34.4	11167.2	2	800.00	15.00	.0
	12.3	-34.2					
35	13.4	-34.1	11001.2	2	800.00	15.00	.0
	14.5	-33.9					
36	15.6	-33.7	10770.5	2	800.00	15.00	.0
	16.6	-33.5					
37	17.7	-33.2	10478.0	2	800.00	15.00	.0
	18.7	-32.9					
38	19.8	-32.6	10126.8	2	800.00	15.00	.0
	20.8	-32.2					
39	20.9	-32.2	964.4	2	800.00	15.00	.0
	21.0	-32.2					
40	22.0	-31.8	9679.1	2	800.00	15.00	.0
	23.0	-31.4					
41	23.8	-31.0	7071.8	2	800.00	15.00	.0
	24.5	-30.7					
42	25.3	-30.4	6607.0	3	.00	26.50	.0
	26.0	-30.0					

1 UTEXAS3 - VER. 1.200 - 12/16/92 - (C) 1985-1992 S. G. WRIGHT
Date: 3: 7:2003 Time: 10:29:15 Input file: Casel.inp
Diablo Canyon Power Plant ISFSI
Stability Analysis - Case 1

TABLE NO. 26

```
*************************************************************
*  Coordinate, Weight, Strength and Pore Water Pressure     *
*  Information for Individual Slices for Conventional       *
*  Computations or First Stage of Multi-Stage Computations. *
*  (Information is for the Critical Shear Surface in the    *
*  Case of an Automatic Search.)                            *
*************************************************************
```

Slice No.	X	Y	Slice Weight	Matl. Type	Cohesion	Friction Angle	Pore Pressure
	26.0	-30.0					
43	26.2	-29.9	1951.7	3	.00	26.50	.0
	26.4	-29.8					
44	27.4	-29.2	8324.6	3	.00	26.50	.0
	28.3	-28.7					
45	29.3	-28.1	7759.9	3	.00	26.50	.0
	30.2	-27.5					
46	30.6	-27.3	3382.3	3	.00	26.50	.0
	31.0	-27.0					
47	31.3	-26.8	2009.3	3	.00	26.50	.0
	31.5	-26.6					
48	32.4	-25.9	6716.0	3	.00	26.50	.0
	33.2	-25.3					
49	34.1	-24.6	6095.8	3	.00	26.50	.0
	34.9	-23.9					
50	35.7	-23.1	5468.9	3	.00	26.50	.0
	36.5	-22.4					
51	36.7	-22.1	1801.0	3	.00	26.50	.0

	37.0	-21.8					
52	37.7	-21.0	4620.1	3	.00	26.50	.0
	38.5	-20.2					
53	39.2	-19.4	4005.6	3	.00	26.50	.0
	39.8	-18.5					
54	40.5	-17.6	3410.0	3	.00	26.50	.0
	41.1	-16.8					
55	41.7	-15.9	2840.7	3	.00	26.50	.0
	42.3	-14.9					
56	42.9	-14.0	2304.5	3	.00	26.50	.0
	43.4	-13.1					
57	43.9	-12.1	1808.3	3	.00	26.50	.0
	44.4	-11.1					
58	44.9	-10.1	1358.2	3	.00	26.50	.0
	45.3	-9.1					
59	45.7	-8.1	960.1	3	.00	26.50	.0
	46.1	-7.1					
60	46.5	-6.1	619.3	3	.00	26.50	.0
	46.8	-5.0					
61	47.1	-4.0	340.3	3	.00	26.50	.0
	47.4	-2.9					
62	47.6	-1.9	127.1	3	.00	26.50	.0
	47.9	-.8					
63	47.9	-.4	7.8	3	.00	26.50	.0
	48.0	-.1					

1 UTEXAS3 - VER. 1.200 - 12/16/92 - (C) 1985-1992 S. G. WRIGHT
Date: 3: 7:2003 Time: 10:29:15 Input file: Casel.inp
Diablo Canyon Power Plant ISFSI
Stability Analysis - Case 1

TABLE NO. 27

```
*************************************************************
*  Seismic Forces and Forces Due to Surface Pressures for   *
*  Individual Slices for Conventional  Computations or the  *
*  First Stage of Multi-Stage Computations.                 *
*  (Information is for the Critical Shear Surface in the    *
*  Case of an Automatic Search.)                            *
*************************************************************
```

				FORCES DUE TO SURFACE PRESSURES			
Slice No.	X	Seismic Force	Y for Seismic Force	Normal Force	Shear Force	X	Y
1	-34.0	0.	.0	0.	0.	-34.0	.0
2	-33.8	0.	-.5	2922.	0.	-33.8	.0
3	-33.3	0.	-1.6	3649.	0.	-33.3	.0
4	-32.7	0.	-2.6	4336.	0.	-32.7	.0
5	-32.0	0.	-3.7	4977.	0.	-32.0	.0
6	-31.2	0.	-4.7	5565.	0.	-31.2	.0
7	-30.3	0.	-5.7	6092.	0.	-30.3	.0
8	-29.3	0.	-6.6	6555.	0.	-29.3	.0
9	-28.2	0.	-7.6	6946.	0.	-28.2	.0
10	-27.0	0.	-8.5	7264.	0.	-27.0	.0
11	-25.7	0.	-9.3	7503.	0.	-25.7	.0
12	-24.3	0.	-10.2	7662.	0.	-24.3	.0
13	-22.8	0.	-11.0	7739.	0.	-22.8	.0
14	-22.0	0.	-11.4	274.	0.	-22.0	.0
15	-21.2	0.	-11.8	7732.	0.	-21.2	.0
16	-19.6	0.	-12.5	7641.	0.	-19.6	.0

17	-18.4	0.	-13.0	2783.	0.	-18.4	.0
18	-18.0	0.	-13.1	378.	0.	-18.0	.0
19	-17.1	0.	-13.4	7372.	0.	-17.1	.0
20	-15.3	0.	-14.0	7087.	0.	-15.3	.0
21	-13.4	0.	-14.6	6728.	0.	-13.5	.0
22	-11.5	0.	-15.1	6297.	0.	-11.5	.0
23	-9.5	0.	-15.6	5800.	0.	-9.6	.0
24	-7.5	0.	-16.0	5242.	0.	-7.5	.0
25	-5.5	0.	-16.3	4629.	0.	-5.5	.0
26	-3.4	0.	-16.6	3968.	0.	-3.4	.0
27	-1.3	0.	-16.9	3267.	0.	-1.3	.0
28	.9	0.	-17.1	2533.	0.	.8	.0
29	3.1	0.	-17.2	1774.	0.	3.0	.0
30	5.2	0.	-17.3	999.	0.	5.1	.0
31	6.7	0.	-17.3	153.	0.	6.6	.0
32	7.5	0.	-17.3	83.	0.	7.3	.0
33	9.1	0.	-17.3	0.	0.	9.1	.0
34	11.3	0.	-17.2	0.	0.	11.3	.0
35	13.4	0.	-17.0	0.	0.	13.4	.0
36	15.6	0.	-16.8	0.	0.	15.6	.0
37	17.7	0.	-16.6	0.	0.	17.7	.0
38	19.8	0.	-16.3	0.	0.	19.8	.0
39	20.9	0.	-16.1	0.	0.	20.9	.0
40	22.0	0.	-15.9	0.	0.	22.0	.0

1 UTEXAS3 - VER. 1.200 - 12/16/92 - (C) 1985-1992 S. G. WRIGHT
Date: 3: 7:2003 Time: 10:29:15 Input file: Case1.inp
Diablo Canyon Power Plant ISFSI
Stability Analysis - Case 1

TABLE NO. 27

```
*************************************************************
*  Seismic Forces and Forces Due to Surface Pressures for   *
*  Individual Slices for Conventional  Computations or the  *
*  First Stage of Multi-Stage Computations.                 *
*  (Information is for the Critical Shear Surface in the    *
*  Case of an Automatic Search.)                            *
*************************************************************
```

Slice No.	X	Seismic Force	Y for Seismic Force	FORCES DUE TO SURFACE PRESSURES Normal Force	Shear Force	X	Y
41	23.8	0.	-15.5	0.	0.	23.8	.0
42	25.3	0.	-15.2	0.	0.	25.3	.0
43	26.2	0.	-14.9	0.	0.	26.2	.0
44	27.4	0.	-14.6	0.	0.	27.4	.0
45	29.3	0.	-14.1	0.	0.	29.3	.0
46	30.6	0.	-13.6	0.	0.	30.6	.0
47	31.3	0.	-13.4	0.	0.	31.3	.0
48	32.4	0.	-13.0	0.	0.	32.4	.0
49	34.1	0.	-12.3	0.	0.	34.1	.0
50	35.7	0.	-11.6	0.	0.	35.7	.0
51	36.7	0.	-11.0	0.	0.	36.7	.0
52	37.7	0.	-10.5	0.	0.	37.7	.0
53	39.2	0.	-9.7	0.	0.	39.2	.0
54	40.5	0.	-8.8	0.	0.	40.5	.0
55	41.7	0.	-7.9	0.	0.	41.7	.0
56	42.9	0.	-7.0	0.	0.	42.9	.0
57	43.9	0.	-6.1	0.	0.	43.9	.0

```
  58     44.9       0.       -5.1       0.       0.     44.9       .0
  59     45.7       0.       -4.1       0.       0.     45.7      -.1
  60     46.5       0.       -3.1       0.       0.     46.5      -.1
  61     47.1       0.       -2.0       0.       0.     47.1      -.1
  62     47.6       0.       -1.0       0.       0.     47.6      -.1
  63     47.9       0.        -.3       0.       0.     47.9      -.1
1       UTEXAS3 - VER. 1.200 - 12/16/92 - (C) 1985-1992 S. G. WRIGHT
        Date:  3: 7:2003   Time: 10:29:15   Input file: Casel.inp
        Diablo Canyon Power Plant ISFSI
        Stability Analysis - Case 1


        TABLE NO. 29
        ********************************************************************
        *  Information Generated During Iterative Solution for the Factor  *
        *  of Safety and Side Force Inclination by Spencer's Procedure     *
        ********************************************************************

              Trial     Trial
             Factor   Side Force    Force      Moment                 Delta
        Iter-   of    Inclination  Imbalance  Imbalance   Delta-F    Theta
        ation  Safety   (degrees)    (lbs.)   (ft.-lbs.)            (degrees)

           1   3.00000   -15.0000  -.7017E+06   .1603E+07
        On iteration   1 the following slices produced
        low denominators in the equations for the factor
        of safety -   55  56  57  58  59  60  61
        First-order corrections to F and THETA .........  -.610E+00  .180E+01
        Values factored by  .820E+00 - Deltas too large   -.500E+00  .148E+01

           2   2.50000   -13.5238  -.4748E+05   .1015E+07
        On iteration   2 the following slices produced
        low denominators in the equations for the factor
        of safety -   55  56  57  58  59  60  61
        First-order corrections to F and THETA .........   .780E+00 -.364E+01
        Values factored by  .641E+00 - Deltas too large    .500E+00 -.233E+01

           3   3.00000   -15.8548   .3618E+05   .2831E+06
        On iteration   3 the following slices produced
        low denominators in the equations for the factor
        of safety -   54  55  56  57  58  59  60  61
        First-order corrections to F and THETA .........   .292E+00 -.689E+00
        Second-order correction - Iteration   1 ........   .311E+00 -.689E+00
        Second-order correction - Iteration   2 ........   .311E+00 -.689E+00
        Second-order correction - Iteration   3 ........   .311E+00 -.689E+00

           4   3.31067   -16.5436   .1058E+04   .2605E+05
        On iteration   4 the following slices produced
        low denominators in the equations for the factor
        of safety -   54  55  56  57  58  59  60  61
        First-order corrections to F and THETA .........   .295E-01 -.735E-01
        Second-order correction - Iteration   1 ........   .298E-01 -.735E-01
        Second-order correction - Iteration   2 ........   .298E-01 -.735E-01

           5   3.34043   -16.6171  -.7271E+00   .1047E+02
        On iteration   5 the following slices produced
        low denominators in the equations for the factor
        of safety -   54  55  56  57  58  59  60  61
        First-order corrections to F and THETA .........   .882E-05 -.279E-04

        Factor of Safety - - - - - - - -     3.340
```

```
Side Force Inclination - - - - -    -16.62
Number of Iterations - - - - - -     5

DENOMINATOR IN EQUATIONS FOR F WAS SMALL FOR   8 SLICES
FIRST AND LAST SLICES WHERE DENOMINATOR WAS LOW -    54    61
1   UTEXAS3 - VER. 1.200 - 12/16/92 - (C) 1985-1992 S. G. WRIGHT
Date:  3: 7:2003   Time: 10:29:15   Input file: Case1.inp
Diablo Canyon Power Plant ISFSI
Stability Analysis - Case 1
```

TABLE NO. 38

```
*****************************************************************
*  Final Results for Stresses Along the Shear Surface           *
*  (Results for Critical Shear Surface in Case of a Search.)    *
*****************************************************************
```

SPENCER'S PROCEDURE USED TO COMPUTE FACTOR OF SAFETY
Factor of Safety = 3.340 Side Force Inclination = -16.62 Degrees

-------- VALUES AT CENTER OF BASE OF SLICE---------

Slice No.	X-center	Y-center	Total Normal Stress	Effective Normal Stress	Shear Stress
1	-34.0	.0	.4	.4	.2
2	-33.8	-1.1	1683.4	1683.4	600.6
3	-33.3	-3.2	2100.4	2100.4	749.3
4	-32.7	-5.3	2502.5	2502.5	892.8
5	-32.0	-7.3	2889.5	2889.5	1030.9
6	-31.2	-9.4	3260.6	3260.6	1163.3
7	-30.3	-11.4	3615.4	3615.4	1289.8
8	-29.3	-13.3	3953.0	3953.0	1410.3
9	-28.2	-15.1	4272.8	4272.8	1524.4
10	-27.0	-17.0	4574.0	4574.0	1631.8
11	-25.7	-18.7	4855.9	4855.9	1732.4
12	-24.3	-20.4	5117.8	5117.8	1825.9
13	-22.8	-22.0	5358.9	5358.9	1911.9
14	-22.0	-22.8	5477.5	5477.5	1954.2
15	-21.2	-23.6	5586.0	5586.0	1992.9
16	-19.6	-25.0	5782.6	5782.6	2063.1
17	-18.4	-25.9	5906.1	5906.1	2107.1
18	-18.0	-26.2	6448.4	6448.4	756.7
19	-17.1	-26.9	6495.8	6495.8	760.5
20	-15.3	-28.1	6568.8	6568.8	766.4
21	-13.4	-29.2	6613.3	6613.3	770.0
22	-11.5	-30.2	6629.5	6629.5	771.3
23	-9.5	-31.1	6617.3	6617.3	770.3
24	-7.5	-32.0	6576.9	6576.9	767.1
25	-5.5	-32.7	6508.4	6508.4	761.6
26	-3.4	-33.3	6411.9	6411.9	753.8
27	-1.3	-33.8	6287.4	6287.4	743.8
28	.9	-34.1	6135.2	6135.2	731.6
29	3.1	-34.4	5955.3	5955.3	717.2
30	5.2	-34.5	5747.9	5747.9	700.6
31	6.7	-34.6	5598.5	5598.5	688.6
32	7.5	-34.6	5503.6	5503.6	681.0
33	9.1	-34.5	5500.3	5500.3	680.7
34	11.3	-34.4	5604.1	5604.1	689.0
35	13.4	-34.1	5695.4	5695.4	696.3

36	15.6	-33.7	5774.3	5774.3	702.7
37	17.7	-33.2	5841.2	5841.2	708.0
38	19.8	-32.6	5896.5	5896.5	712.5
39	20.9	-32.2	5924.6	5924.6	714.7
40	22.0	-31.8	5944.9	5944.9	716.4

1

-------- VALUES AT CENTER OF BASE OF SLICE---------

Slice No.	X-center	Y-center	Total Normal Stress	Effective Normal Stress	Shear Stress
41	23.8	-31.0	5976.1	5976.1	718.9
42	25.3	-30.4	6183.3	6183.3	922.9
43	26.2	-29.9	6207.8	6207.8	926.5
44	27.4	-29.2	6233.6	6233.6	930.4
45	29.3	-28.1	6279.4	6279.4	937.2
46	30.6	-27.3	6317.0	6317.0	942.9
47	31.3	-26.8	6336.9	6336.9	945.8
48	32.4	-25.9	6371.9	6371.9	951.1
49	34.1	-24.6	6445.8	6445.8	962.1
50	35.7	-23.1	6551.1	6551.1	977.8
51	36.7	-22.1	6654.2	6654.2	993.2
52	37.7	-21.0	6786.8	6786.8	1013.0
53	39.2	-19.4	7090.0	7090.0	1058.2
54	40.5	-17.6	7618.0	7618.0	1137.0
55	41.7	-15.9	8632.3	8632.3	1288.4
56	42.9	-14.0	10994.2	10994.2	1641.0
57	43.9	-12.1	20187.5	20187.5	3013.1
58	44.9	-10.1	-44229.5	-44229.5	-6601.6
59	45.7	-8.1	-6362.6	-6362.6	-949.7
60	46.5	-6.1	-2287.8	-2287.8	-341.5
61	47.1	-4.0	-873.2	-873.2	-130.3
62	47.6	-1.9	-250.4	-250.4	-37.4
63	47.9	-.4	-37.7	-37.7	-5.6

```
CHECK SUMS - (ALL SHOULD BE SMALL)
SUM OF FORCES IN VERTICAL DIRECTION     =          .02  (=  .243E-01)
     SHOULD NOT EXCEED      .100E+03
SUM OF FORCES IN HORIZONTAL DIRECTION   =          .07  (=  .719E-01)
     SHOULD NOT EXCEED      .100E+03
SUM OF MOMENTS ABOUT COORDINATE ORIGIN  =       -10.27  (= -.103E+02)
     SHOULD NOT EXCEED      .100E+03
SHEAR STRENGTH/SHEAR FORCE CHECK-SUM    =          .01  (=  .672E-02)
     SHOULD NOT EXCEED      .100E+03

///// WARNING ///// EFFECTIVE OR TOTAL NORMAL STRESS ON SHEAR
                    SURFACE IS NEGATIVE AT POINTS ALONG THE
                    LOWER ONE-HALF OF THE SHEAR SURFACE -
                    SOLUTION MAY NOT BE A VALID SOLUTION.
///// WARNING ///// EFFECTIVE OR TOTAL NORMAL STRESS ON SHEAR
                    SURFACE IS NEGATIVE AT POINTS ALONG THE
                    LOWER ONE-HALF OF THE SHEAR SURFACE -
                    SOLUTION MAY NOT BE A VALID SOLUTION.

///// WARNING ///// SHEAR STRESS AT SOME POINTS ALONG THE SHEAR
                    SURFACE IS NEGATIVE - SOLUTION MAY NOT BE A
                    VALID SOLUTION.
///// WARNING ///// SHEAR STRESS AT SOME POINTS ALONG THE SHEAR
```

```
                    SURFACE IS NEGATIVE - SOLUTION MAY NOT BE A
                    VALID SOLUTION.
1       UTEXAS3 - VER. 1.200 - 12/16/92 - (C) 1985-1992 S. G. WRIGHT
        Date:  3: 7:2003   Time: 10:29:15   Input file: Case1.inp
        Diablo Canyon Power Plant ISFSI
        Stability Analysis - Case 1
```

TABLE NO. 39

```
*****************************************************************
*  Final Results for Side Forces and Stresses Between Slices.   *
*  (Results for Critical Shear Surface in Case of a Search.)    *
*****************************************************************
```

SPENCER'S PROCEDURE USED TO COMPUTE FACTOR OF SAFETY
Factor of Safety = 3.340 Side Force Inclination = -16.62 Degrees

---------- VALUES AT RIGHT SIDE OF SLICE ----------

Slice No.	X-Right	Side Force	Y-Coord. of Side Force Location	Fraction of Height	Sigma at Top	Sigma at Bottom
1	-34.0	0.	.0	.475	.4	.5
2	-33.6	3487.	-1.1	.464	1210.7	1876.8
3	-33.0	7695.	-2.4	.438	1082.4	2367.1
4	-32.4	12526.	-3.7	.421	989.1	2788.4
5	-31.6	17878.	-5.0	.407	902.3	3177.3
6	-30.8	23646.	-6.3	.396	816.6	3540.8
7	-29.8	29722.	-7.6	.386	730.4	3880.5
8	-28.8	35999.	-8.8	.378	643.3	4196.7
9	-27.6	42367.	-10.1	.370	555.4	4488.9
10	-26.4	48722.	-11.4	.363	467.0	4756.6
11	-25.0	54958.	-12.6	.357	378.4	4999.0
12	-23.6	60974.	-13.8	.351	290.3	5215.3
13	-22.1	66675.	-14.9	.345	203.2	5404.8
14	-22.0	66869.	-14.9	.345	200.2	5410.9
15	-20.4	72147.	-16.0	.340	114.7	5571.7
16	-18.7	76932.	-17.1	.335	31.6	5704.0
17	-18.1	78558.	-17.4	.333	1.9	5745.2
18	-18.0	78934.	-17.5	.333	-13.8	5773.8
19	-16.2	86083.	-18.8	.316	-304.4	6298.1
20	-14.4	92619.	-20.0	.303	-565.1	6751.5
21	-12.5	98480.	-21.1	.291	-805.3	7146.7
22	-10.5	103618.	-22.1	.280	-1031.8	7493.7
23	-8.5	107992.	-23.1	.270	-1250.1	7800.3
24	-6.5	111578.	-23.9	.259	-1464.2	8073.0
25	-4.4	114359.	-24.8	.249	-1677.8	8317.5
26	-2.3	116333.	-25.5	.238	-1894.1	8539.2
27	-.2	117510.	-26.3	.227	-2116.1	8743.4
28	2.0	117912.	-26.9	.215	-2347.2	8935.2
29	4.1	117573.	-27.6	.201	-2590.6	9120.6
30	6.3	116540.	-28.1	.186	-2850.5	9305.9
31	7.0	116079.	-28.3	.181	-2936.4	9365.3
32	8.0	115300.	-28.6	.173	-3065.7	9453.7
33	10.2	113127.	-29.1	.155	-3363.0	9650.6
34	12.3	110265.	-29.6	.134	-3681.4	9850.0
35	14.5	106705.	-30.1	.111	-4022.1	10050.8
36	16.6	102441.	-30.7	.084	-4386.4	10252.0
37	18.7	97478.	-31.2	.053	-4776.4	10452.7
38	20.8	91824.	-31.7	.016	-5194.1	10652.2

39	21.0	91237.	-31.8	.012	-5236.3	10671.5
40	23.0	84840.	-32.4	BELOW	-5687.5	10868.4

1

---------- VALUES AT RIGHT SIDE OF SLICE ----------

Slice No.	X-Right	Side Force	Y-Coord. of Side Force Location	Fraction of Height	Sigma at Top	Sigma at Bottom
41	24.5	79522.	-33.0	BELOW	-6053.8	11016.0
42	26.0	73544.	-33.6	BELOW	-6400.4	11098.3
43	26.4	71654.	-33.9	BELOW	-6508.6	11120.6
44	28.3	62866.	-35.1	BELOW	-7004.1	11201.1
45	30.2	53430.	-36.9	BELOW	-7523.6	11241.6
46	31.0	48861.	-38.1	BELOW	-7770.1	11242.1
47	31.5	45994.	-39.0	BELOW	-7922.9	11235.2
48	33.2	35449.	-43.4	BELOW	-8469.9	11156.9
49	34.9	24259.	-52.7	BELOW	-9013.4	10961.3
50	36.5	12385.	-81.8	BELOW	-9522.4	10583.7
51	37.0	7963.	-115.2	BELOW	-9687.7	10387.6
52	38.5	-4987.	129.5	ABOVE	-10054.1	9580.7
53	39.8	-18972.	19.5	ABOVE	-10154.6	8189.0
54	41.1	-34448.	2.5	ABOVE	-9689.0	5744.4
55	42.3	-52446.	-4.1	.729	-7992.0	1250.9
56	43.4	-75891.	-7.4	.433	-3340.4	-7827.0
57	44.4	-119787.	-9.4	.158	10904.5	-31617.2
58	45.3	-22028.	-6.9	.249	1173.7	-5815.8
59	46.1	-7775.	-5.0	.294	248.6	-2358.9
60	46.8	-2596.	-3.4	.337	-11.1	-985.9
61	47.4	-604.	-1.7	.419	-103.3	-297.7
62	47.9	-30.	-.4	.561	-51.6	-23.9
63	48.0	1.	-1.6	BELOW	.0	.0

```
CHECK SUMS - (ALL SHOULD BE SMALL)
SUM OF FORCES IN VERTICAL DIRECTION     =          .02  (=  .243E-01)
     SHOULD NOT EXCEED      .100E+03
SUM OF FORCES IN HORIZONTAL DIRECTION   =          .07  (=  .719E-01)
     SHOULD NOT EXCEED      .100E+03
SUM OF MOMENTS ABOUT COORDINATE ORIGIN =       -10.27  (= -.103E+02)
     SHOULD NOT EXCEED      .100E+03
SHEAR STRENGTH/SHEAR FORCE CHECK-SUM    =          .01  (=  .672E-02)
     SHOULD NOT EXCEED      .100E+03

///// WARNING ///// FORCES BETWEEN SLICES ARE NEGATIVE AT POINTS
                    ALONG THE LOWER ONE-HALF OF THE SHEAR SURFACE -
                    SOLUTION MAY NOT BE A VALID SOLUTION.
///// WARNING ///// FORCES BETWEEN SLICES ARE NEGATIVE AT POINTS
                    ALONG THE LOWER ONE-HALF OF THE SHEAR SURFACE -
                    SOLUTION MAY NOT BE A VALID SOLUTION.

***** CAUTION ***** SOME OF THE FORCES BETWEEN SLICES ACT AT POINTS
                    ABOVE THE SURFACE OF THE SLOPE OR BELOW THE
                    SHEAR SURFACE - EITHER A TENSION CRACK MAY BE
                    NEEDED OR THE SOLUTION MAY NOT BE A VALID SOLUTION.


END-OF-FILE ENCOUNTERED WHILE READING COMMAND
WORDS - END OF PROBLEM(S) ASSUMED
```